European Commission

JRC TECHNICAL REPORT

Report on the biogeochemical model of the North-Western European Shelf

Friedland, R., Stips, A., Grizzetti, B., de Roo, A., Lessin, G.

2020

Joint Research Centre

EUR 30168 EN

Contact information
Name: René Friedland
Address: Via E. Fermi, TP270, Ispra, Varese, Italy
Email: jrc-mmf@ec.europa.eu, rene.friedland@ec.europa.eu
Tel.: +39-0332-78947

EU Science Hub
https://ec.europa.eu/jrc

JRC120213

EUR 30168 EN

PDF	ISBN 978-92-76-17866-8	ISSN 1831-9424	doi:10.2760/78173

Luxembourg: Publications Office of the European Union, 2020

How to cite this report: Friedland, R., Stips, A., Grizzetti, B., de Roo, A. and Lessin, G., *Report on the biogeochemical model of the North-Western European Shelf,* Publications Office of the European Union, Luxembourg, 2020, ISBN 978-92-76-17866-8, doi:10.2760/78173, JRC120213.

Contents

1 Introduction ... 2
2 Material and method ... 5
2.1 Model setup ... 5
2.2 Riverine nutrient and freshwater inputs ... 10
2.3 Validation data sets for hydrographical properties ... 17
2.4 Validation data sets for biogeochemical properties ... 20
3 Results ... 28
3.1 Sea surface height compared to gauge data ... 28
3.2 Sea surface temperature (compared to satellite data) ... 29
3.3 Sea surface salinity (compared to satellite data) ... 30
3.4 Salinity and temperature compared to climatologies (KNSC and GINS) ... 31
3.5 Mixing zones and current fields ... 32
3.6 State of MSFD eutrophication indicators ... 33
3.7 Seasonal climatologies ... 37
3.8 Model results compared to satellite data ... 42
3.9 ICES COMPEAT data ... 47
3.10 Assessment for AMM7 regions ... 49
3.11 Station data ... 53
4 Summary ... 55
References ... 56

1 Introduction

Marine and coastal waters all around Europe and the globe are heavily threatened by eutrophication, the excessive accumulation of nutrients in the water resulting in potentially toxic algal blooms and regions with nearly no oxygen in the water, preventing any underwater life (Nixon, 1995). Hence, clean oceans and seas are addressed by the 2030 Agenda for Sustainable Development of the United Nations ([1]) as well as by Directive 2008/56/EC of the European Parliament and of the European Council (Marine Strategy Framework Directive (2008/56/EC)).

The accumulation of (inorganic) nutrients in the Greater North Sea region has already been reported for decades, for example a first target to half the riverine nutrient loads was set in 1988 (PARCOM, 1988). Using the years 2006 to 2014, the third eutrophication status assessment (OSPAR, 2017) of the Convention for the Protection of the Marine Environment of the North-East Atlantic (OSPAR) led to the identification of non-problematic, potential problematic and problematic areas (see Figure 1). All problematic and potential problematic areas are located along the southern and eastern parts of the North Sea and along the shoreline of France.

Currently, strong efforts are being made to update the eutrophication assessment, especially within the OSPAR working group on Hazardous Substances and Eutrophication (HASEC ([2])), leading to revised assessment units. A first, yet not finalised approach, is to implement and apply the ICES COMPEAT tool ([3]) (see Figure 2). The preliminary assessment to compare the present state with set targets, resulted in a worsened classification as more regions are now assessed as 'Not Good'. These regions are again mostly located in the southern and eastern North Sea, but now also many (coastal) waters around UK and in the Celtic and Irish Sea are classified as 'Not Good' (see Figure 2).

To support the integrated assessment and develop the ability to test future threads or suitable measures to improve the water quality, the Marine Modelling Framework (MMF) of JRC was extended by a fully coupled three-dimensional model of the Greater North Sea, Celtic Sea and Irish Sea. The developed model was supposed to incorporate the dominating hydrodynamical features as well as a sophisticated model of the lower trophic levels (LTL), suitable to allow scenario simulations and validated using up-to-date observations. While a wide branch of coupled 3d-models for the North Sea region already exists, e.g. shown in Moll and Radach (2003), the newly developed JRC model was chosen to base on GETM and ERSEM. GETM was selected as hydrodynamical engine of the model to be in a methodologial agreement with the other LTL models of MMF and because it was already shown that GETM is well suitable for the modelling of the Greater North Sea (e.g. Stips et al. (2016), Pätsch et al. (2017), Gräwe et al. (2015)). Further, it allows easy incorporation of up-to-date LTL models like ERSEM, which was already successfully used for the simulation of the biogeochemistry of the Greater North Sea (Butenschön et al., 2016). Nevertheless, many other LTL models were also applied to the region, e.g. ERGOM (Maar et al., 2011), ECOSMO (Daewel and Schrum, 2013), ECOHAM (Große et al., 2016), ERSEM-BFM (van Leeuwen et al., 2015) or even combined to a model ensemble (Lenhart et al., 2010).

([1]) https://sustainabledevelopment.un.org/sdgs
([2]) https://www.ospar.org/work-areas/hasec
([3]) https://ocean.ices.dk/core/compeat?assessmentperiod=20062014_Test

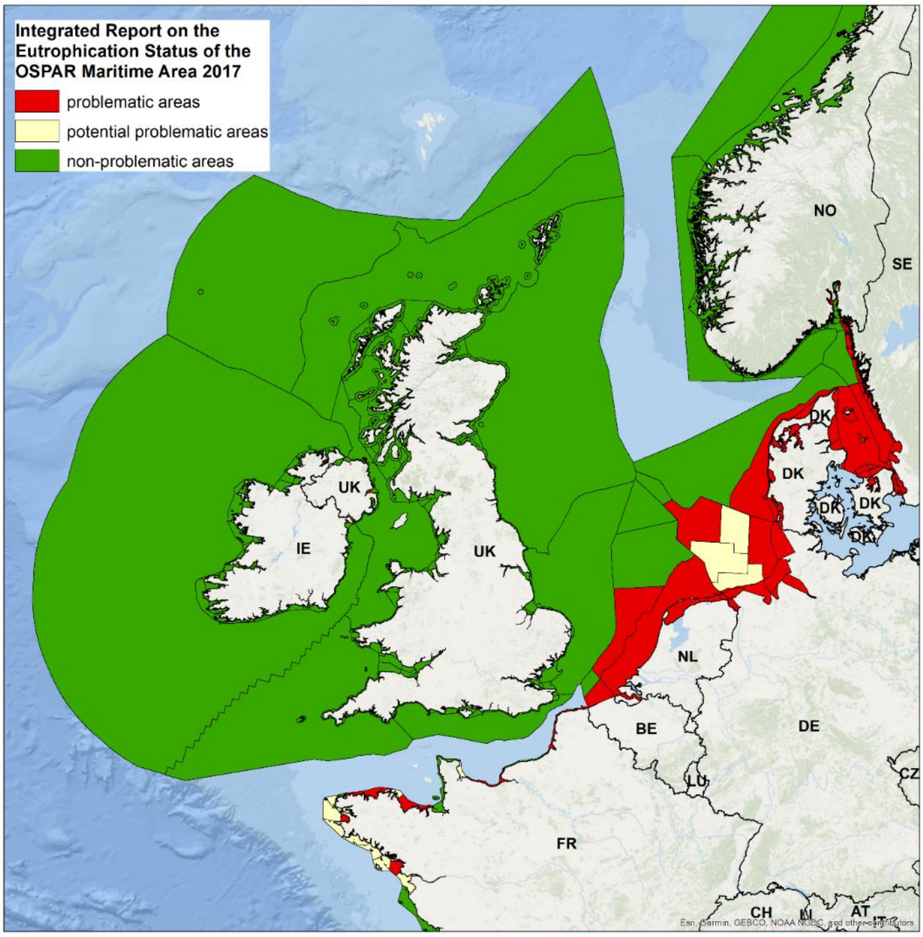

Figure 1: Result of the integrated eutrophication assessment (4) by (OSPAR, 2017)

(4) https://odims.ospar.org/layers/geonode:ospar_eut_status_2017_06_001/metadata_detail

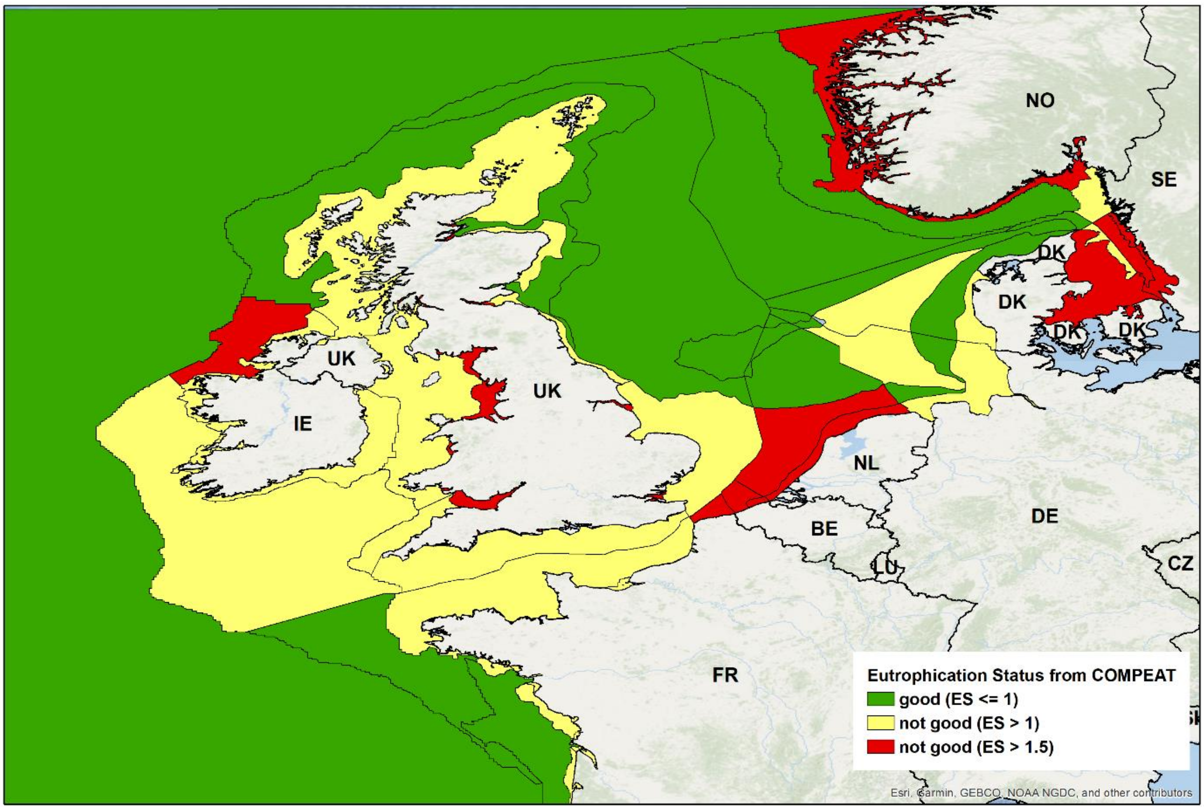

Figure 2: Result of the eutrophication assessment, computed with ICES COMPEAT

2 Material and method

2.1 Model setup

Based on a collaboration with PML and NIOZ a 3d-model system of the North-Western European Shelf (NWES) was developed. It covers the region between 46.4° N-63° N and 17.5° W-13.1° E (see Figure 3) and includes the Greater North Sea and surrounding areas (Skagerrak and Kattegat in the east, Norwegian Sea in the North, English Channel and Celtic Sea in the South, Irish Sea and parts of deep Atlantic Ocean in the West). The model system is a fully coupled 3d-hydrodynamical-biogeochemical model of the lower trophic web. The hydrographical part is based on the General Estuarine Transport Model (GETM ([5])). By using the Framework for Aquatic Biogeochemical Models (FABM; Bruggeman and Bolding (2014)), the European Regional Seas Ecosystem Model (ERSEM; Butenschön et al. (2016)) was coupled dynamically to the hydrodynamic model engine. The model simulations covered 8 years (2005-2012), restricted by the riverine inputs.

The horizontal grid cells of the model region are equidistant with a resolution of 0.08° in x-direction and 0.05° in y-direction, resulting in a cell size of 4.04-6.13 km (x-direction) and 5.56 km (y). For the vertical decomposition, adaptive coordinates were chosen, which adjust the layer height depending on the vertical stratification. To avoid numerical instabilities, the minimal height of the surface and bottom cell was set to 0.5 m. It has been shown that adaptive coordinates are advantageous for the simulation of stratified waters like the North or Baltic Sea (Gräwe et al., 2015). The bathymetry of the model domain (Figure 3a) was initially taken from North-West European Shelf Operational Oceanographic System (NOOS ([6]); Stips et al. (2016)), but was adjusted to include some shallow parts of the Wadden Sea. A spatially variable bottom roughness (Figure 3b) was chosen, which was used as optimisation parameter to enhance the match of modelled and observed tides.

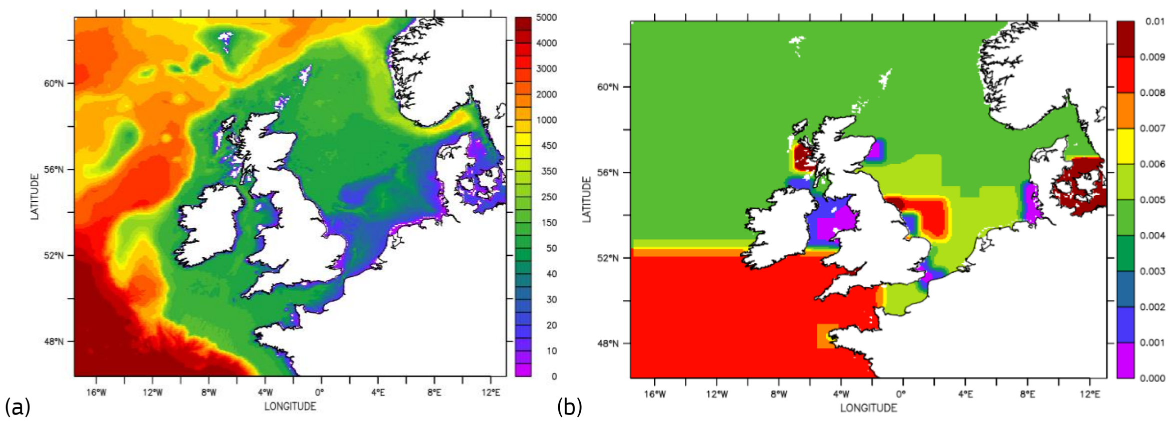

Figure 3: Used topography (a; m) and bottom roughness (b; m) of the NWES-model

The used version of ERSEM is freely available ([7]) (upon registration), a previous version of ERSEM was used already by JRC MMF (Garcia-Gorriz et al., 2016). It consists of dissolved inorganic nutrients (ammonium, nitrate, phosphate, carbon, silicate) and has a sophisticated growth model for phytoplankton, which is divided

([5]) http://www.getm.eu
([6]) http://www.noos.cc
([7]) https://gitlab.ecosystem-modelling.pml.ac.uk/stable/ERSEM

into four functional groups (see Figure 4). Each group has its specific ecological niche and requirements. Nutrients are uptaken in a variable ratio (and not following the Redfield ratio like in most other biogeochemical models). This allows them to adapt their growth to changes of the nutrient limitations. While previous studies (Ford et al., 2017) have shown a good agreement of the different modelled groups with observations, the analyses within this report are focused on the integrated Chlorophyll-a content of all phytoplankton groups, as MSFD is using this as a central eutrophication indicator (D5.C2). ERSEM further incorporates three functional zooplankton groups and several benthic models of different complexities. For the present study, the benthic model with the lowest complexity ([8]), the so-called 'benthic returns', was used to reduce the computational efforts.

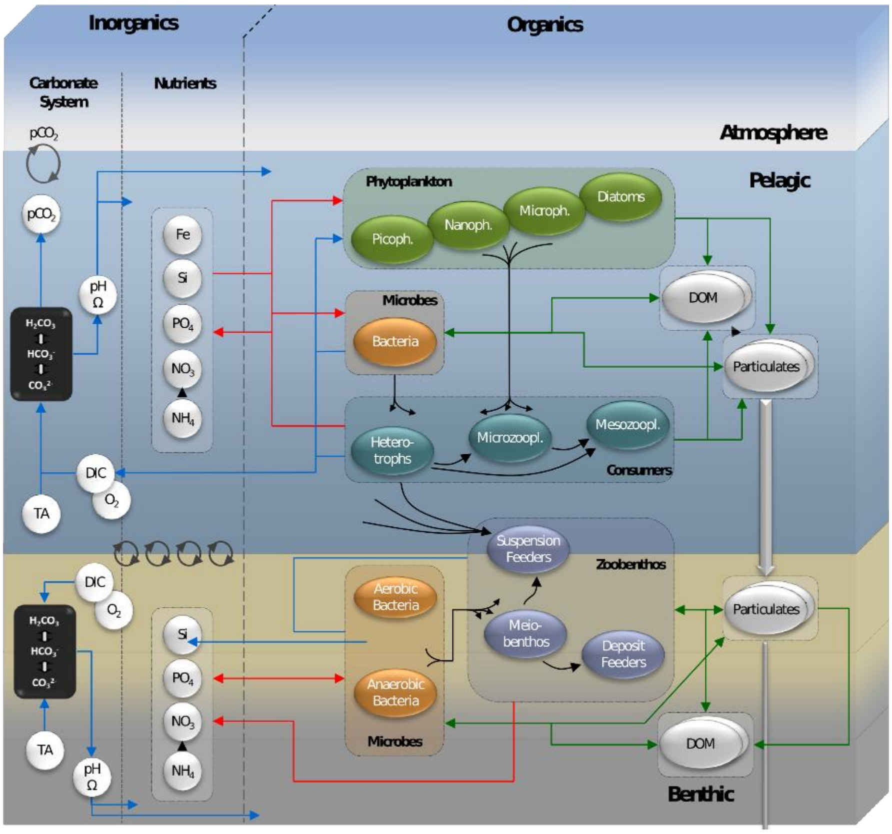

Figure 4: Schematic overview of the European Regional Seas Ecosystem Model (ERSEM; taken from ([9]))

Atmospheric forcing fields ([10]) were taken from the European Centre for Medium Range Weather Forecast (ECMWF, using ERA5 ([11])) in agreement with the other marine model of JRC ([12]). Sea level data and surface currents at the open boundaries were generated in temporal resolution of 30 minutes from the tide model provided by Oregon State University ([13]). They were enhanced by the daily deviation from the long-term mean using HYCOM ([14]) (Cummings and Smedstad, 2013). The 2d-boundaries are following the spatial gradients of

([8]) Following fabm-ersem-15.06-L4-noben-docdyn-iop.yaml
([9]) https://www.pml.ac.uk/Modelling_at_PML/Models/ERSEM
([10]) 10 m winds, 2 m temperature, 2 m dewpoint temperature, cloud cover, mean sea level pressure, precipitation
([11]) https://www.ecmwf.int/en/forecasts/datasets/reanalysis-datasets/era5
([12]) Taken from /ACQUA/COMMONDATA/ECMWF/ncdf_era5
([13]) http://volkov.oce.orst.edu/tides/AO.html
([14]) http://www.hycom.org

the sea surface height from the global model (see Figure 5), especially with a higher water level at the Baltic Sea boundary (due to the nature of the Baltic Sea, where freshwater inputs exceed evaporation, so that a net export of water into the North Sea must take place). Dominated by the Gulf Stream, along the western boundary of NWES the positive U-currents indicate an inflow into the region, while a major part is leaving again through the northern boundary, following the positive V-currents (see Figure 5). Using the salinity and water temperature fields from HYCOM, the climatological means were computed at the open boundaries. This approach allows to use the open boundaries for later scenario simulations without adjusting them further. On the other hand, the simulation results got slightly worse along the boundaries, as the short-term variability was not included. The fields along the southern boundary had to be adjusted, using the mean values from World Ocean Atlas 2018 (WOA2018 ([15])).

Using observational data covering the inorganic nutrients (phosphate, nitrate, ammonium and silicate), dissolved oxygen, dissolved inorganic carbon and alkalinity from WOA2018, climatological values (in a monthly resolution) were computed and processed to be used along the open boundaries. Furthermore, winter values from WOA2018 were processed to generate the necessary initial conditions (referring to early January). Thereafter, the values were fitted to the model bathymetry and vertically adjusted to be utilised as model input. Using these fields as first initial conditions, a full simulation of NWES covering a five-year period was conducted. At the end of this spin-up phase, stable annual biogeochemical cycles were recognisable. Afterwards, hydrographical and biogeochemical variables (Figures 6 and 7) were selected from the end of the spin-up phase and processed to provide initial conditions for the later simulations.

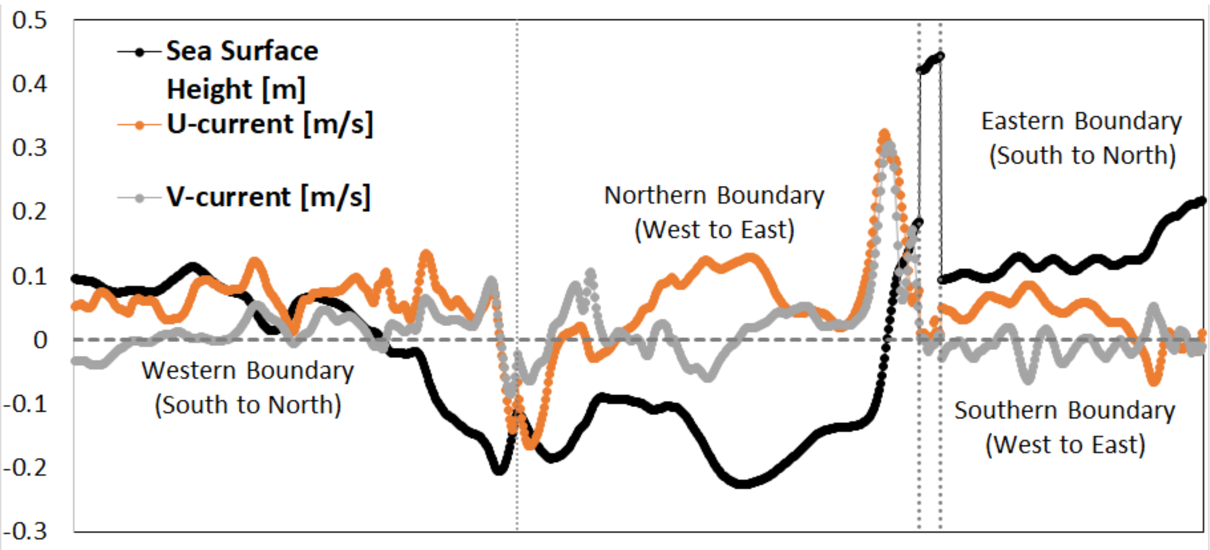

Figure 5: Sea Surface Height (black), U- and V-components of the currents (orange and gray) along the open boundaries averaged over the complete simulation period.

([15]) https://www.nodc.noaa.gov/OC5/woa18

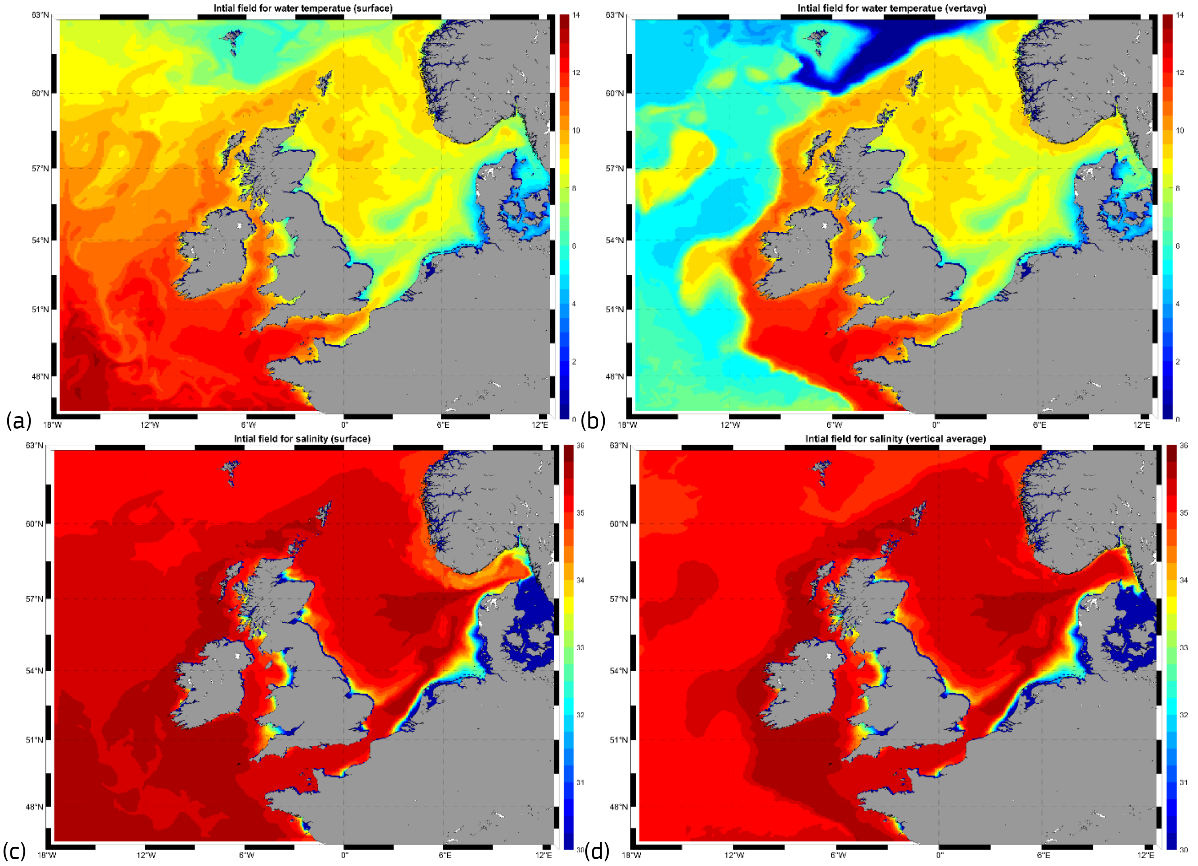

Figure 6: Initial fields of water temperature (a, b) and salinity (c, d) of the NWES setup, shown are surface values (a, c) and vertical averages (b, d) of both

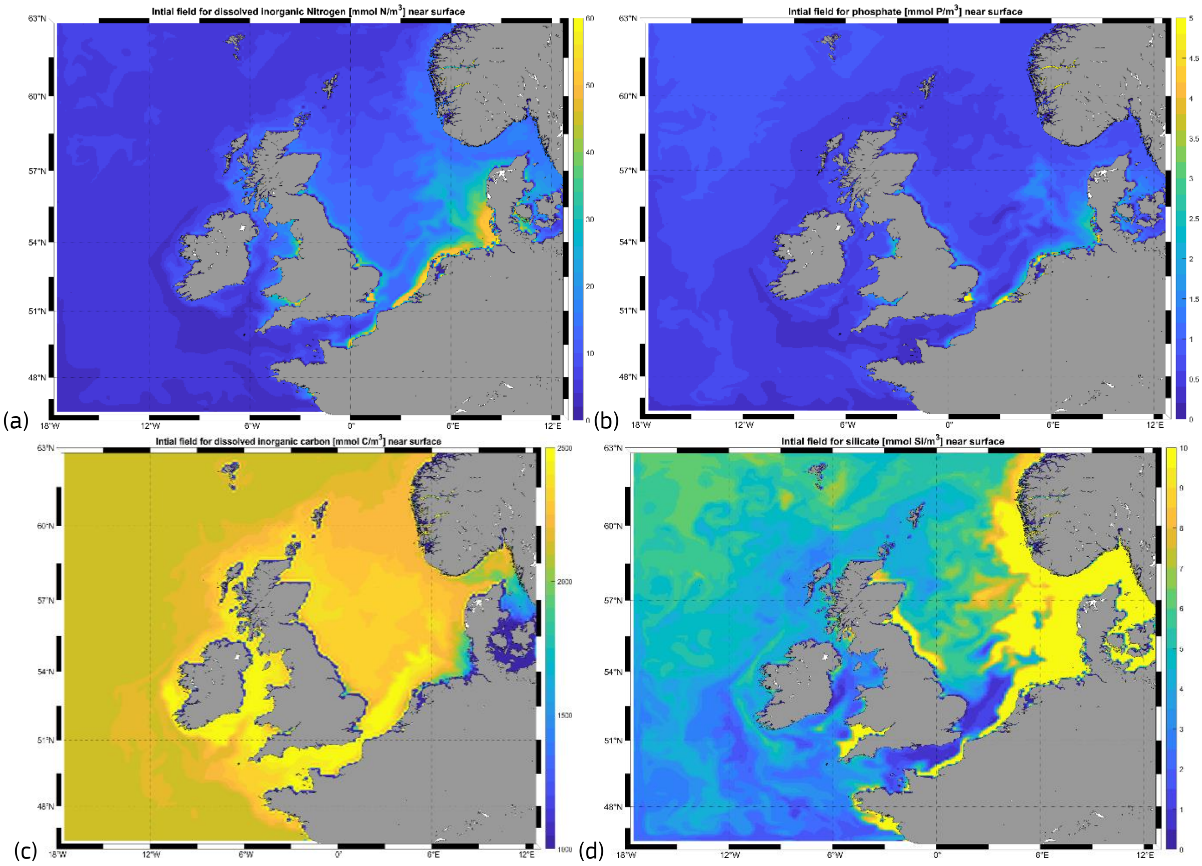

Figure 7: Initial fields of dissolved inorganic nitrogen (a), phosphate (b), dissolved inorganic carbon (c) and silicate (d) of the NWES setup, only surface values are shown

2.2 Riverine nutrient and freshwater inputs

Riverine nutrient and freshwater inputs were provided by JRC's catchment models GREEN (Grizzetti et al., 2012, Grizzetti et al., 2019) and LISFLOOD (De Roo et al., 2000, Van Der Knijff et al., 2010). GREEN is a statistical GIS-based model covering the whole of Europe, including the nutrient loads entering the North-Western European Shelf (Figures 8-10). The nutrient and freshwater loads were provided at the land-sea-interface, following the classification of outflow points from GREEN, which incorporated the freshwater flux provided by the LISFLOOD model. LISFLOOD is a grid-based rainfall-runoff-water resources model, which simulates the daily water balance of Europe using 5 km grid cells. It takes water abstractions and return flows for irrigation, livestock, industry, energy cooling, public water usage, and ecosystem constraints into account. The output of both catchment models is provided with a spatially very high resolution, resulting in roughly 15 000 inflow points for the NWES setup. These were merged into the nearest grid cell of the hydrodynamic model. As only annual values of freshwater runoff and nutrient loads could be provided, a temporal downscaling was conducted, using climatological cycles computed from the publicly available catchment model HYPE ([16]). As the biogeochemical model needs the inorganic nutrient loads (Ammonium, Nitrate, and Phosphate), Total Nitrogen and Phosphorus provided by GREEN were used to estimate the inorganic loads ([17]). Constant conversion factors were assumed, computed from the ICG EMO nutrient load database.

To validate the freshwater runoff and riverine nutrient loads, a variety of observed data for the biggest rivers was merged, provided by:

- Global Runoff Data Centre ([18]);
- Global Nutrient Export from WaterSheds 2 (Mayorga et al., 2010);
- European Environment Agency ([19]);
- Publicly available databases (OSPAR Data and Information Management System ([20]); UK National River Flow Archive ([21]); Hydro-Data provided by the Irish Office of Public Works ([22]);
- OSPAR Intersessional Correspondence Group on Eutrophication Modelling (ICG EMO ([23]));
- Literature sources (see Table 1).

The riverine freshwater runoffs and nutrient loads provided by LISFLOOD and GREEN fit very well with the observations (see Figures 11-13). Correlations between reported and modelled riverine nutrient loads are overall high and the linear regression is close to 1.

Table 1: Used literature sources for the validation of the riverine loads

Reference	River

([16]) https://hypeweb.smhi.se/explore-water/historical-data/europe-time-series
([17]) Ammonium and Nitrate are 5 % and 75 % of Total Nitrogen, while Phosphate is 50 % of Total Phosphorus.
([18]) https://www.bafg.de/GRDC/EN/01_GRDC/grdc_node.html
([19]) https://www.eea.europa.eu/data-and-maps/data/waterbase-rivers-10
([20]) https://odims.ospar.org
([21]) https://nrfa.ceh.ac.uk/data/search
([22]) http://waterlevel.ie/hydro-data/list.html#
([23]) Provided by *Sonja* v *Leeuwen* (NIOZ, pers. comm.), see Lenhart et al. (2010); when forcing the NWES simulation with ICG EMO the freshwater inputs were scaled by a factor of 0.9 to improve the salinity gradients.

Hartmann et al. (2011)	Rhine
Hesse and Krysanova (2016)	Elbe
Howden et al. (2010)	Thames
Ménesguen et al. (2019)	Loire, Seine
Minaudo et al. (2015)	Loire
Mockler et al. (2017)	Shannon
Passy et al. (2013), Thieu et al. (2010)	Scheldt, Seine, Somme
Passy et al. (2016)	Seine
Tockner et al. (2009)	Elbe, Loire, Rhine
Radach and Pätsch (2007)	Elbe, Ems, Rhine, Weser
Romero et al. (2013)	Loire, Scheldt, Seine, Somme, Vilaine

(a) (b)

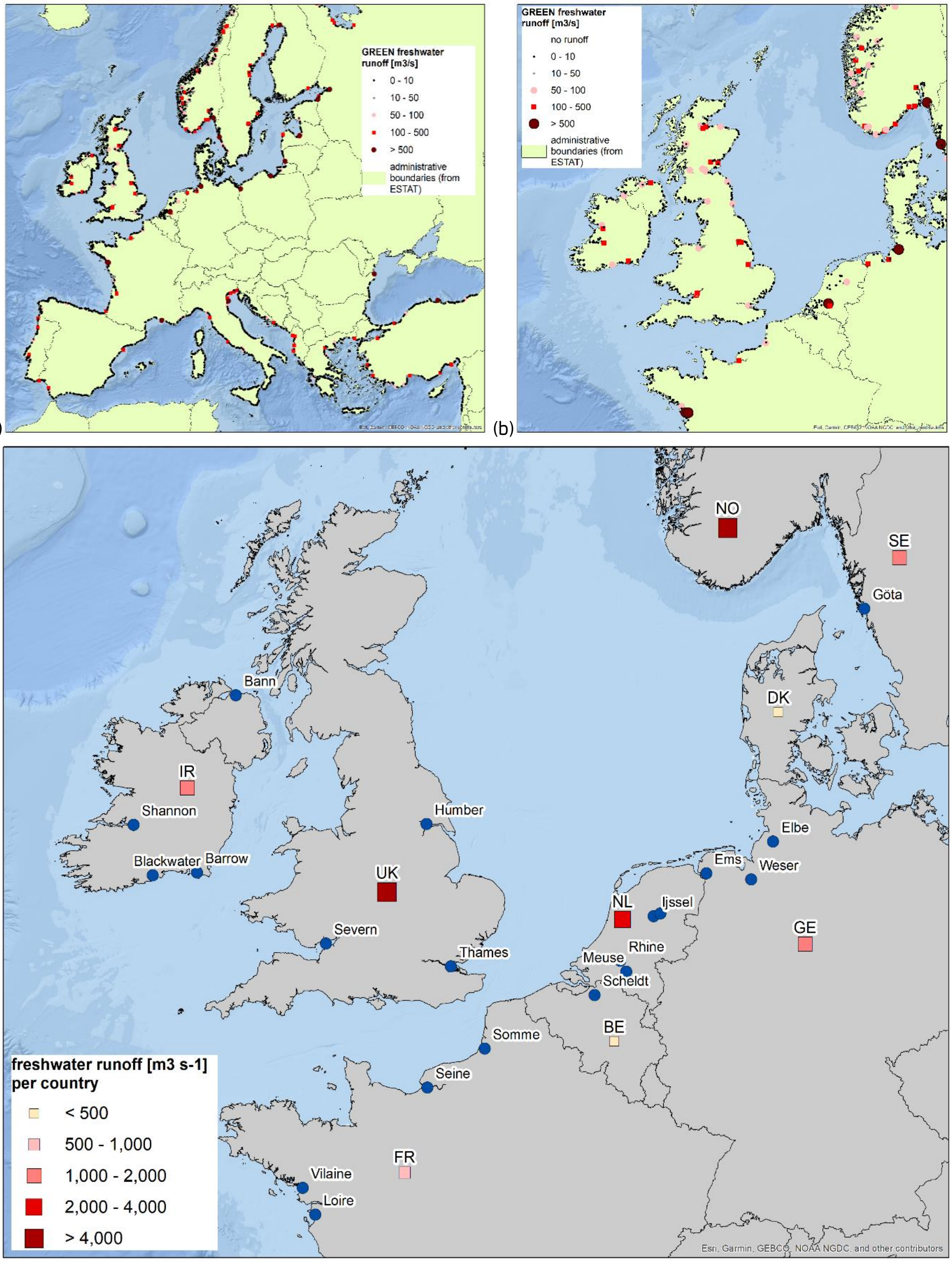

(c)

Figure 8: Freshwater runoff [m3 s-1] into the European seas (a), zoomed into the NWES region (b) and summed per country (c, highlighted are the biggest rivers)

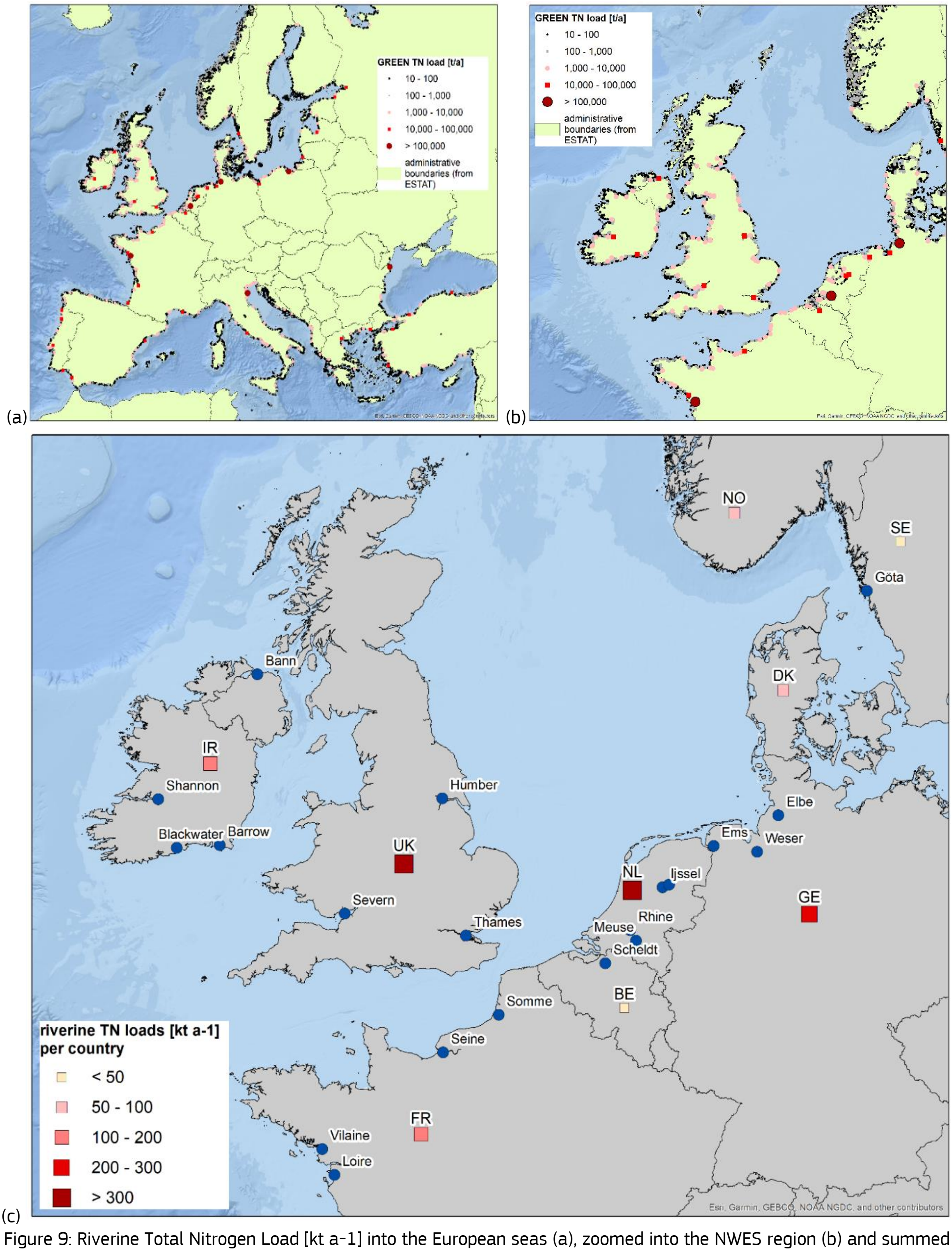

Figure 9: Riverine Total Nitrogen Load [kt a-1] into the European seas (a), zoomed into the NWES region (b) and summed per country (c, highlighted are the biggest rivers)

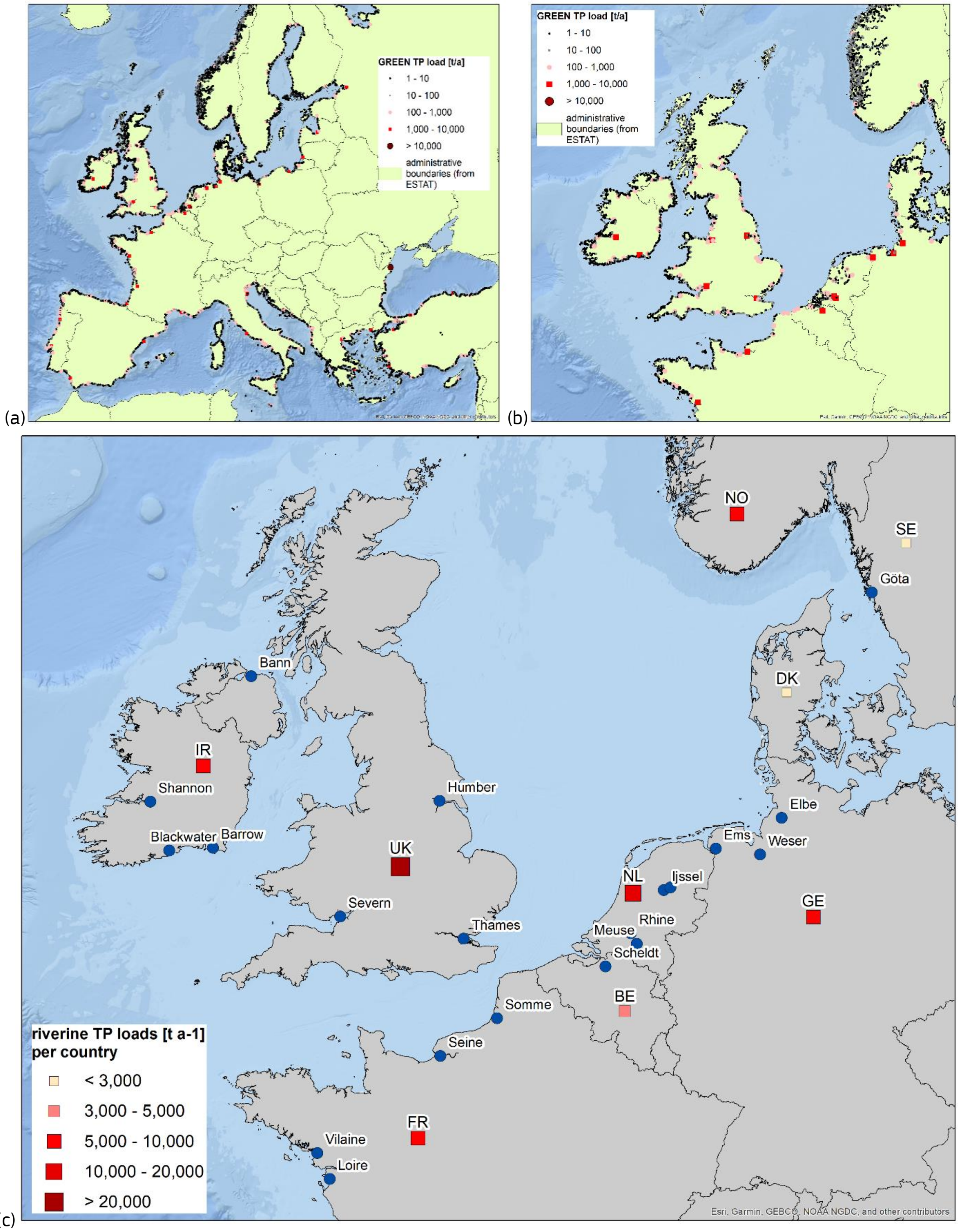

Figure 10: Riverine Total Phosphorus Load [kt a-1] into the European seas (a), zoomed into the NWES region (b) and summed per country (c), highlighted are the biggest rivers)

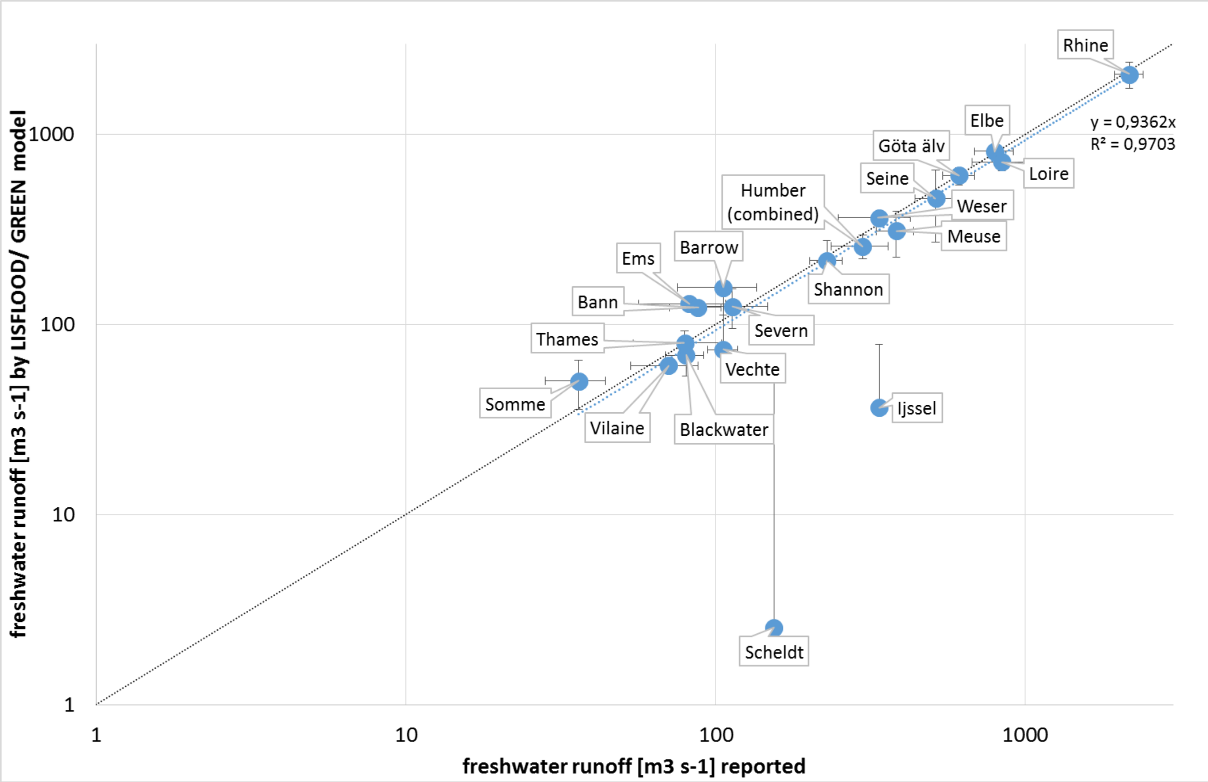

Figure 11: Comparison of reported freshwater runoff [m3 s-1] with LISFLOOD/GREEN model

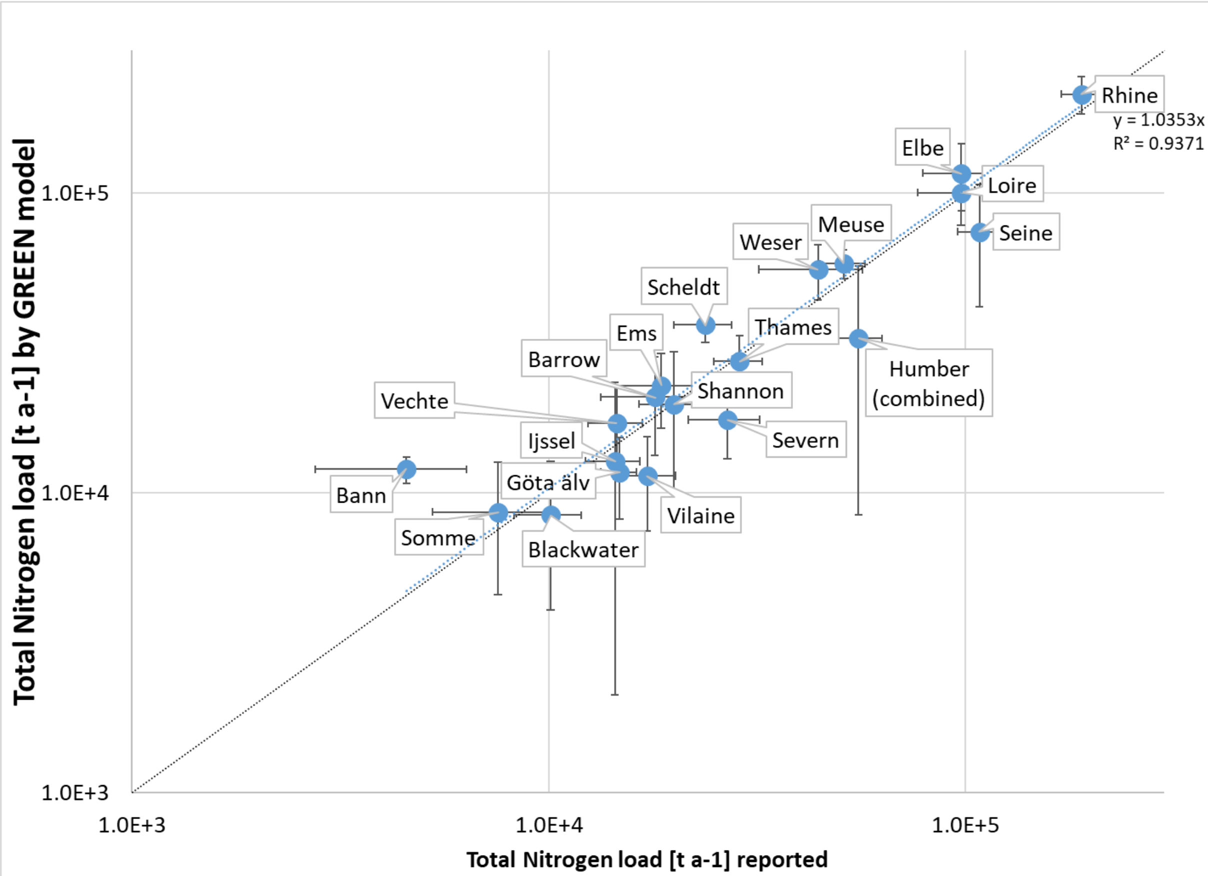

Figure 12: Comparison of reported Total Nitrogen load [t a-1] with GREEN model

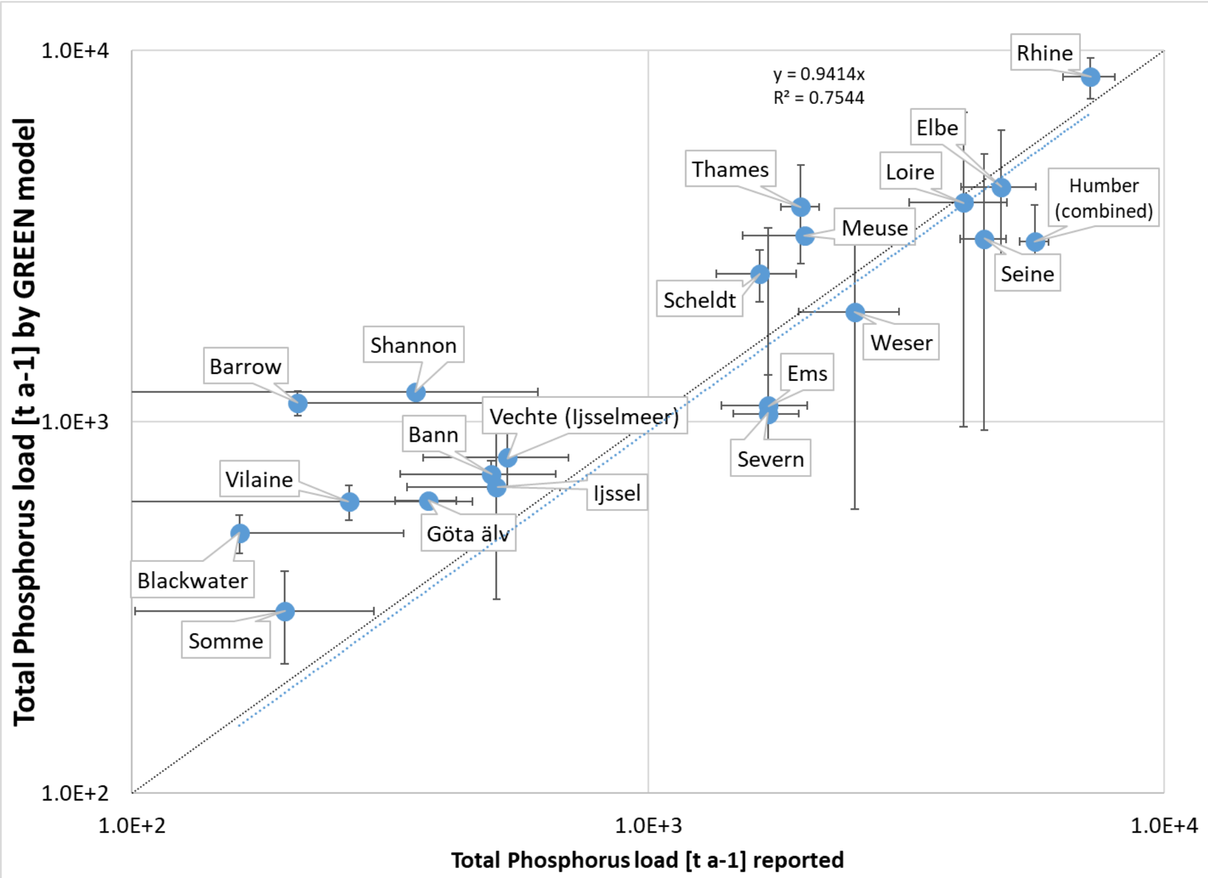

Figure 13: Comparison of reported Total Phosphorus load [t a-1] with GREEN model

2.3 Validation data sets for hydrographical properties

For the calibration and validation of the NWES model, a wide range of observational data sets was used. First, sea gauge data for stations along all coasts (see Figure 14) was taken from EMODnet ([24]) and further processed. Two sets of Sea Surface Temperature (SST) fields derived from satellite data were taken from COPERNICUS. The gap-free 'High Resolution L4 Sea Surface Temperature', reprocessed by IFREMER ([25]) was used with a very high temporal (daily) and spatial resolution (0.04°, see Figure 15a), as well as the ESA CCI SST ([26]) data set based on OSTIA, which has a slightly coarser spatial resolution (0.05°, see Figure 15b). ESA CCI ([27]) (Boutin et al., 2019) is further providing satellite data for the sea surface salinity (see Figure 16). The KLIWAS North Sea Climatology (KNSC ([28]); (Bersch *et al.*, 2013)) was further incorporated. The data set contains the monthly means of water temperature and salinity on a 0.5 × 0.25° grid (79 vertical layers; see Figure 17), but the number of usable observations varies strongly. As the NWES-model has a finer horizontal and temporal resolution, the monthly mean for all cells with a KNSC grid box was computed. Further, the observations collected at the World Ocean Database (WOD ([29])) were processed on a daily basis for the grid cells of the NWES-model (Figure 18) for a straightforward comparison with the model results. Further, at WOD a climatology covering the years 2005-2012 for the Greenland, Iceland and Norwegian Seas (GINS ([30])) is provided on a quite fine horizontal grid of 0.1°.

Following van Leeuwen *et al.* (2015), the North Sea can be divided into five regions according to their vertical density gradients (permanently stratified or mixed, seasonally stratified, intermittently stratified or dominated by freshwater influence). This classification was compared with a model-based estimation of the frequency of stratification (Figure 32).

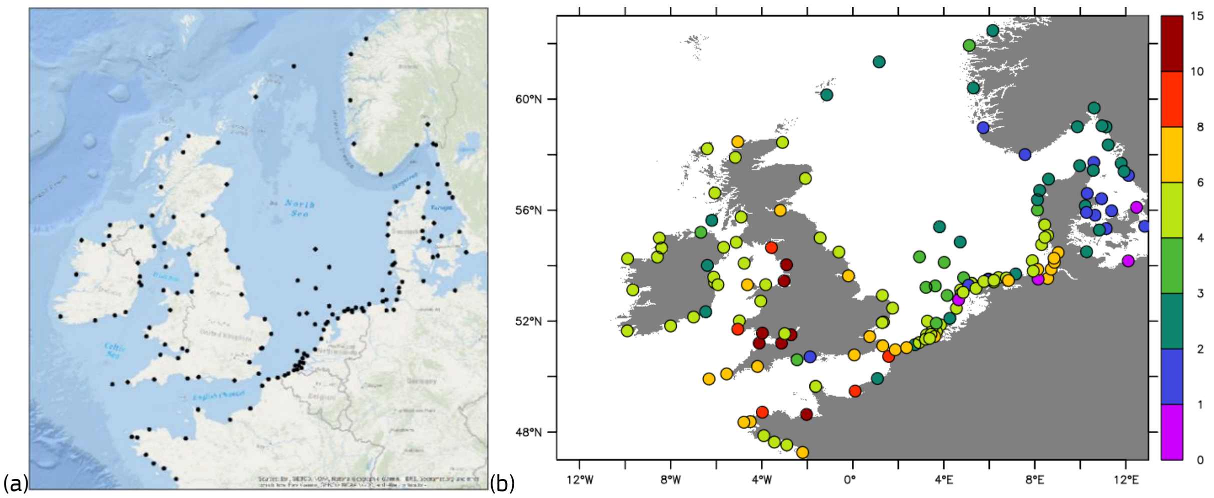

Figure 14: Used gauge stations taken from EMODnet (left) and computed tidal range [m] (right)

([24]) http://www.emodnet-physics.eu/Portal
([25])http://resources.marine.copernicus.eu/?option=com_csw&view=details&product_id=SST_NWS_SST_L4_REP_OBSERVATIONS_010_023
([26]) http://marine.copernicus.eu/services-portfolio/access-to-products/?option=com_csw&view=details&product_id=SST_GLO_SST_L4_REP_OBSERVATIONS_010_024
([27]) http://cci.esa.int/salinity
([28]) https://icdc.cen.uni-hamburg.de/1/daten/ocean/knsc-hydrographic.html
([29]) https://www.nodc.noaa.gov/OC5/WOD/pr_wod.html
([30]) https://www.nodc.noaa.gov/OC5/regional_climate/gin-seas-climate

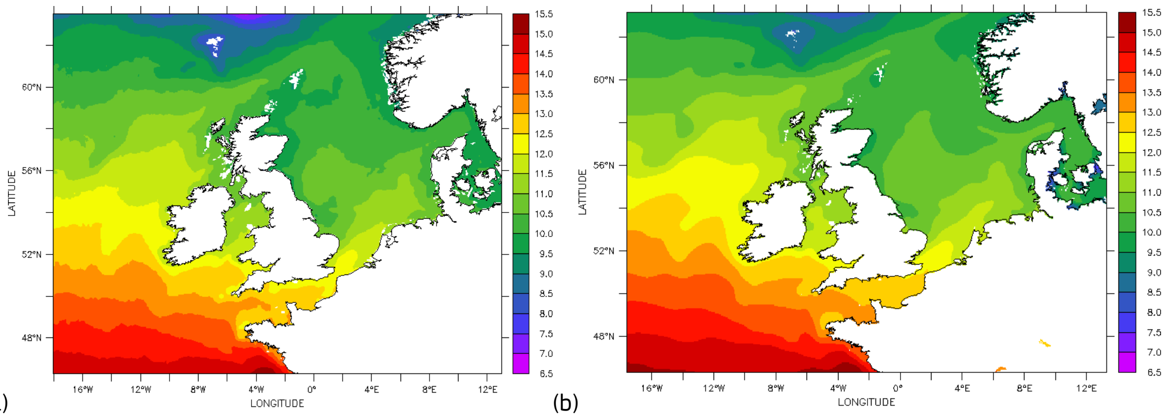

(a) (b)
Figure 15: Average SST derived from satellite data processed by IFREMER (a) and ESA SST CCI project using OSTIA (b)

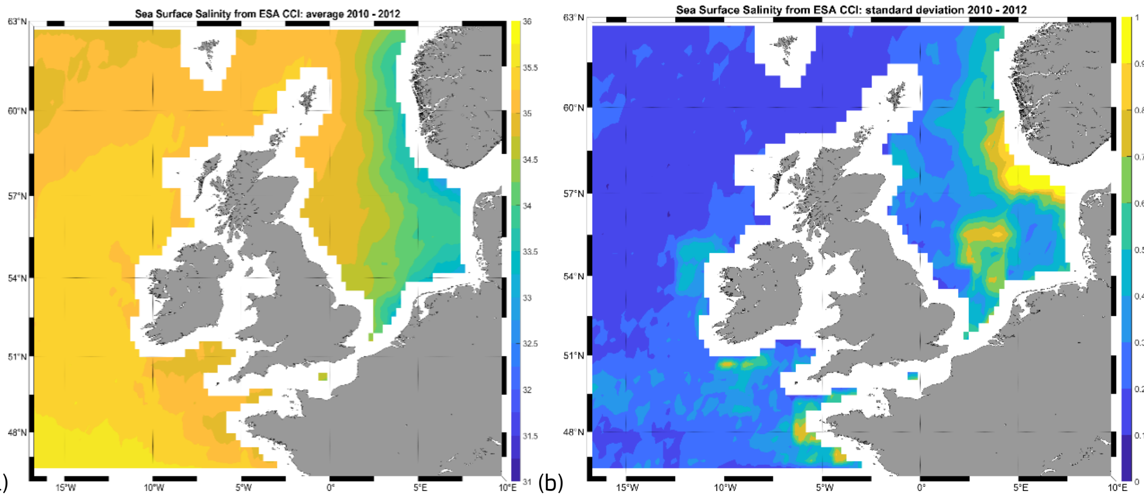

(a) (b)
Figure 16: Average SSS (a) and standard deviation (b) derived from satellite data provided by ESA SST CCI

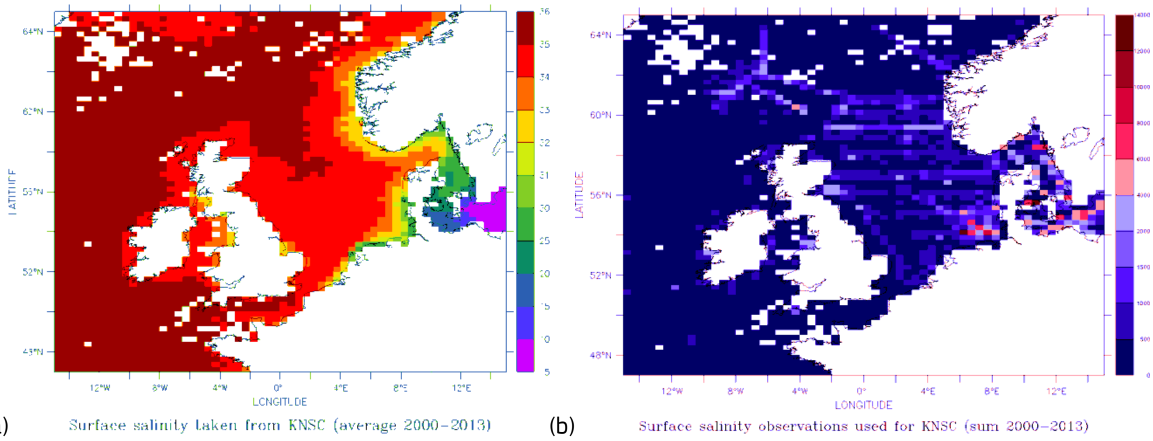

(a) (b)
Figure 17: Average Sea Surface Salinity (a) computed from KNSC and number of observations per grid box (b)

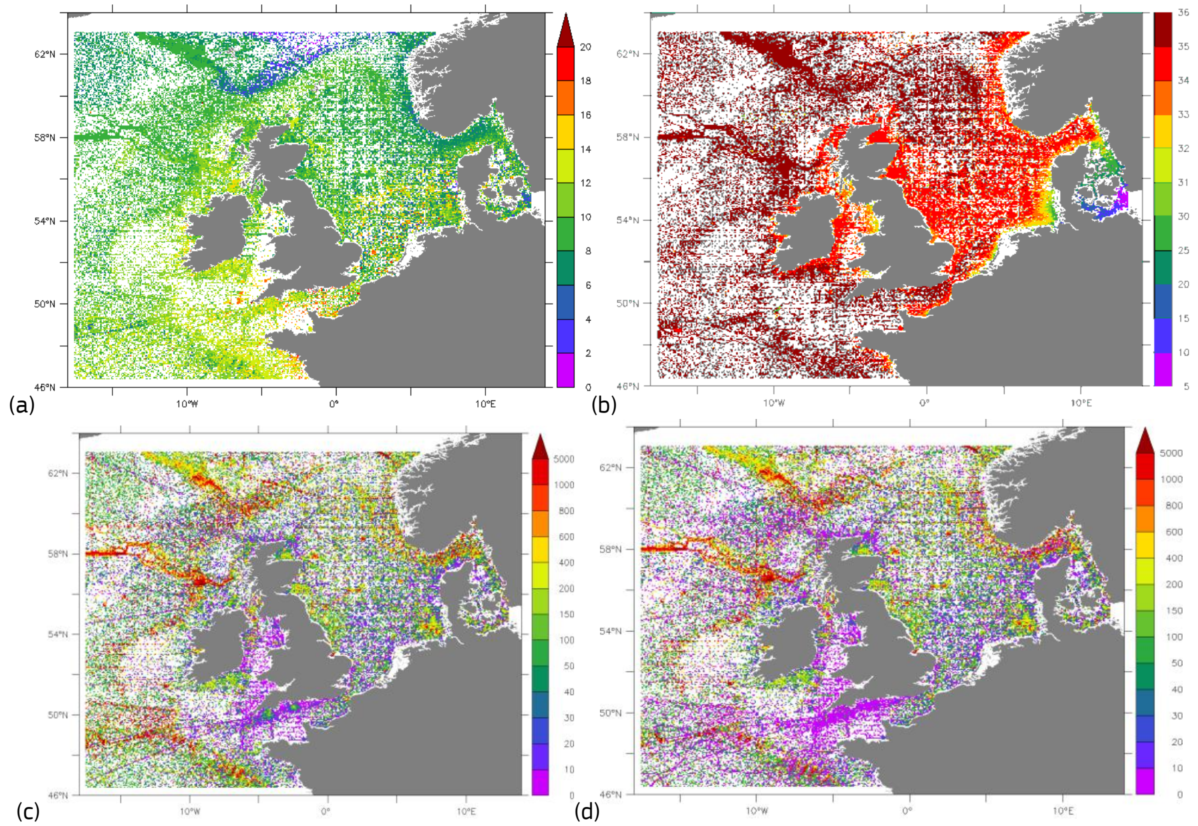

Figure 18: Water temperature (a) and salinity (b) taken from WOD averaged over all depth layers together with number of observations per grid point for water temperature (c) and salinity (d)

2.4 Validation data sets for biogeochemical properties

For the calibration and validation of the biogeochemical part of the NWES model, a wide range of observational data sets was used. Only variables related to indicators of MSFD descriptor 5 (eutrophication) were selected. The used data sets span from single station data, like the WCO long-term monitoring station L4 ([31]) and Helgoland Roads (Wiltshire et al., 2008) taken from PANGAEA ([32]), over publicly available databases, providing raw observations (like ICES database ([33]) or WOD ([34]), which both vary substantially in the distribution of included data, see Figure 20). As the observation provided by the two databases is very scattered, they were merged for 13 regions (AMM7, see Figure 19), as suggested by Edwards et al. (2012) and Wakelin et al. (2012).

Further, the North Sea Biogeochemical Climatology (NSBC ([35]); Hinrichs et al. (2017); see Figure 21) was used, which provides monthly averages for every year (level 2 data), as well as an optimally interpolated monthly climatology (level 3 data). Emodnet Chemistry ([36]) provides another seasonal climatology (but only for the North Sea area, see Figure 22). Two satellite data sets were used to validate the Chlorophyll-a concentrations (see Figure 23). Therefore, monthly averaged data provided at Environmental Marine Information System (EMIS ([37])) and daily data from the Copernicus Marine environment monitoring service ([38]) was used. Due to the different temporal resolution of the two satellite data sets, they vary strongly in the data availability for the model validation (see Figures 23e, f). The comparison with satellite data was extended by including the light attenuation (kd490 taken from EMIS ([39]), see Figure 25), as well as two estimations of the net primary productivity (see Figure 24) taken from COPERNICUS ([40]) and Ocean Productivity ([41]) (VGPM, CBPM, EPPLEY). Both data sets have a decreasing data availability towards North. Finally, the observations gathered within ICES COMPEAT tool (Figures 2, 26) were used, which are currently applied to assess the ecological state of the OSPAR regions.

Following the methods of Edman and Omstedt (2013), the model quality was classified into three groups (excellent, good and improvable). Therefore, the correlation coefficient (R) between observed and modelled concentrations was computed, as well as the root mean square deviation (RMSD), which was divided by the standard deviation from the observation to calculate the value of the cost function (see Figure 34).

([31]) https://westernchannelobservatory.org.uk/l4_nutrients.php
([32]) https://www.pangaea.de
([33]) https://ocean.ices.dk/HydChem/HydChem.aspx?plot=yes
([34]) https://www.nodc.noaa.gov/OC5/SELECT/dbsearch/dbsearch.html
([35]) https://icdc.cen.uni-hamburg.de/1/daten/ocean/knsc-hydrographic0/;
([36]) http://ec.oceanbrowser.net/emodnet-combined/#0
([37]) http://emis.jrc.ec.europa.eu/satellite/2km/EMIS_A_CHLA.xml
([38]) http://marine.copernicus.eu/services-portfolio/access-to-products
([39]) https://data.jrc.ec.europa.eu/dataset/f43226c2-c346-4e3c-9828-86428a16335f
([40]) http://marine.copernicus.eu/services-portfolio/access-to-products/?option=com_csw&view=details&product_id=OCEANCOLOUR_GLO_CHL_L4_REP_OBSERVATIONS_009_082
([41]) http://sites.science.oregonstate.edu/ocean.productivity/index.php

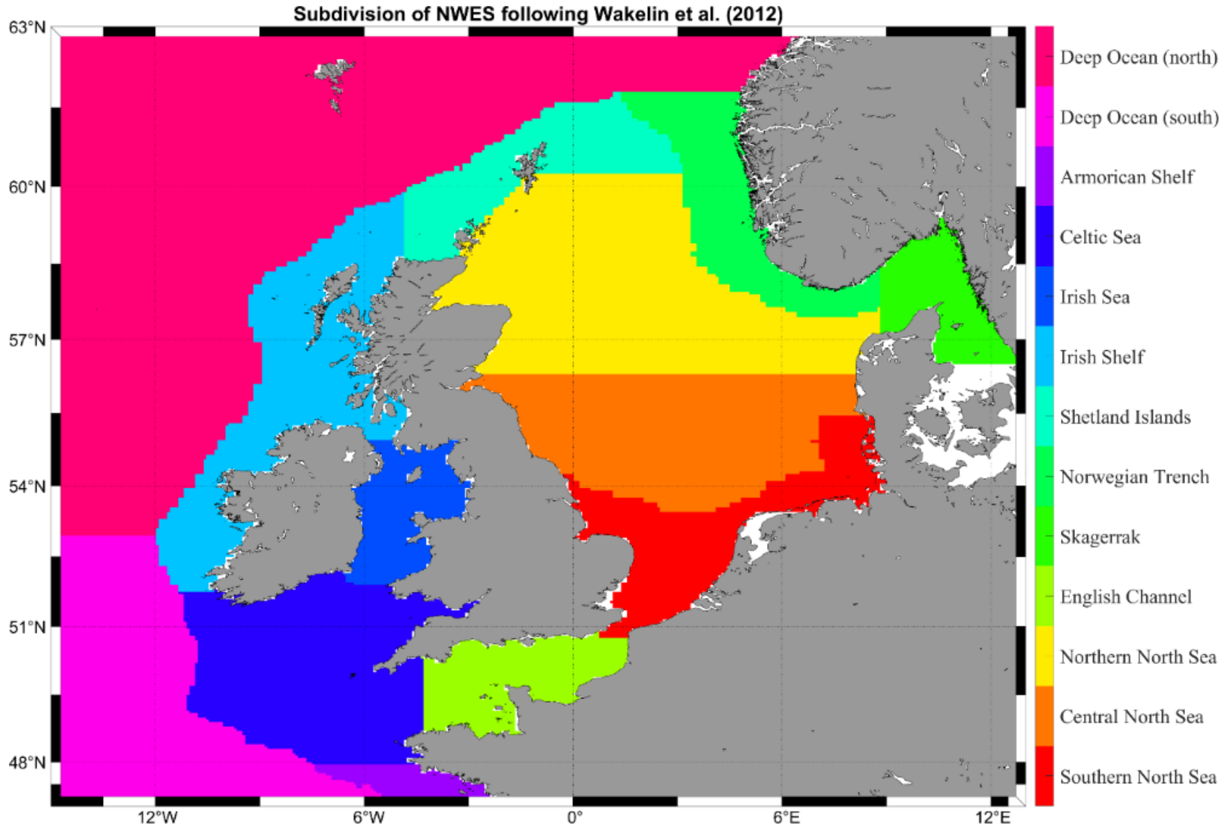

Figure 19: Subdivisions of the NWES region used for the model validation

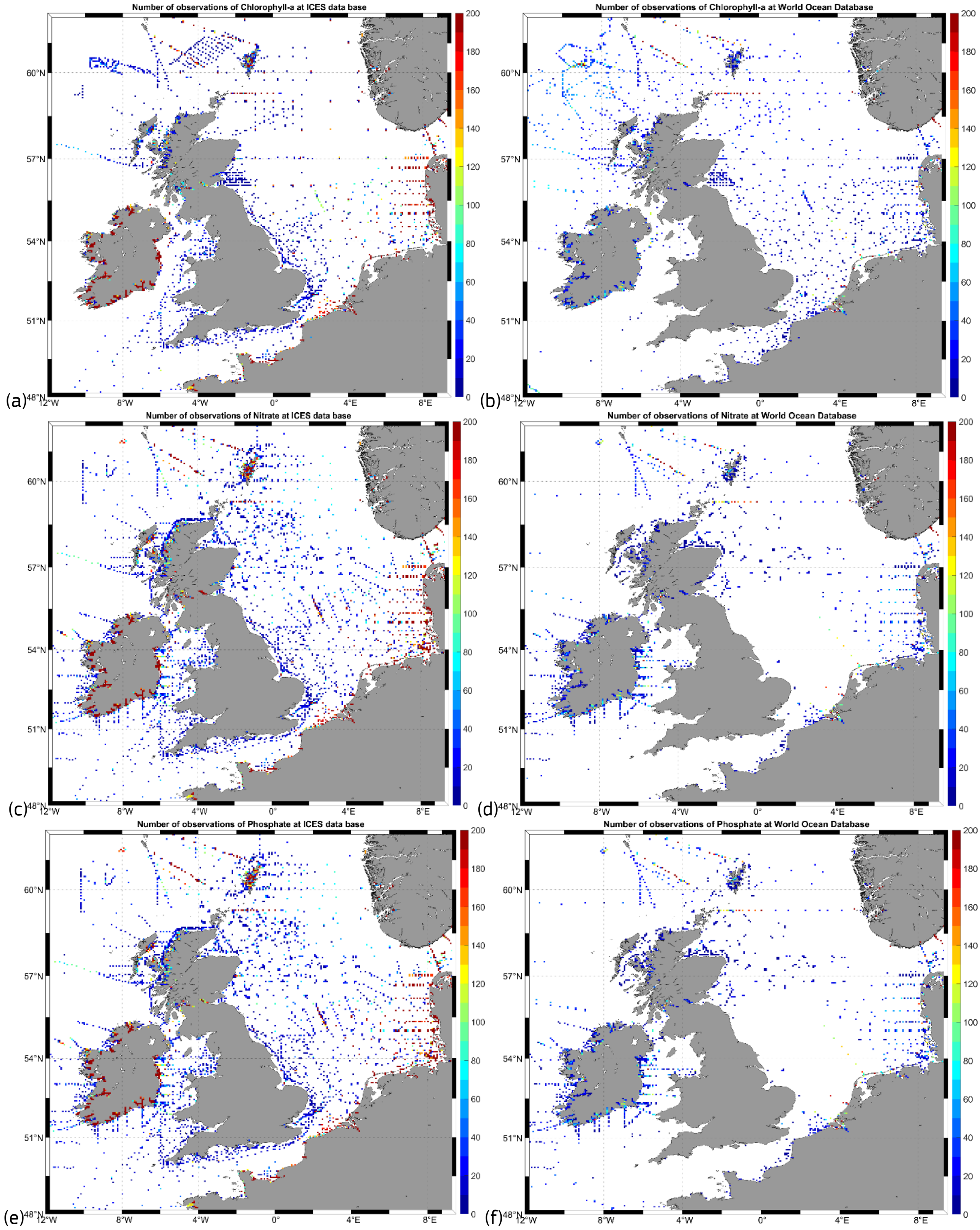

Figure 20: Number of observations for different biogeochemical variables (Chlorophyll-a, Nitrate and Phosphate) from ICES data base (a, c, e) and World Ocean Database (b, d, f)

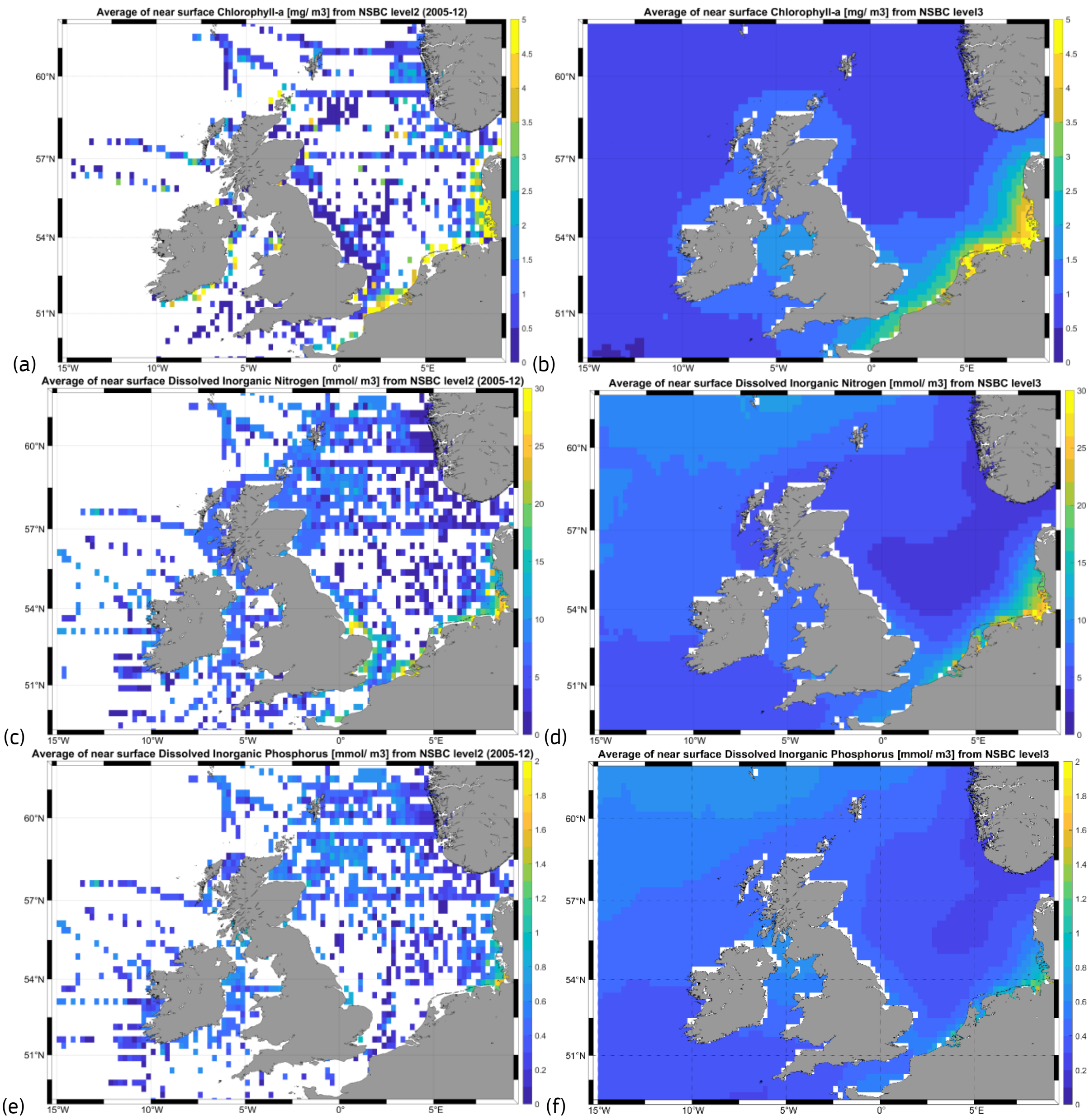

Figure 21: Near-surface concentrations of Chlorophyll-a (a, b), Dissolved Inorganic Nitrogen (c, d) and Phosphate (e, f) taken from NSBC level 2 data (a, c, e) from 2005 to 2012 and from NSBC level 3 climatology (b, d, f)

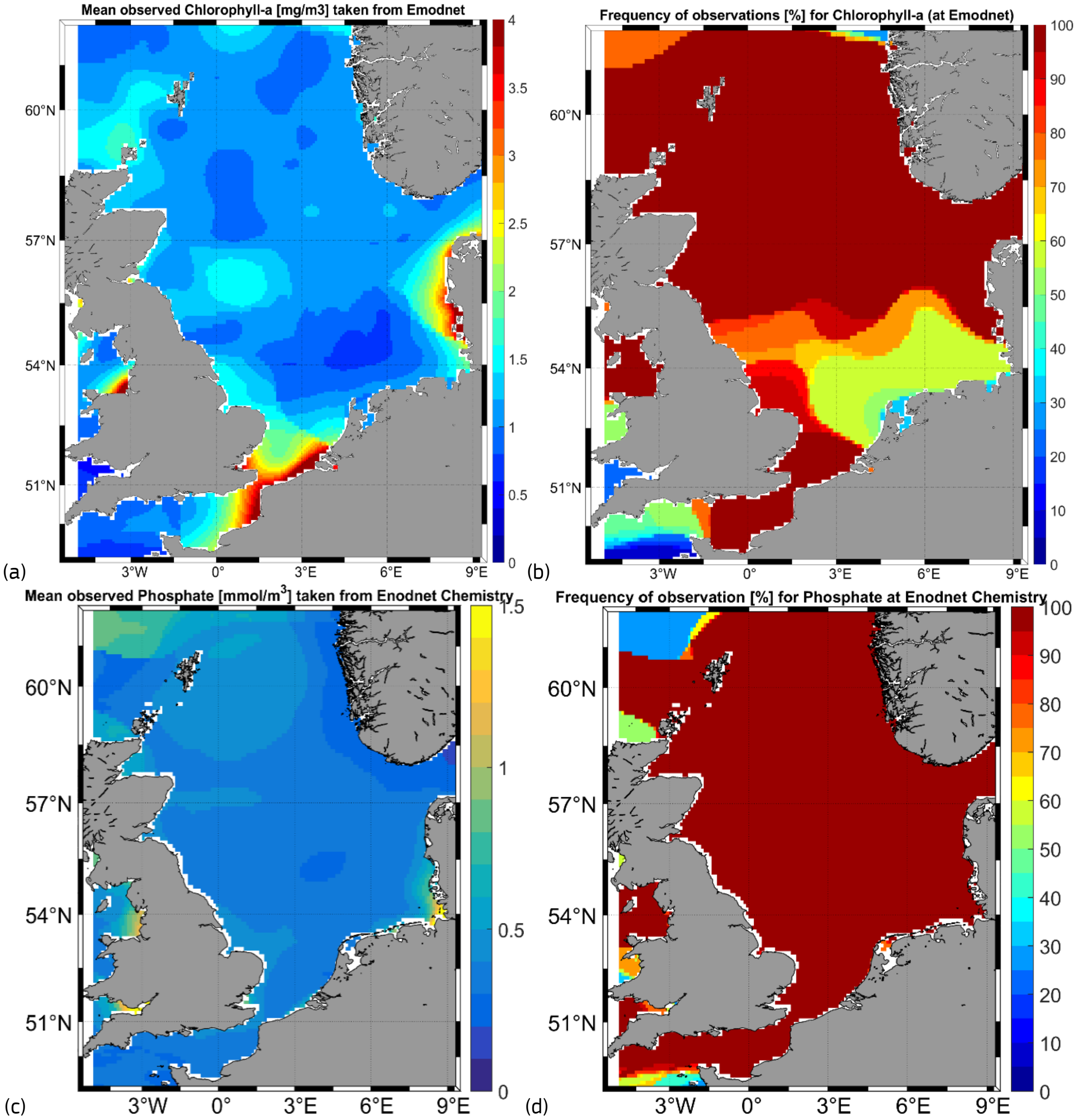

Figure 22: Mean observed Chlorophyll-a concentration (a) and Phosphate (c) taken from Emodnet Chemistry together with the frequency of available observations (b, d) at Emodnet

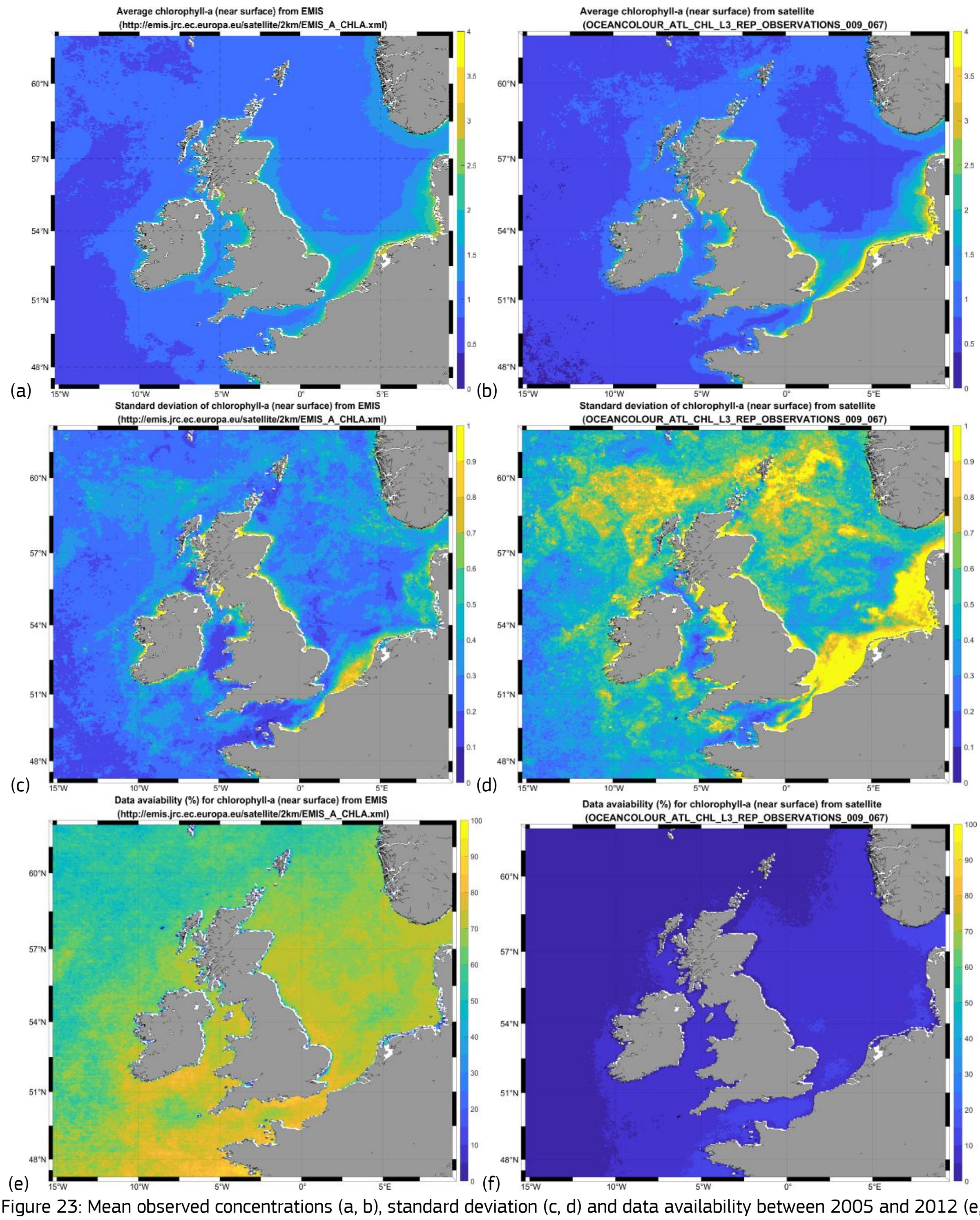

Figure 23: Mean observed concentrations (a, b), standard deviation (c, d) and data availability between 2005 and 2012 (e, f) of Chlorophyll-a taken from two satellite data products (a, c, e from EMIS, b, d, f from COPERNICUS data service)

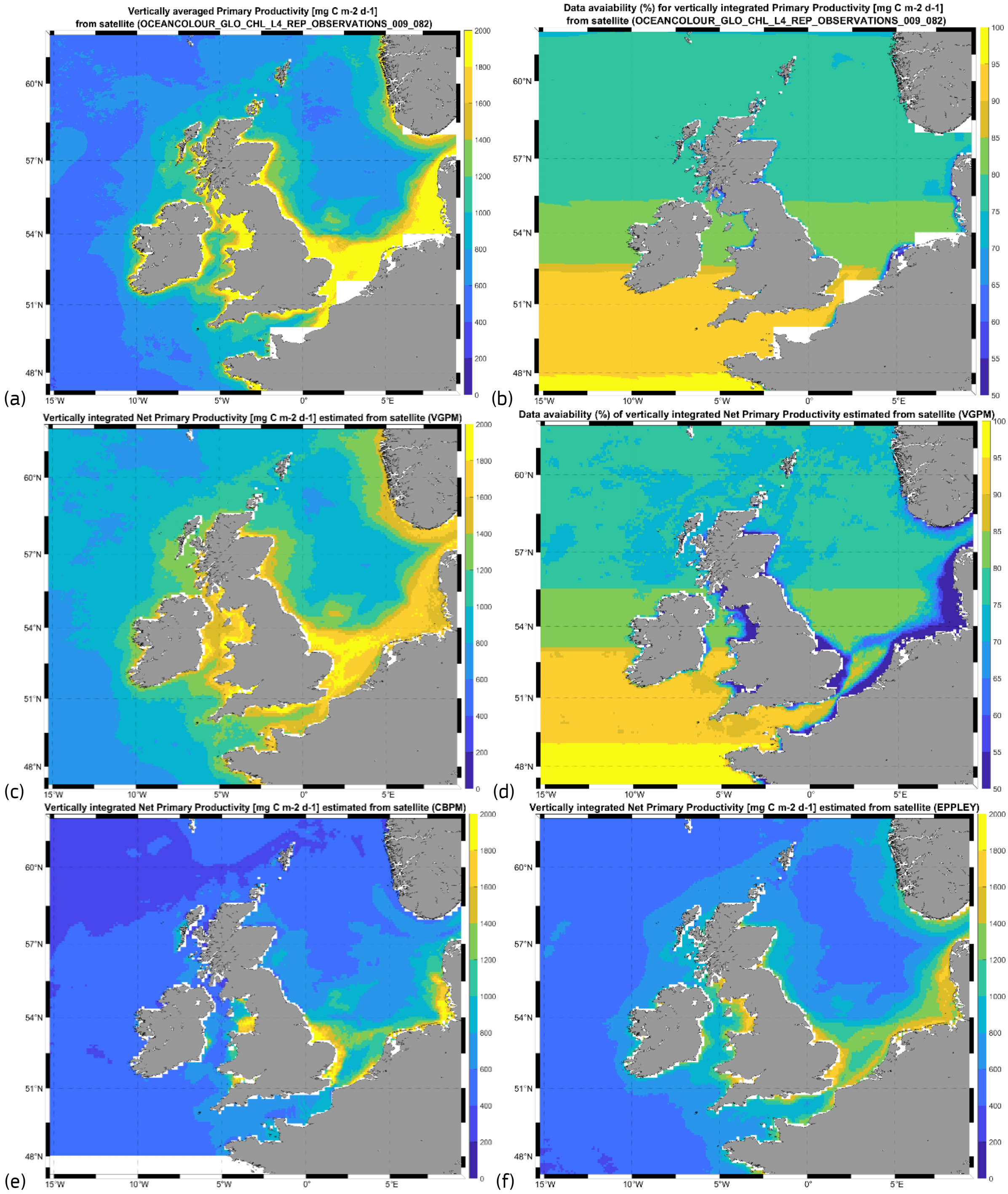

Figure 24: Mean vertically averaged Net Primary Production [mg C m-2 d-1] estimated by COPERNICUS (a) and Ocean Productivity models: (c) VGPM; (e) CBPM; (f) EPPLEY), together with the data availability (b, d)

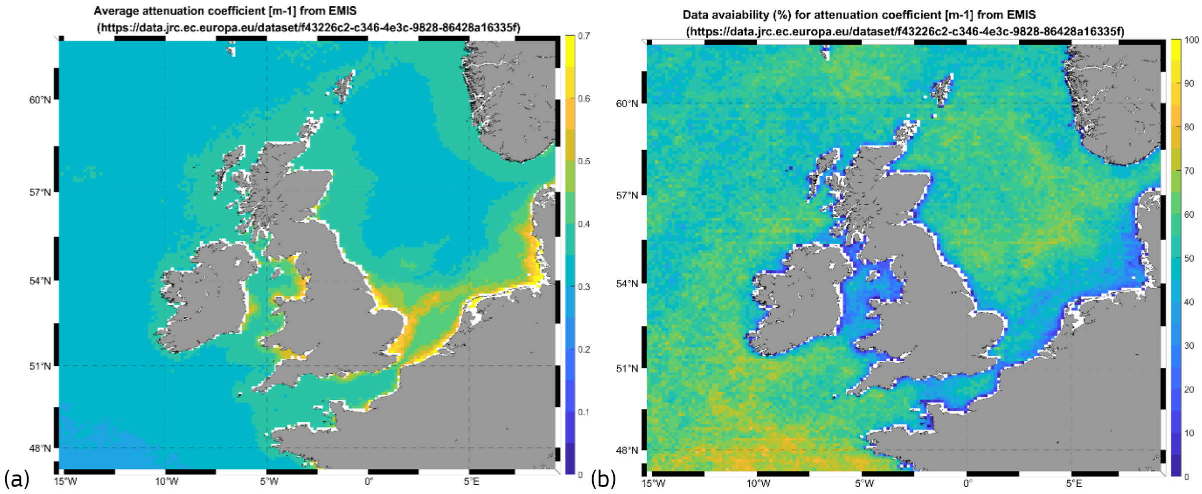

Figure 25: Mean diffuse attenuation coefficient [m-1] at 490 nm taken from EMIS (a) and data availability (b)

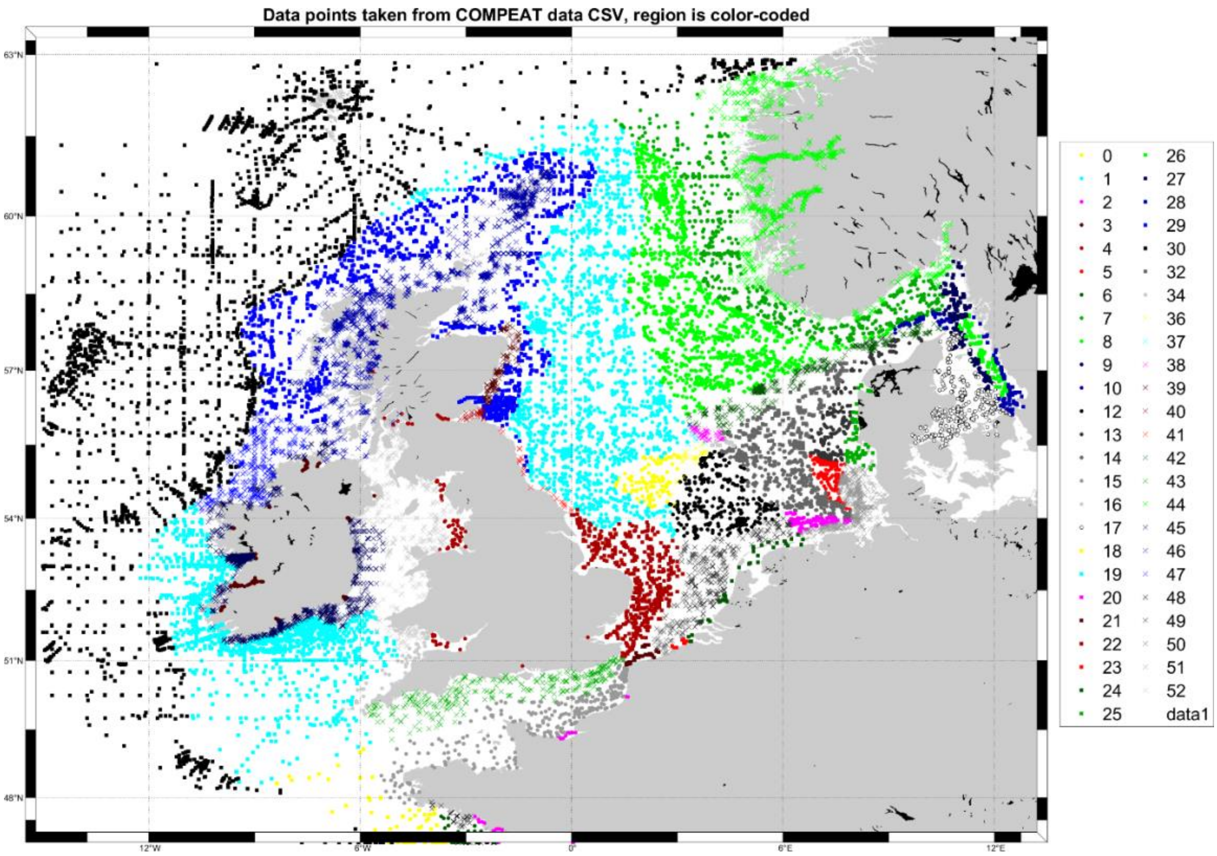

Figure 26: Spatial distribution of the data points within the single assessment units of ICES COMPEAT

3 Results

3.1 Sea surface height compared to gauge data

Compared with the gauge data from EMODnet (see Figure 14), a good agreement between observed and modelled sea surface height (Figure 26) was revealed for the stations, which are dominated by ebb and flood. Stations with a lower tidal range (e.g. along the Danish and Swedish coasts) showed lower correlations (Figure 27), indicating that the model system is well able to reproduce the dominating tides, while the small-scale variations of the sea surface height can be improved in the model. This is also obvious for some stations, especially along the German and UK coast, which are suffering from the coarse horizontal model resolution worsening the model's ability to reproduce complex systems, like Wadden Sea, Severn Estuary or Isle of Islay.

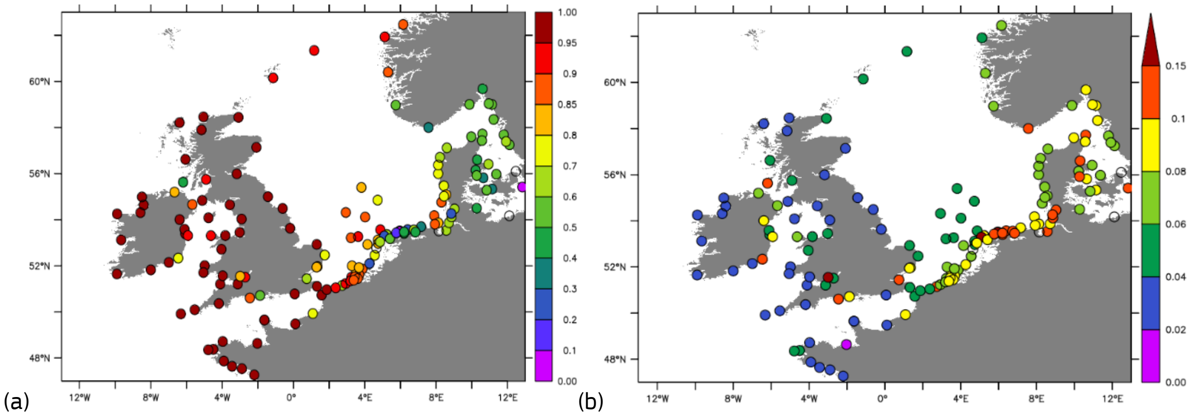

Figure 26: Correlation coefficients (a) and RMSE scaled by the tidal range (b) between modelled and observed sea surface height at the gauge stations taken from EMODnet

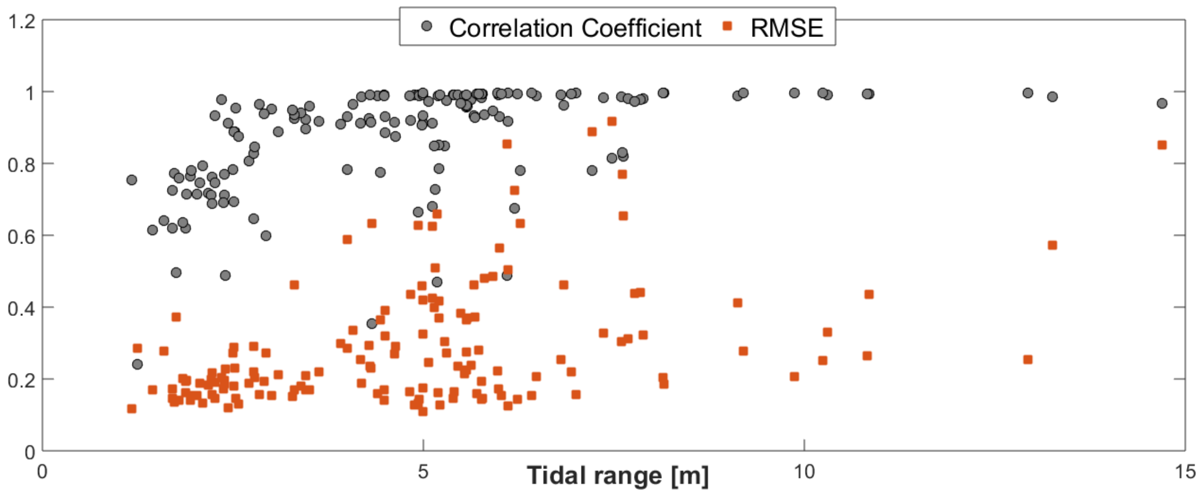

Figure 27: Correlation coefficients (grey) and RMSE scaled by the tidal range (red) as function of the tidal range

3.2 Sea surface temperature (compared to satellite data)

Comparing the modelled SST with satellite data (Figure 15), resulted in a mostly good agreement (indicated by high correlation coefficients: 0.953 for IFREMER and 0.963 for OSTIA), although some regional differences between the two data sets occurred (Figure 28). Lowest correlations occur around the Faroe Islands and along the western coast of Norway. For both data sets, the mean difference averaged over the NWES region is negative (IFREMER: – 0.75K, OSTIA: – 0.40K), indicating that the modelled SST is too high. This is especially the case in the North Sea, Celtic Sea and Irish Sea, while in the deep ocean model SST is slightly too low.

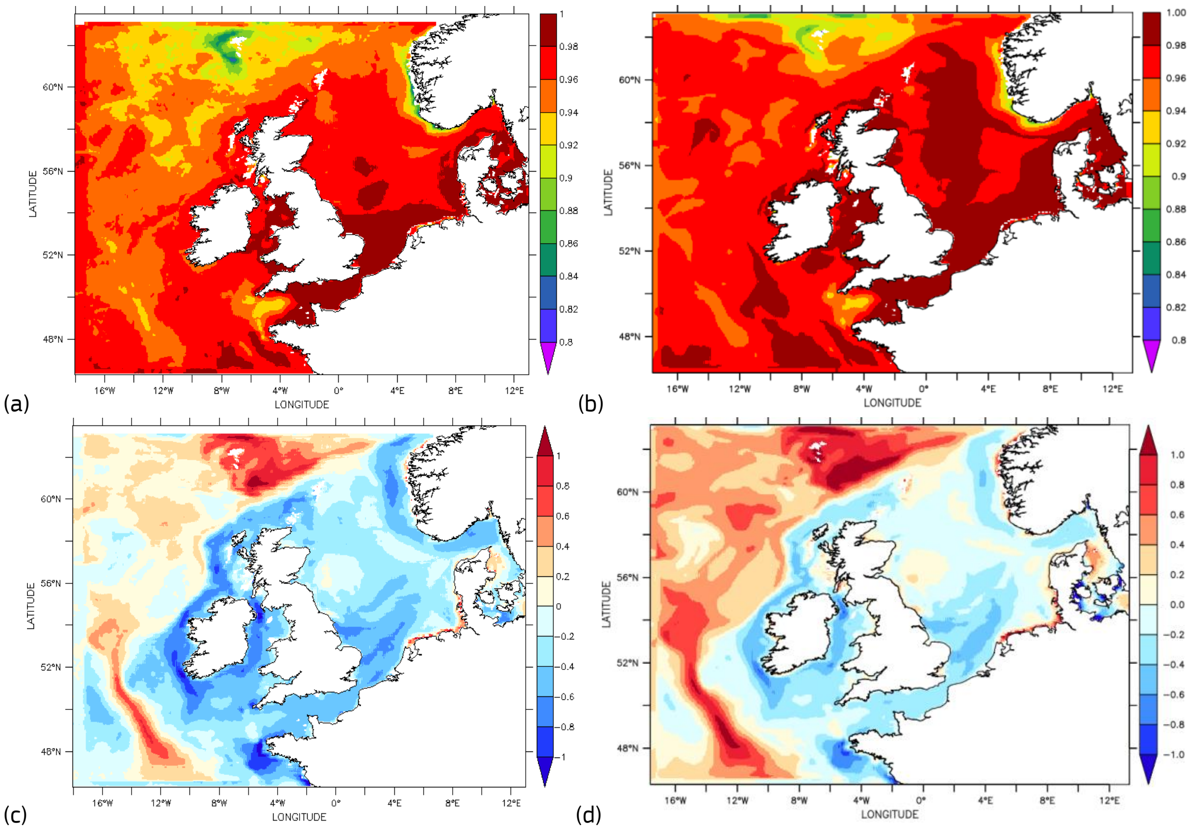

Figure 28: Correlation coefficients (a, b) and mean differences (c, d; in K) between modelled and observed SST taken from IFREMER (a, c) and OSTIA (b, d) accompanied by the mean differences (negative differences denote regions, where the model SST is too high)

3.3 Sea surface salinity (compared to satellite data)

Comparing the modelled SSS with satellite data (Figure 16), resulted in a mostly good agreement (see Figure 29), although some regional differences occur. Correlation is 0.65 and mean difference is approximately – 0.12, indicating that, averaged over the whole region, the modelled salinity is slightly too high. This overestimation occurs especially in the Northern North Sea and the Celtic Sea, while salinity is too low along the east coast of UK and in the eastern part of the North Sea.

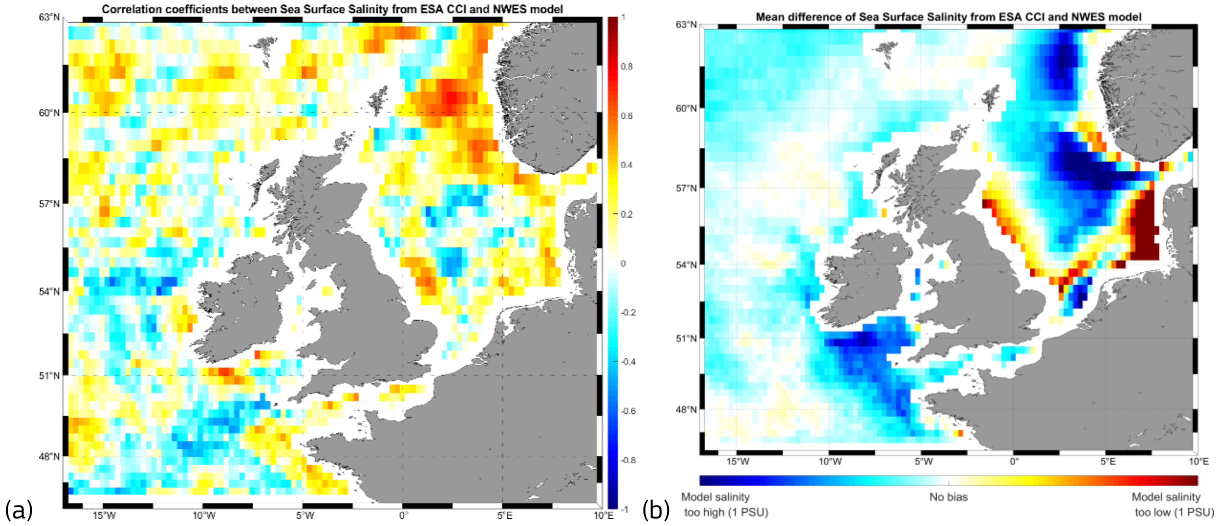

Figure 29: Correlation coefficients (a) and mean differences (b) between modelled and observed SSS taken from ESA SSS CCI (negative differences denote regions, where the model SSS is too high)

3.4 Salinity and temperature compared to climatologies (KNSC and GINS)

As already seen from the SSS comparison (Figure 29), the salinity, especially along the southern and eastern shore of the North Sea, is mostly too low in the model. This is mainly caused by the missing estuaries of Rhine, Elbe or Humber (due to the coarse model resolution), where a substantial mixing of fresh and marine waters takes place. Nevertheless, the overall correlation is still quite high (0.87 if all depths are used, 0.92 for only the surface values), while the mean differences of the vertically averaged salinity (0.15) as well as of the surface salinity (0.46) are positive (see Figure 31). Dominated by the strong annual cycle (Figure 30), the water temperature has an even better correlation (0.97 for KNSC and 0.96 for GINS). It has a small positive bias for both data sets (0.21 K for KNSC and 0.33 K for GINS), occurring mainly in the deep ocean but also in most parts of the North Sea, while modelled water temperature in the south-western North Sea, as well as in the Celtic and Irish Seas is slightly too high (Figure 30). Compared to spatially quite coherent results gained from the satellite data (Figure 28), the comparison with water temperature fields of KNSC is more uneven, as the monthly means are strongly influenced by the available observations for every month, which vary between the grid cells.

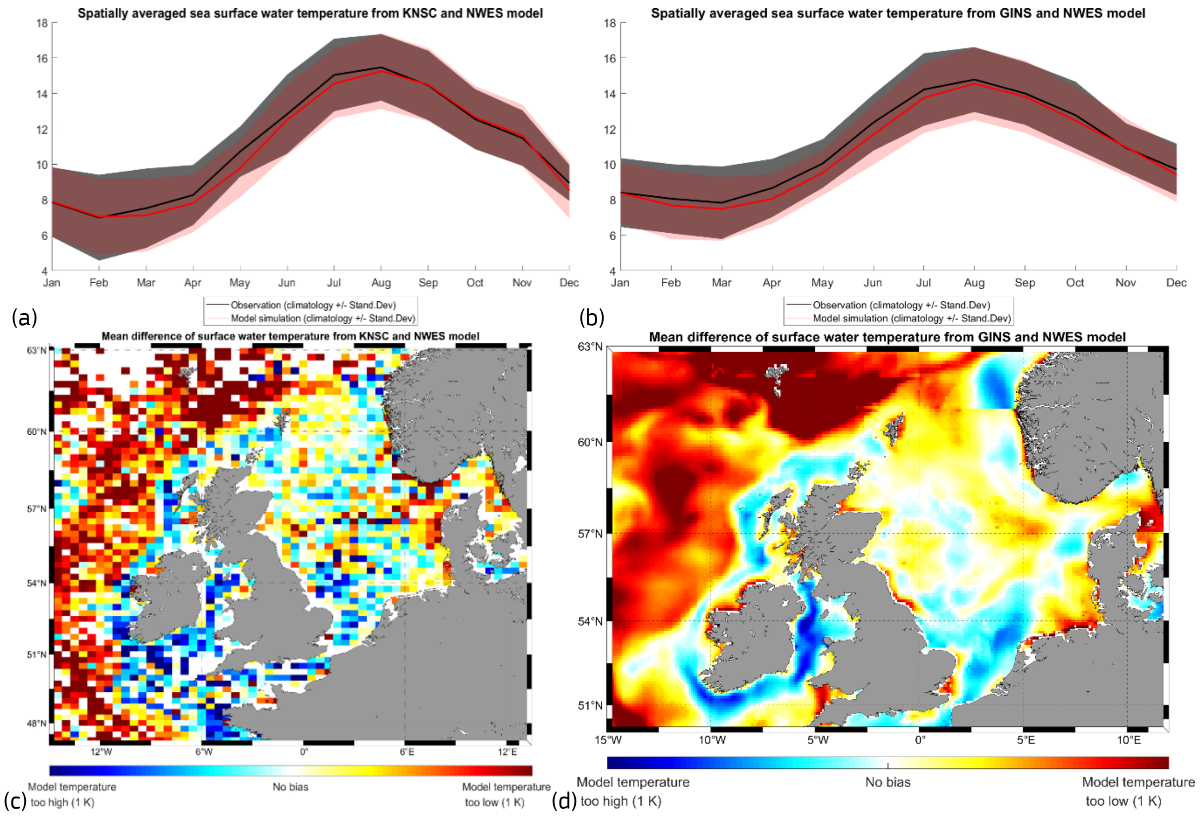

Figure 30: Average sea surface temperature from KNSC data set (black) and NWES model (red) averaged over the region covered by KNSC (a) and GINS (b); and mean differences between observed SST from KNSC (c) and GINS (d) compared to NWES model (negative differences denote regions, where the model SST is too high)

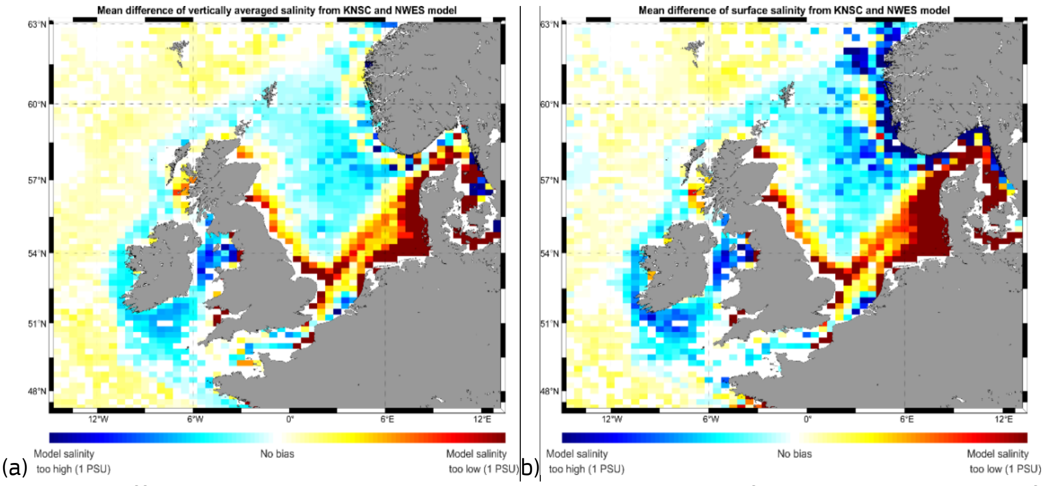

Figure 31: Mean differences between modelled and observed salinity, using data from all depths (a) and only for the surface (b); negative differences denote regions, where the model temperature or salinity are too high)

3.5 Mixing zones and current fields

Comparing the stratification regions as identified by van Leeuwen et al. (2015) with the model results (Figure 32) reveals a good qualitative agreement, except for the seasonally stratified region in the northern part of the North Sea. On the other hand, the permanently mixed and intermittently stratified regions in the English Channel and Southern North Sea are matching well. The prevailing, anti-clockwise current system is well reproduced by the NWES model (Figure 33). There is a strong inflow from the English Channel into the North Sea, as well as through the central northern boundary, while the outflow mainly takes place along the Norwegian coast. In the southern North Sea, the water from the English Channel is mixing with water masses that have been transported along the eastern coast of UK. In the central part of the North Sea, the Dooley current is especially visible in the vertically averaged fields. On the other hand, there is a strong current along the continental shelf west and north of Ireland.

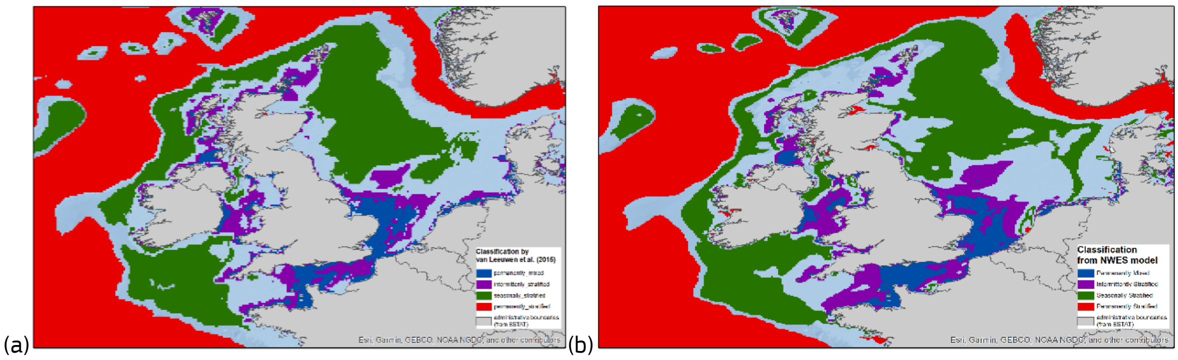

Figure 32: Classification of the North Sea to different stratification regions following van Leeuwen et al. (2015) ((a) as published; (b) calculated from NWES model)

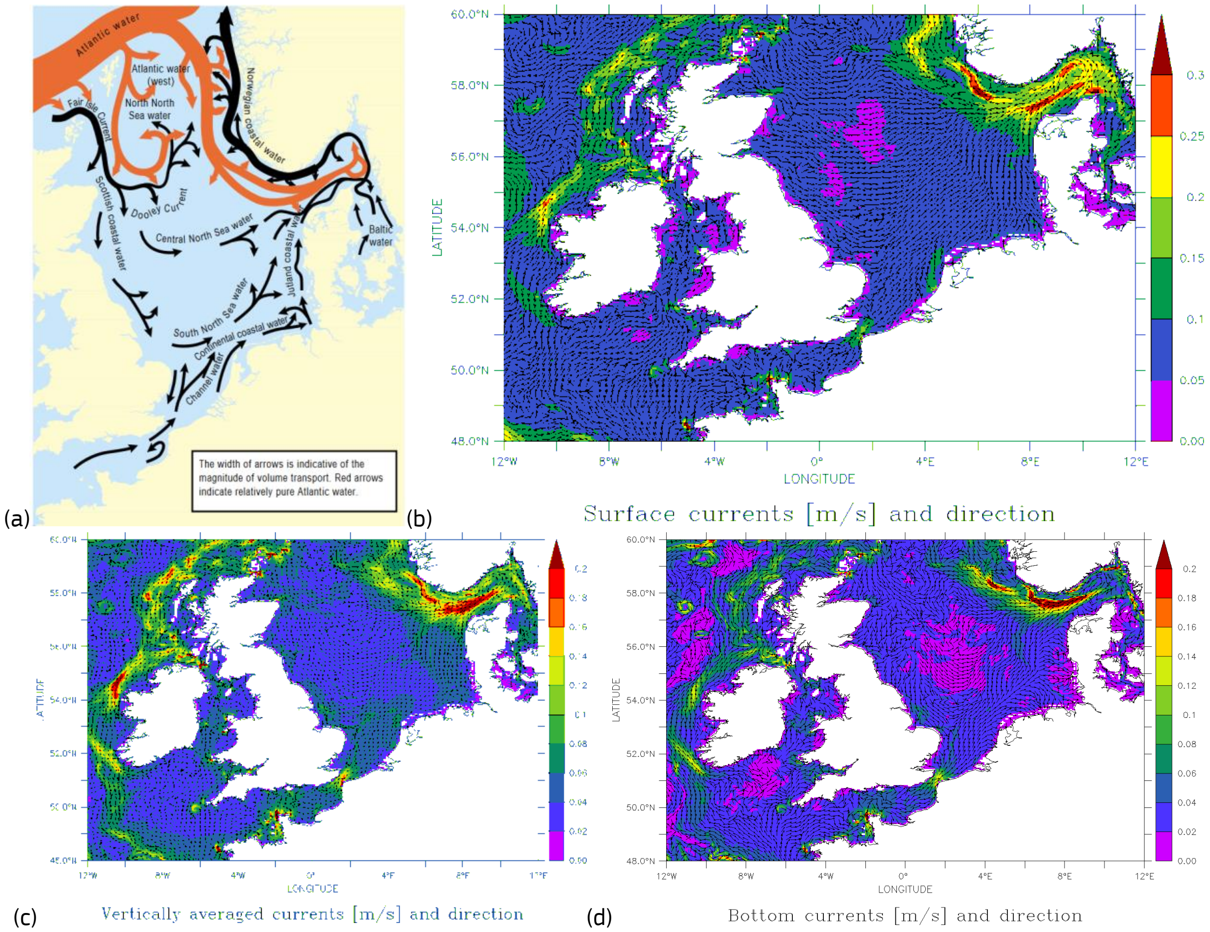

Figure 33: Scheme of the general circulation in the North Sea (a, taken from (OSPAR, 2000)) and mean currents from NWES model at different depth (b) surface, (c) vertically averaged, (d) near-bottom; colour-coded is current speed in m s-1)

3.6 State of MSFD eutrophication indicators

In Figure 34 the NWES model quality is shown for the validation of all biogeochemical variables in comparison to all data sets presented afterwards. The results differ strongly for each variable and between the different observations. The best results are achieved for Phosphate and Chlorophyll-a, while Ammonium, Nitrate and Silicate are mostly improvable.

The average over the whole simulation period (2005-2012) of the central eutrophication indicators Chlorophyll-a, Dissolved Inorganic Nitrogen (DIN, sum of Ammonium and Nitrate) and Phosphate are presented in Figures 35-37. All show strong spatial gradients, with highest values along the southern and eastern shore of the North Sea and along the UK coast. All three near-surface indicators follow strong annual cycles (Figure 38). While the nutrient concentrations reach their annual maximum values during winter season, Chlorophyll-a concentrations are highest during spring (North Sea) and summer (Celtic Sea). The vertical averaged concentrations show less developed annual cycles.

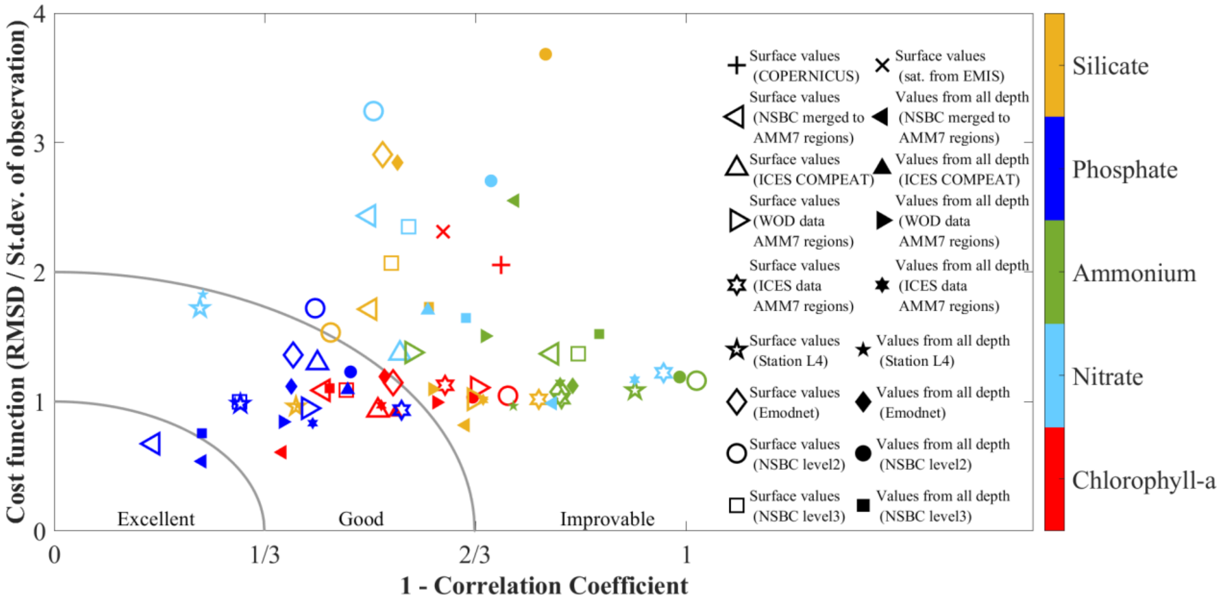

Figure 34: Classification of the validation results for the main biogeochemical variables (colour-coded) following Edman et al. (2013) using all data sets

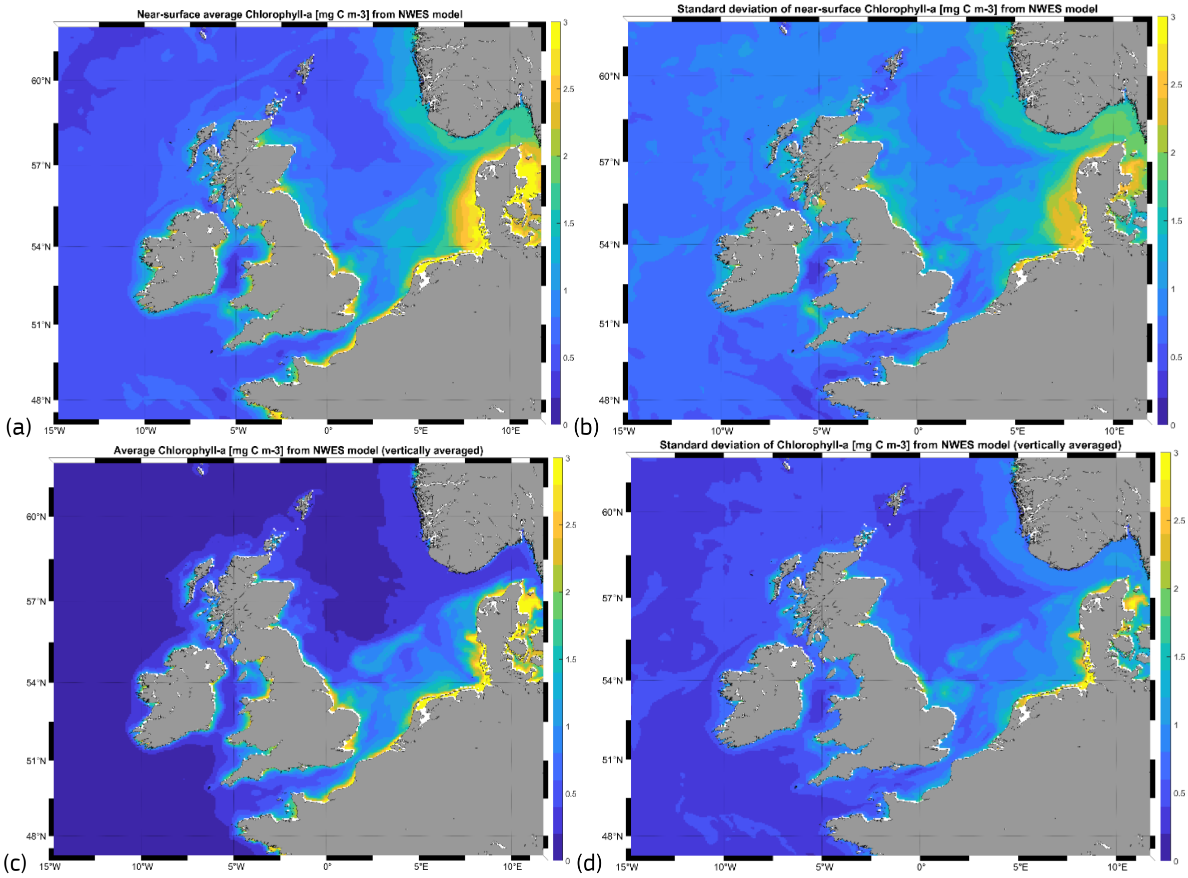

Figure 35: Average Chlorophyll-a concentration [mg m-3] from NWES model near the surface (a) and vertically averaged (c) together with the standard deviation (b, d)

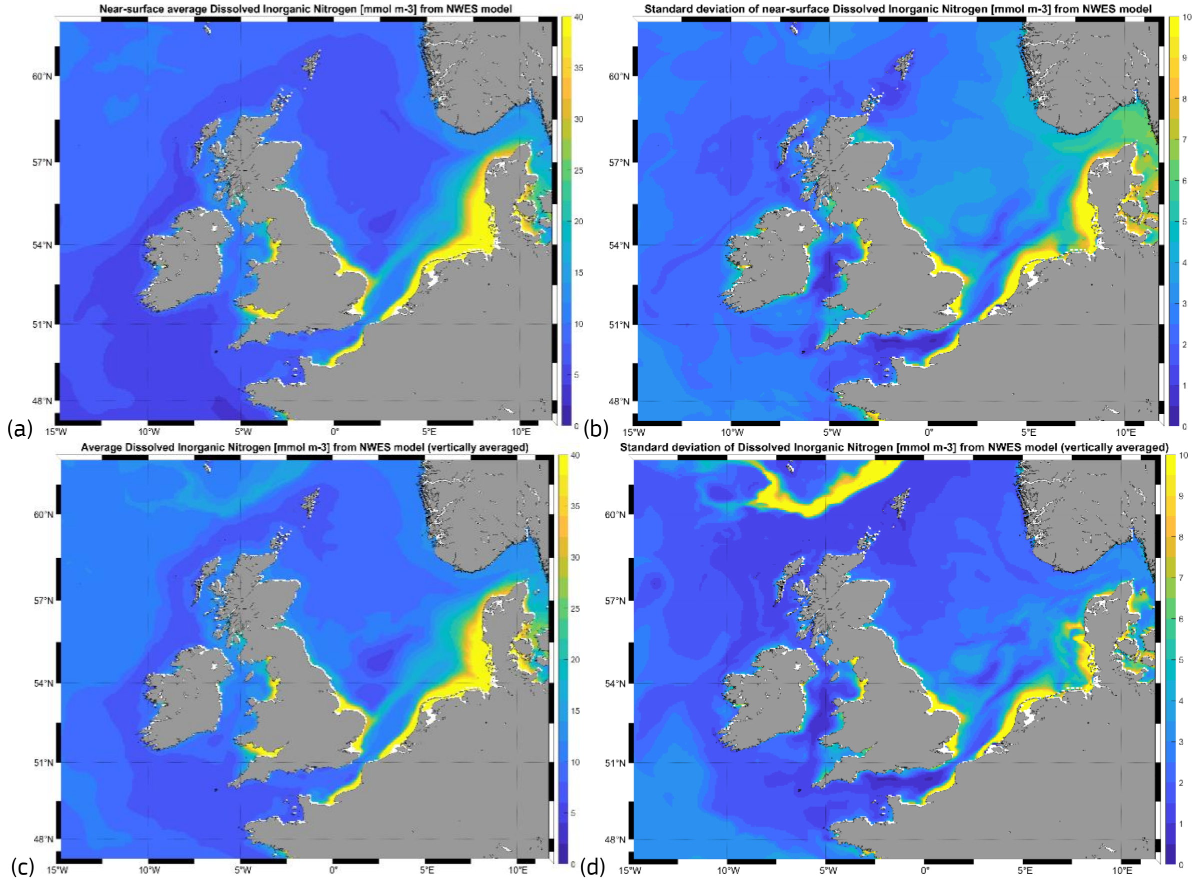

Figure 36: Average DIN concentration [mmol m-3] from NWES model near the surface (a) and vertically averaged (c) together with the standard deviation (b, d)

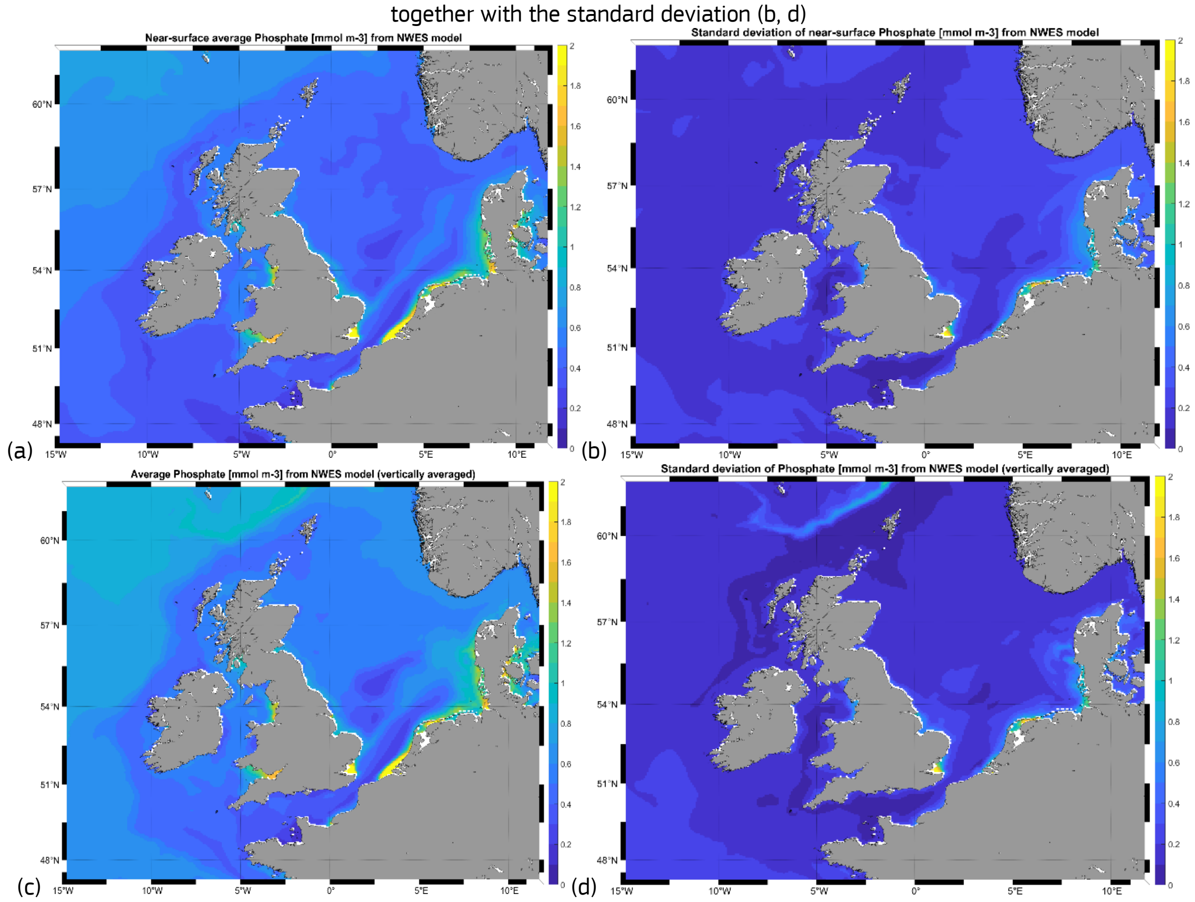

Figure 37: Average Phosphate concentration [mmol m-3] from NWES model near the surface (a) and vertically averaged (c) together with the standard deviation (b, d)

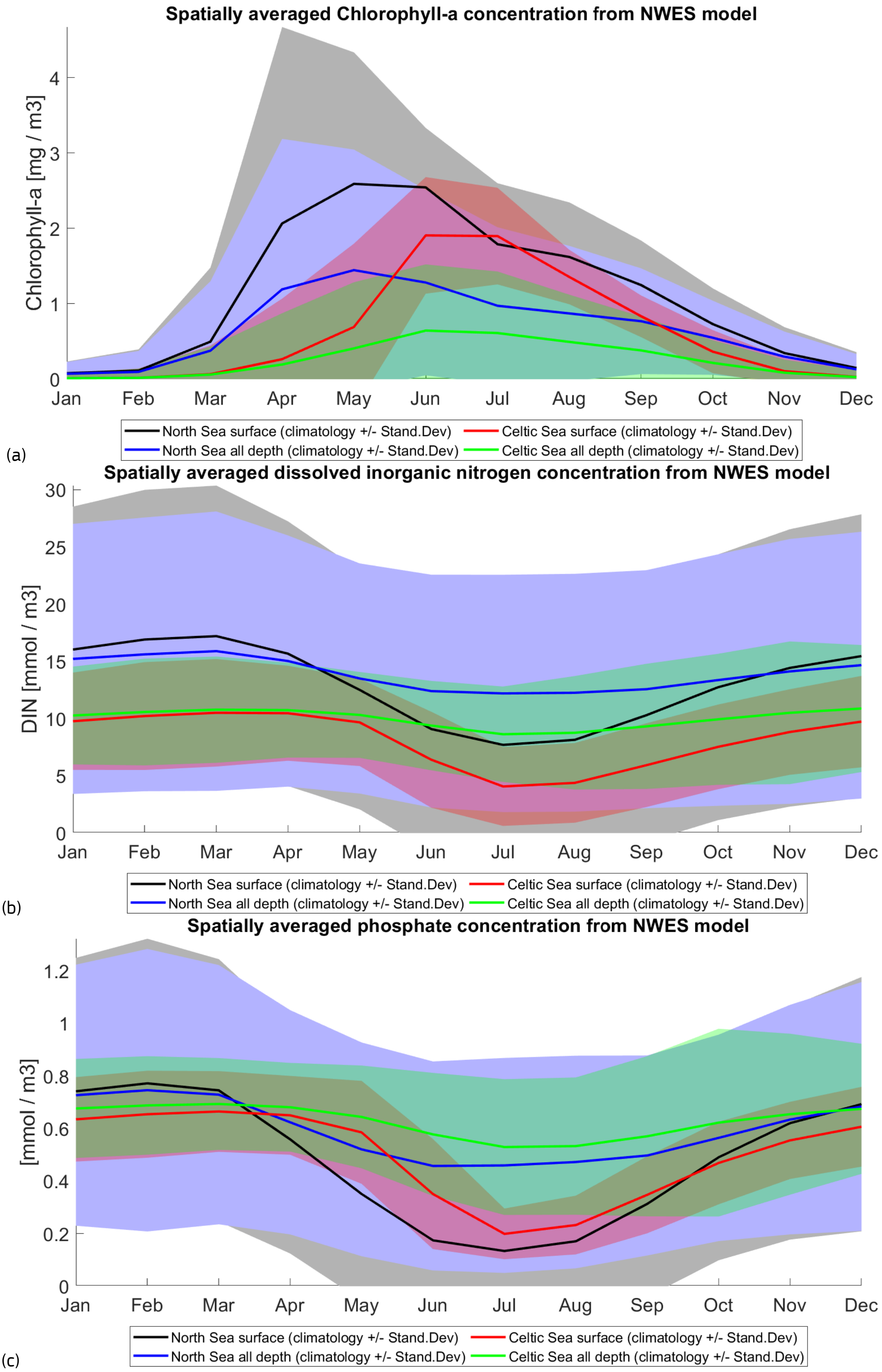

Figure 38: Climatology of concentrations of Chlorophyll-a (a), Ammonium + Nitrate (b) and Phosphate (c) averaged for North Sea and Celtic Sea using only surface values and all depths

3.7 Seasonal climatologies

Using the seasonal climatologies provided by Emodnet Chemistry to compare with the model results (see Figure 39), revealed a good agreement for Chlorophyll-a and Phosphate, while Ammonium and Silicate are improvable. Comparing to the model results with observations gathered by NSBC level 3 data, resulted in high correlation coefficients for all assessed variables (Figures 40, 41, 42), indicating that the seasonal cycles are well reproduced. The only exception is Chlorophyll-a in the central North Sea, where correlations are quite low. The assessment revealed only little differences of the model quality if all depths are evaluated or only near-surface values. Overall, the difference between observed and modelled Chlorophyll-a concentration is positive (Figures 40(b), (d)). This indicates that the model values are too low, especially in the Irish Sea and the southern North Sea (this is opposite to the comparison result from Emodnet Chemistry, see Figure 39(a)). While the phosphate concentration difference is mostly around 0 (Figure 41), DIN concentrations in the model have a strong bias with too high values at NWES model. This is especially the case in the southern and eastern North Sea, where DIN concentrations should be strongly reduced due to denitrification taking place in the sediments, which is missing in the present model setup.

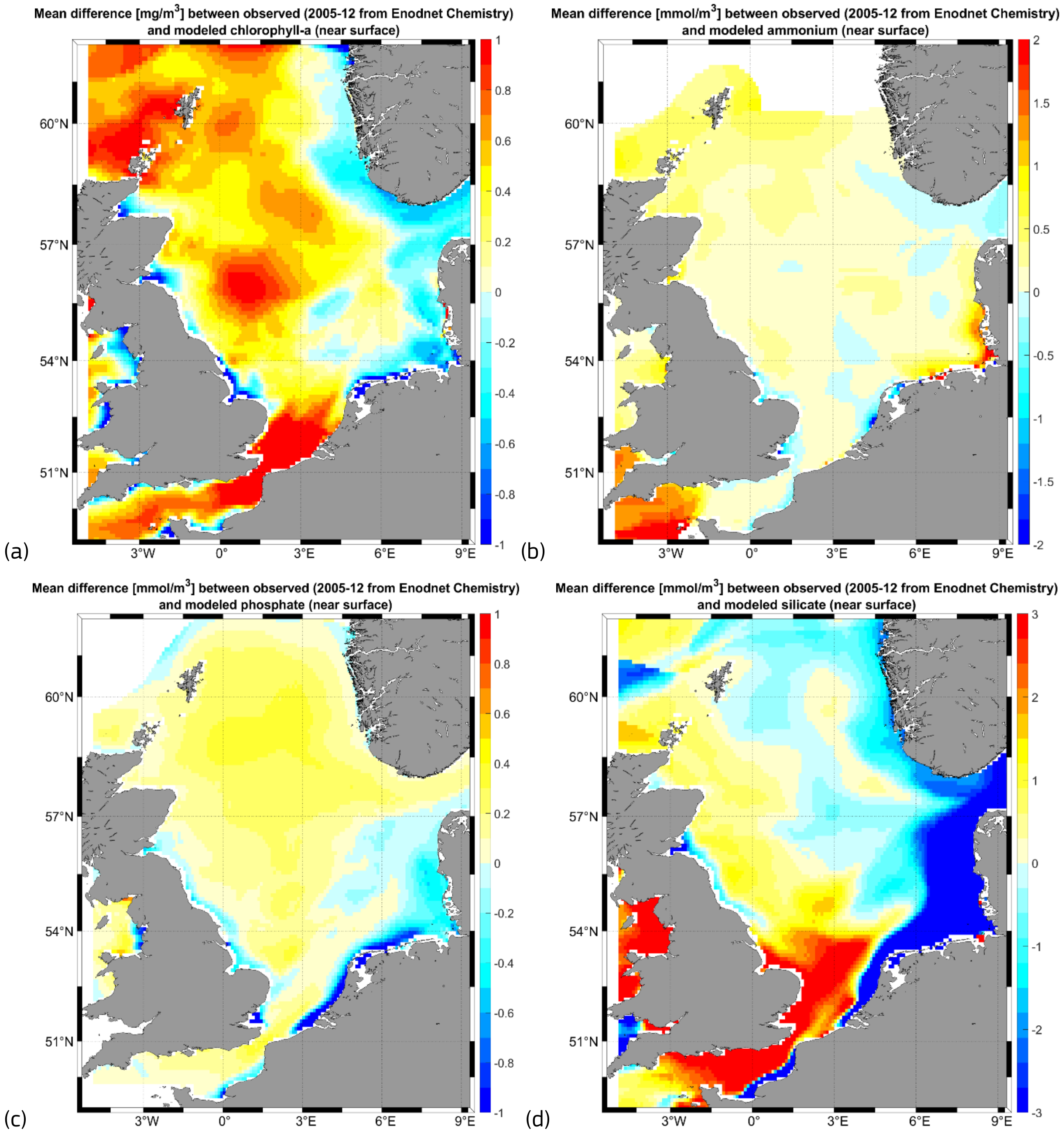

Figure 39: Mean differences between observed concentrations (taken from Emodnet Chemistry) and modelled ones, evaluated for Chlorophyll-a (a), Ammonium (b), Phosphate (c) and Silicate (d) [negative differences denote regions, where the model concentrations are too high]

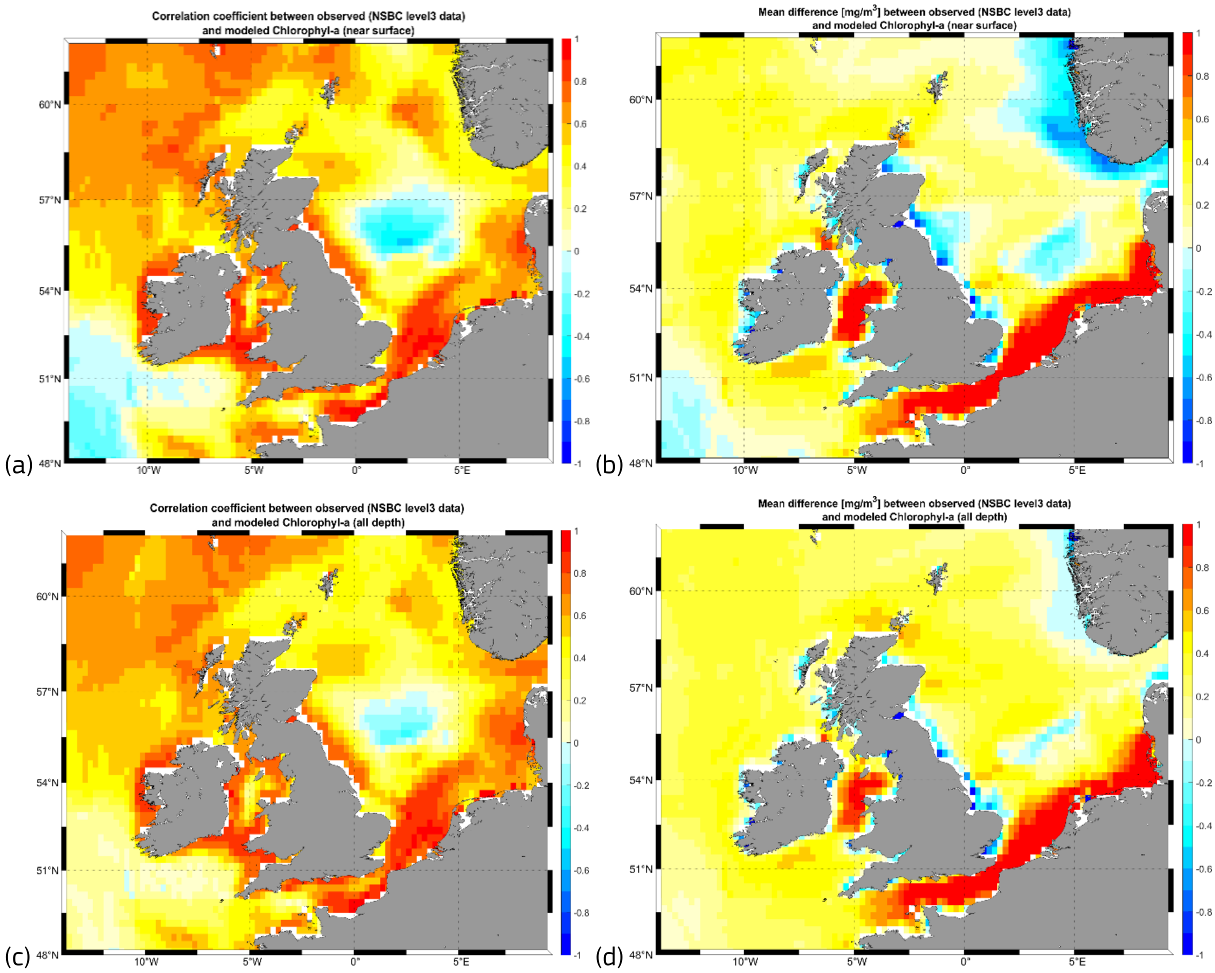

Figure 40: Correlation (a, c) and mean differences (b, d) between observed Chlorophyll concentration (taken from NSBC level 3) and modelled ones, evaluated for near-surface values (a, b) and for all depth layers (c, d) [negative differences denote regions, where the model concentrations are too high]

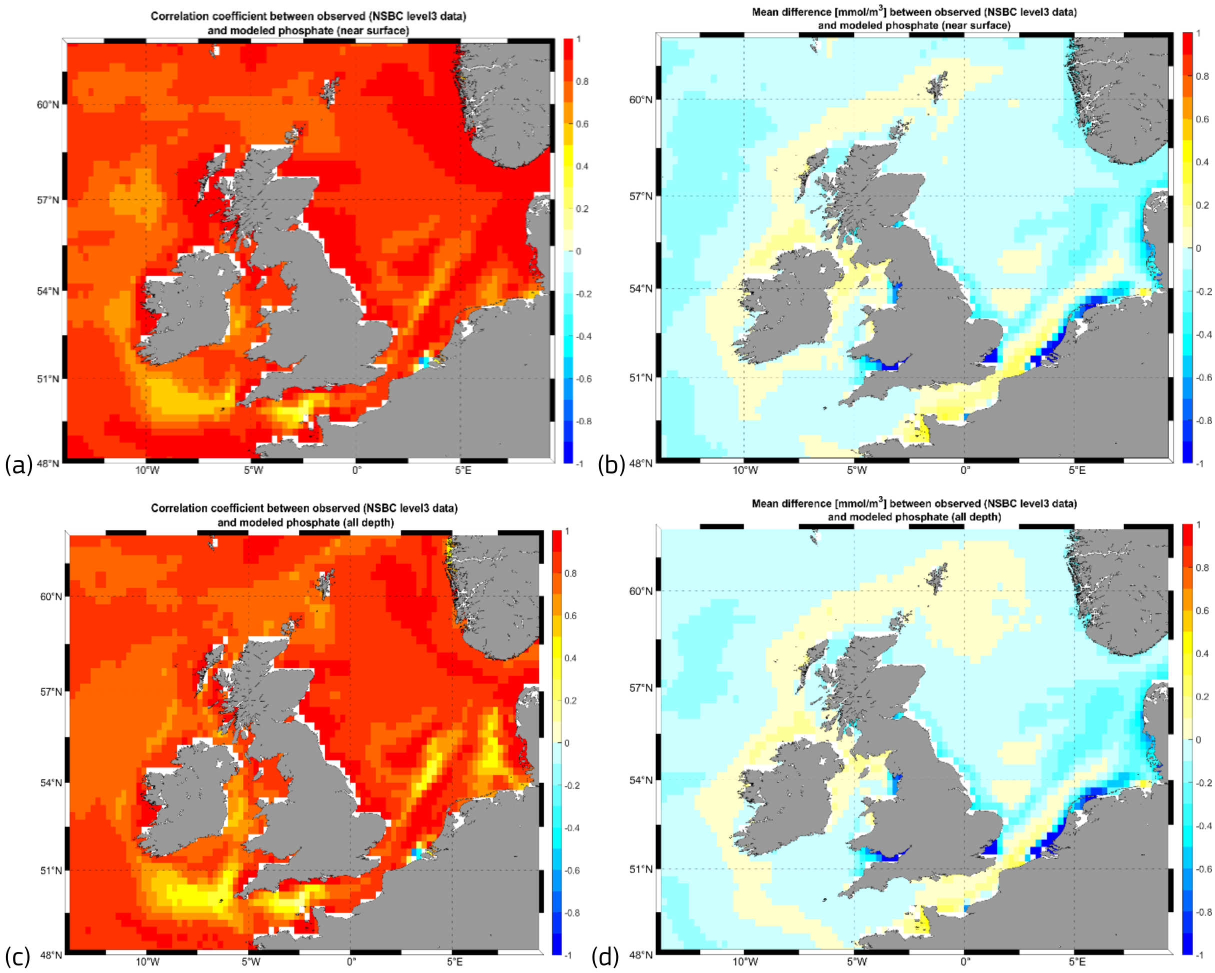

Figure 41: Correlation (a, c) and mean differences (b, d) between observed Phosphate concentration (taken from NSBC level 3) and modelled ones, evaluated for near-surface values (a, b) and for all depth layers (c, d) [negative differences denote regions, where the model concentrations are too high]

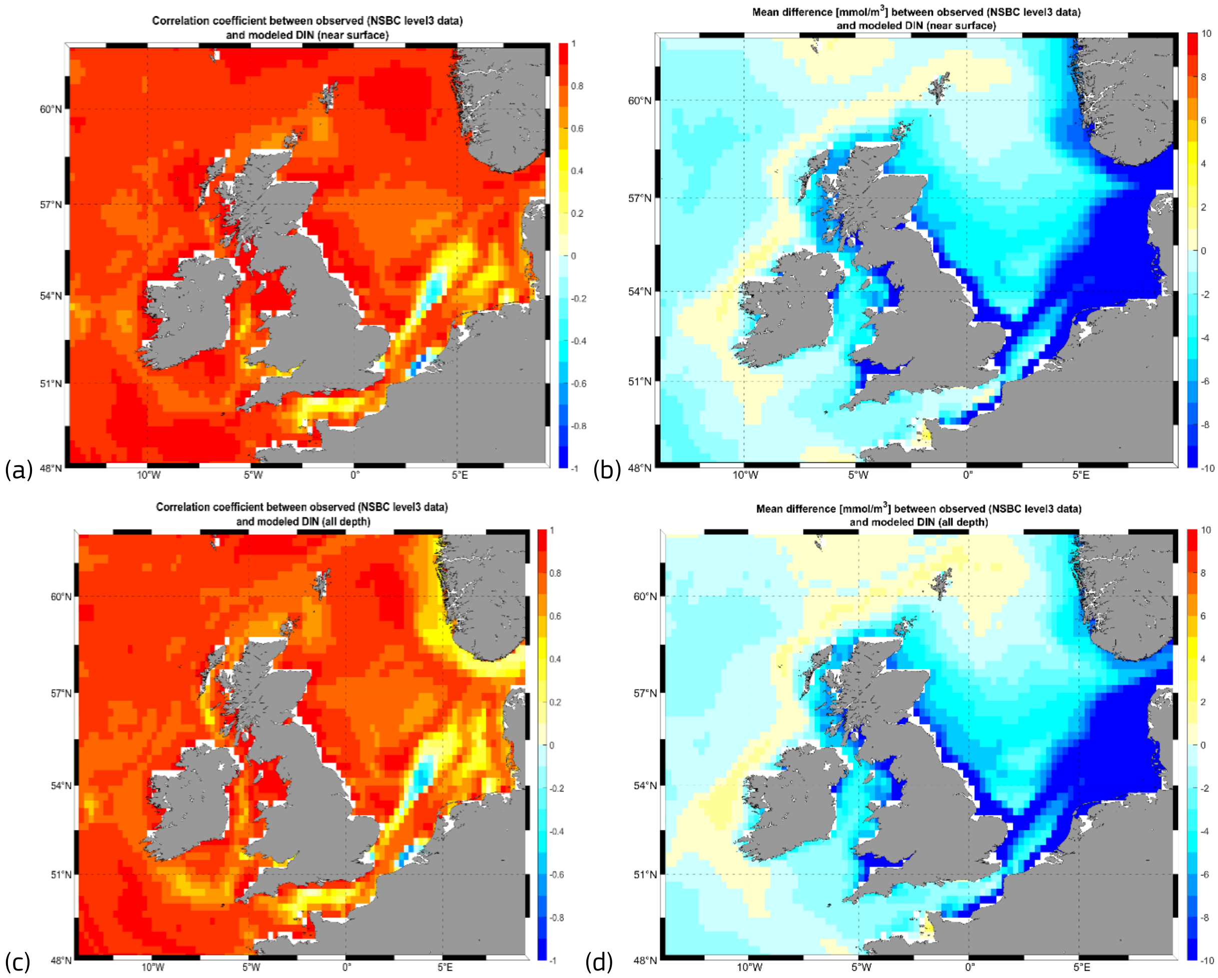

Figure 42: Correlation (a, c) and mean differences (b, d) between observed DIN (Nitrate + Ammonium) concentration (taken from NSBC level 3) and modelled ones, evaluated for near-surface values (a, b) and for all depth layers (c, d) [negative differences denote regions, where the model concentrations are too high]

3.8 Model results compared to satellite data

Several satellite products covering the NWES regions were used for the model validation. The results differ substantially between the individual data sets. For Chlorophyll-a taken from EMIS RMSD between observations and model is quite high (1.14) and correlation only fair (R = 0.38). Especially in the southern and eastern North Sea, the Chlorophyll-a computed by the model is too high (see Figure 44). One problem is thereby the strong underestimation of the light attenuation (see Figure 45), due to the missing inorganic suspended matter (SPM, incorporated in the coupled 3d-model, e.g. by van der Molen et al. (2017)), which is dominating the availability of light strongly (Capuzzo et al., 2013). The statistics are even worse for the comparison with the COPERNICUS Chlorophyll-a data set (RMSD: 1.93; R = 0.29; see Figure 43). The vertically integrated Primary Productivity was compared with different data sets derived from satellite data (see Figures 46, 47). The model results are strongly underestimating, resulting in high RMSDs (COPERNICUS: 1 169, VGPM: 1 340, CBPM: 622.8, EPPLEY: 680.3 mg C m-2 d-1) and low correlations (COPERNICUS: 0.17, VGPM: 0.17, CBPM: 0.12, EPPLEY: 0.14). Nevertheless, the extremely high values from the satellite products of up to 5 000 mg C m-2 d-1 seem unrealistically high (Weston *et al.* (2005) reported values between 456-1 015 mg C m-2 d-1; Westberry *et al.* (2008) up to 1 500 mg C m-2 d-1; and Skogen and Moll (2000) reported also only values below 1 000 mg C m-2 d-1) and may cause the strong bias.

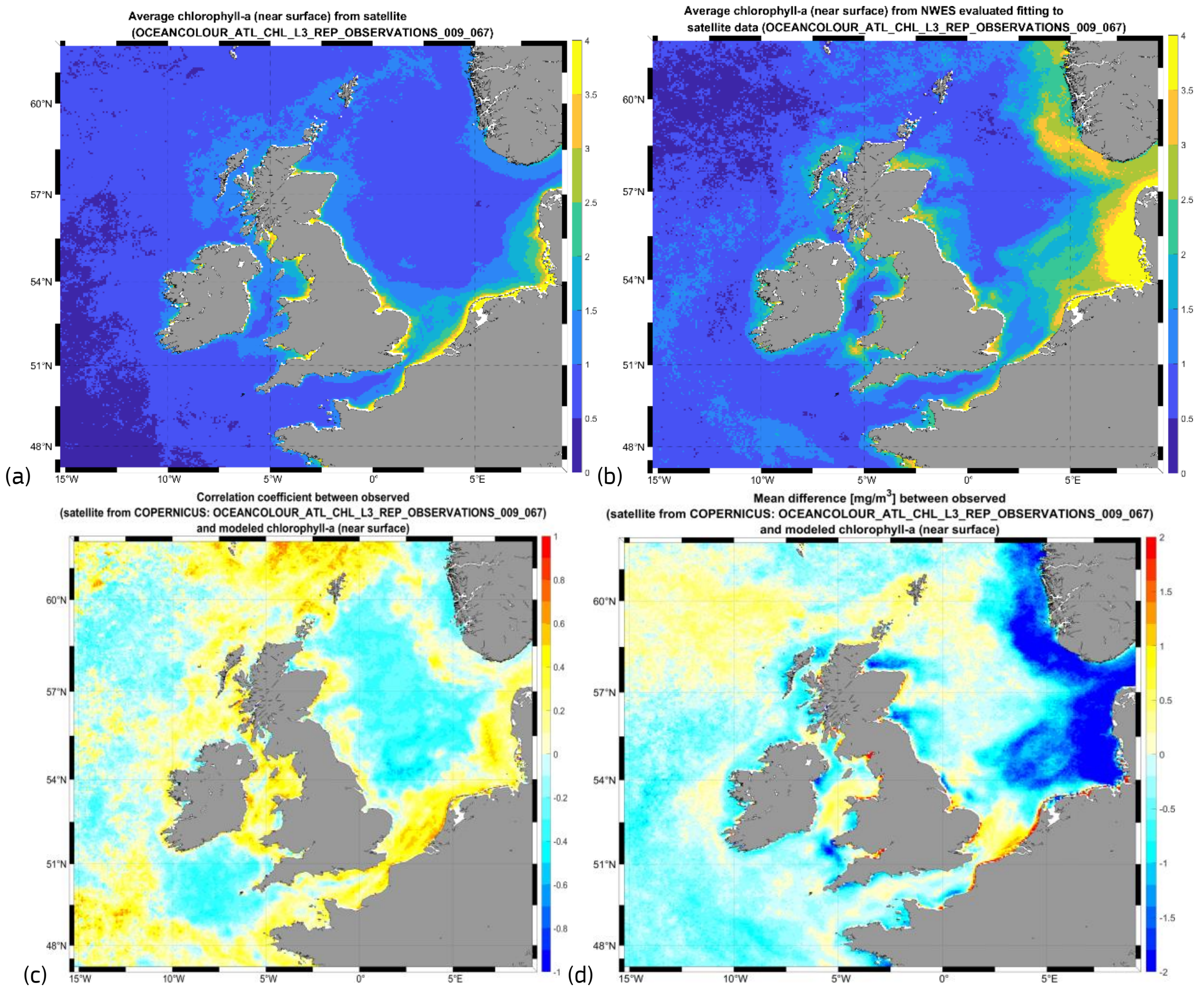

Figure 43: Mean concentrations [mg C m-3] of observed (a; taken from COPERNICUS data service) and modelled (b) near-surface Chlorophyll-a, correlation (c) and mean difference (d; negative differences denote regions, where the model Chlorophyll-a is too high) between both data sets

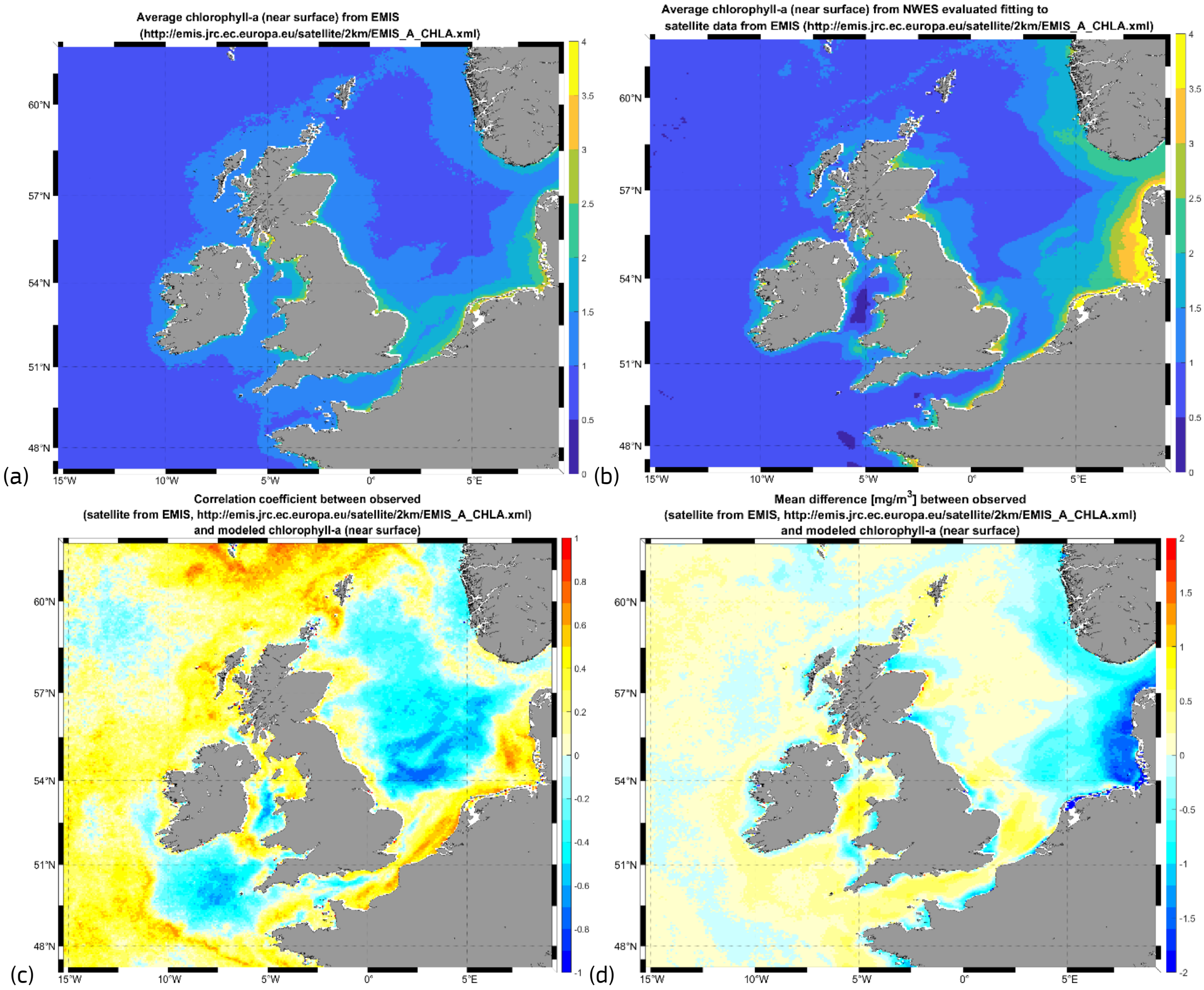

Figure 44: Mean concentrations [mg C m-3] of observed (a; taken from EMIS) and modelled (b) near-surface Chlorophyll-a, correlation (c) and mean difference (d; negative differences denote regions, where the model Chlorophyll-a is too high) between both data sets

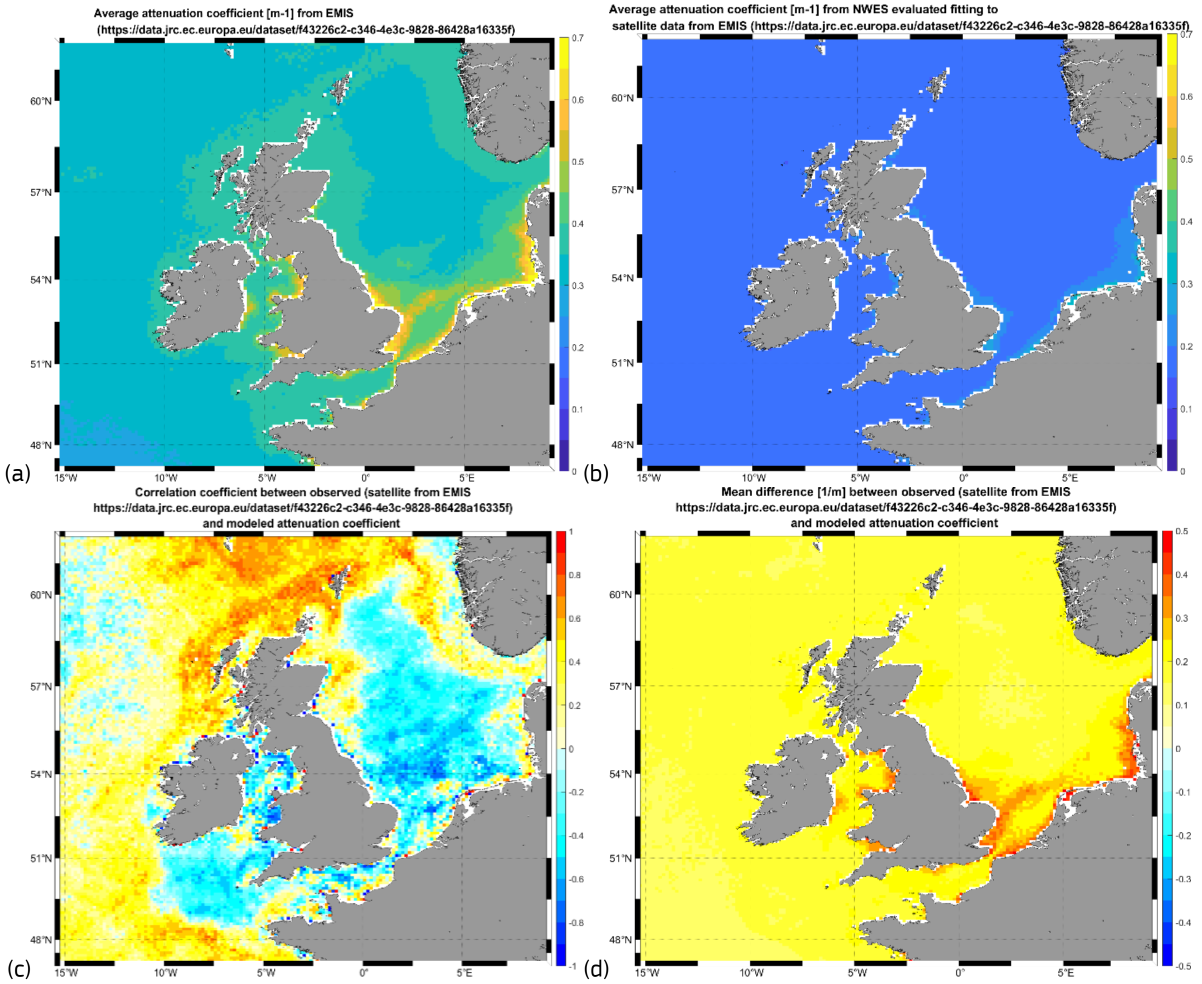

Figure 45: Mean attenuation [m-1] as observed (a; taken from EMIS) and modelled (b), correlation (c) and mean difference (d; positive differences denote regions, where the model attenuation is too low) between both data sets

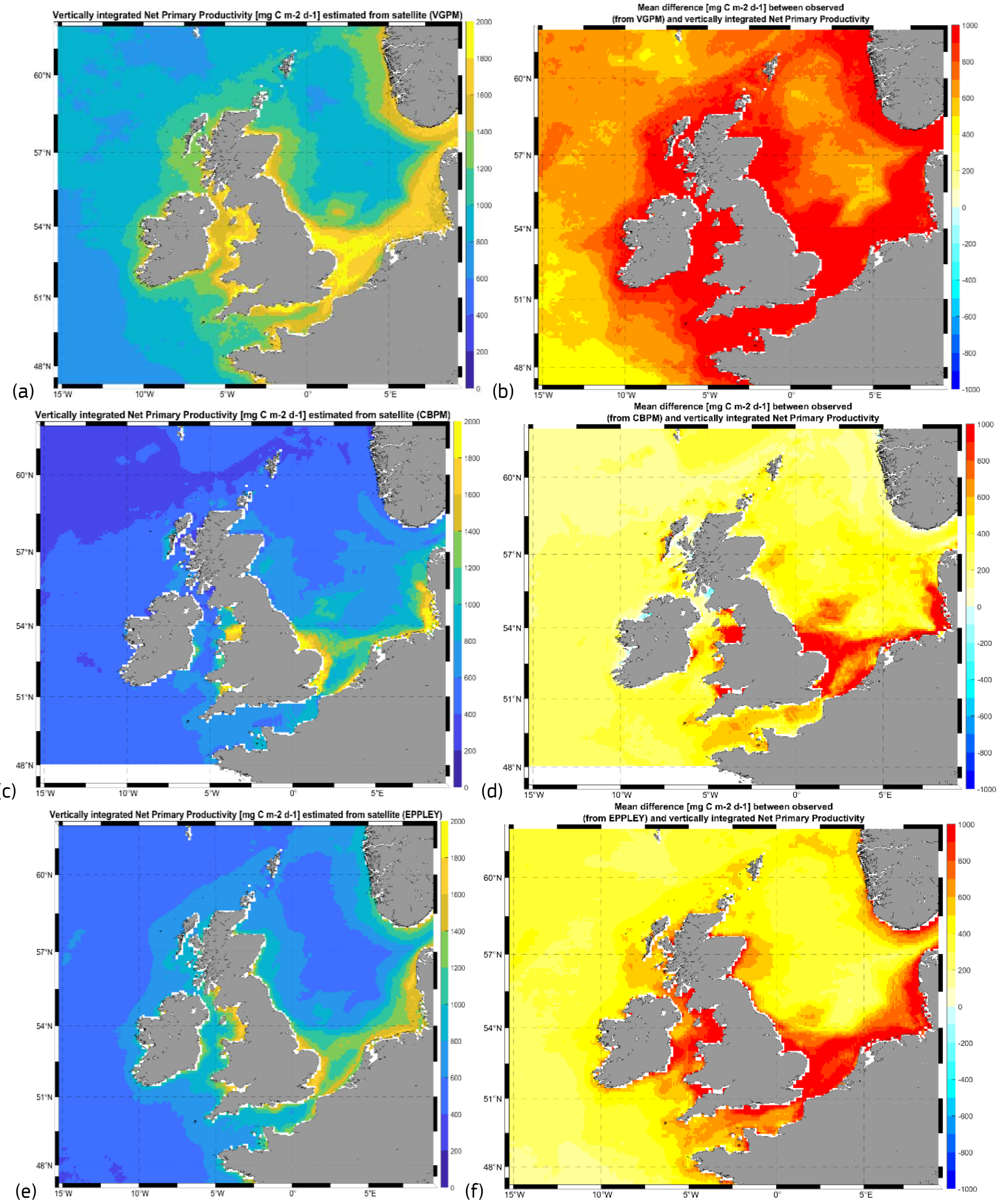

Figure 46: Mean vertically averaged Net Primary Production [mg C m-2 d-1] estimated using VGPM (a); the ratio between VGPM and model values (b), correlation (c) and mean difference between both data sets (d; positive differences denote regions, where the model attenuation is too low)

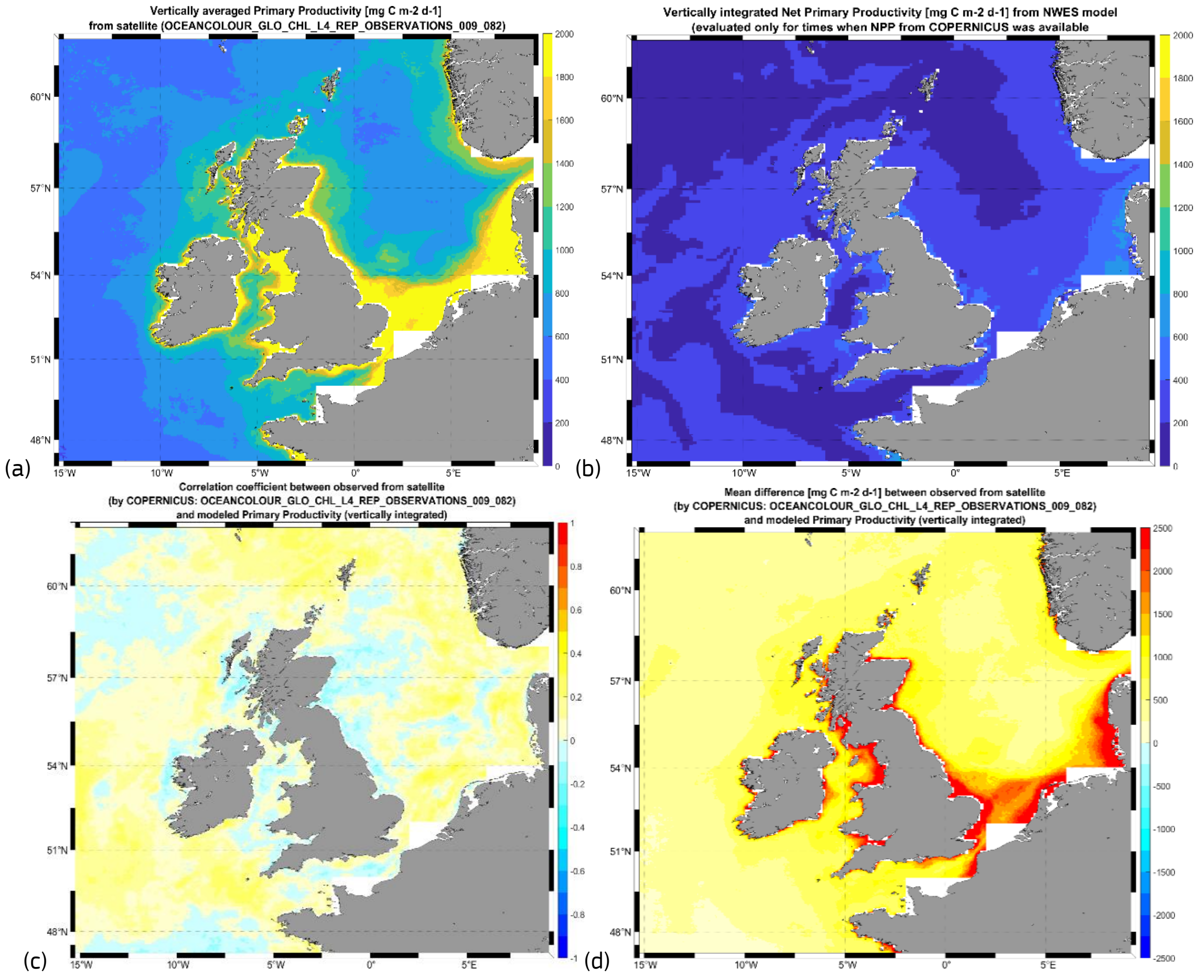

Figure 47: Mean vertically averaged Net Primary Production [mg C m-2 d-1] taken from COPERNICUS (a) and modelled (b), correlation (c) and mean difference (d; positive differences denote regions, where the model attenuation is too low) between both data sets

3.9 ICES COMPEAT data

Following the subdivision proposed by the OSPAR working group ICG EMO and implemented by ICES COMPEAT tool, the model quality regarding Chlorophyll-a (see Figure 48), Dissolved Inorganic Nitrogen (Figure 49) and Phosphate (Figure 50) was assessed (based on the climatologies computed for every assessment unit) using the same classification system as in Figure 34.

The classification resulted, for Phosphate, in an excellent model quality, except for the eastern North Sea and linked to it the Norwegian Trench and Skagerrak area. Further, Chlorophyll-a is also excellent in most coastal areas, while it is mostly improvable in the open sea parts. Dissolved Inorganic Nitrogen is classified only for one region as excellent, due to the too high values in most of the regions.

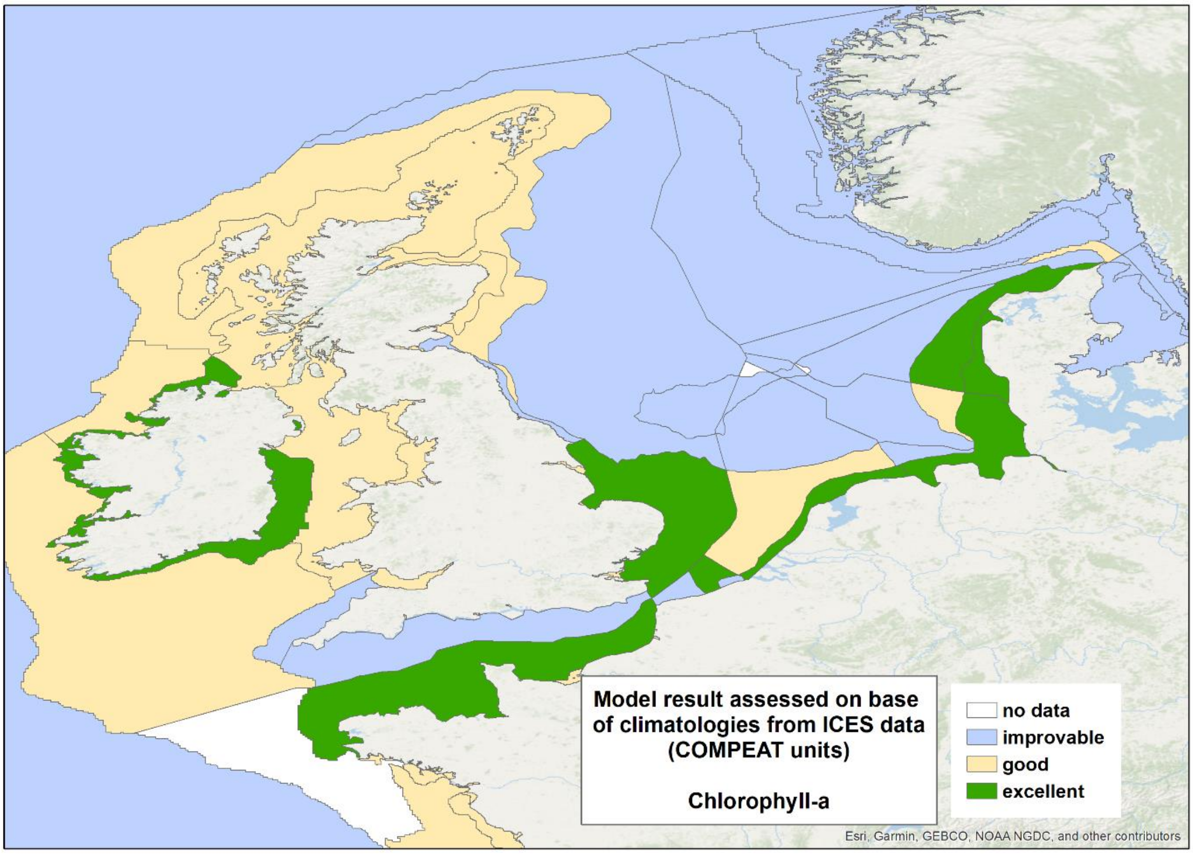

Figure 48: Classification of Chlorophyll-a model quality compared to COMPEAT

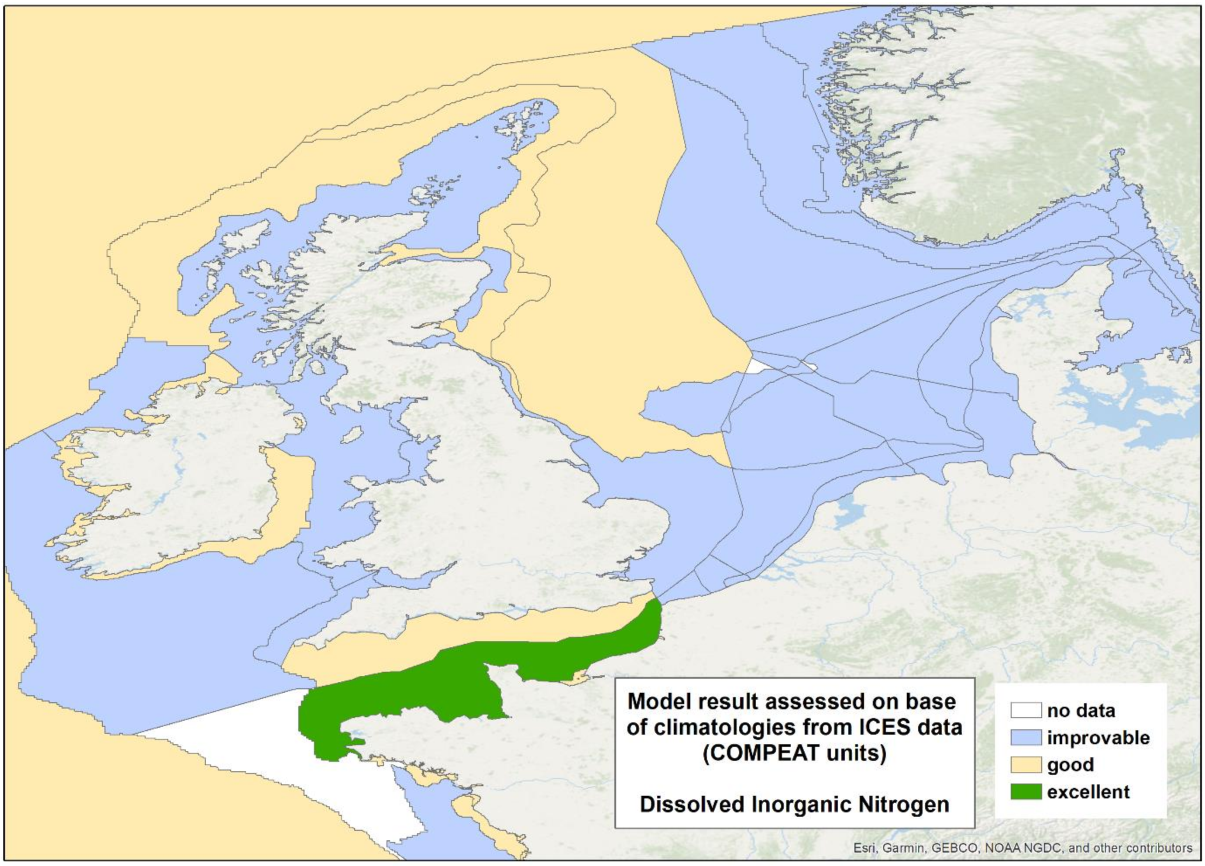

Figure 49: Classification of Dissolved Inorganic Nitrogen model quality compared to COMPEAT

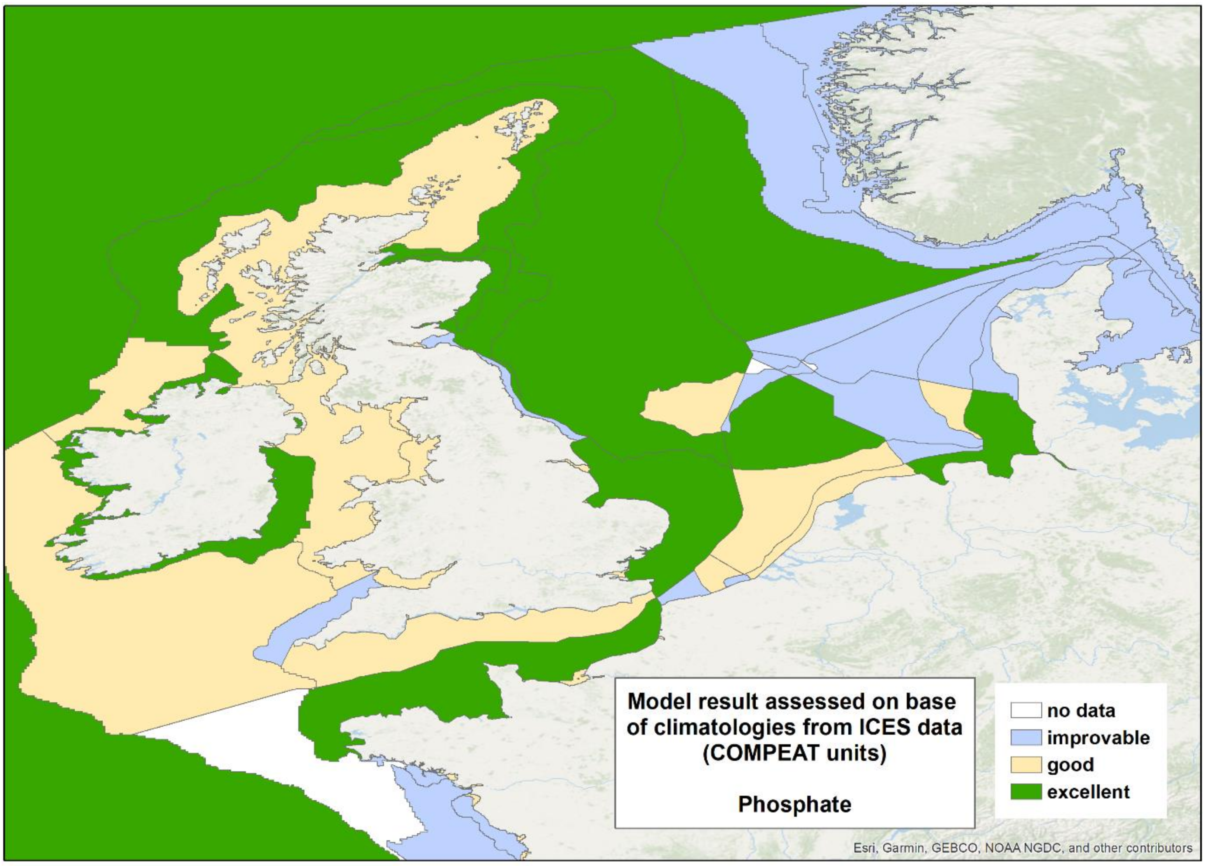

Figure 50: Classification of Dissolved Inorganic Phosphorus (Phosphate) model quality compared to COMPEAT

3.10 Assessment for AMM7 regions

Using the AMM7 region (see Figure 19), model results and observations (using ICES data, WOD and NSBC level 3) were spatially averaged and compared. In Figures 52 and 53 the computed climatologies for some regions of the North Sea and Celtic Sea are shown in detail. While the model shows a strong annual cycle, the observed concentrations differ strongly between the single data sets.

Further, the model quality was assessed for all regions for the near-surface values and using all depth layers (see Figure 51). Overall the classification results in the best results for the comparison with NSBC. For all data sets, the surface values showed higher correlations compared to all depths. The high correlations indicate that the dominating annual cycles are well reproduced. On the other hand, the cost function for Nitrate had mostly higher values, due to the overestimation of Nitrate at NWES model (especially Southern and Central North Sea, Skagerrak and Norwegian Trench).

Using the light attenuation from the NWES model, Secchi Depth (often used as indirect eutrophication indicator) was computed. In Figure 54 it is compared to observations gathered from ICES and an estimate using the attenuation from EMIS. Due to the underestimation of the attenuation, Secchi Depth is mostly everywhere too high in the model, especially in the southern North Sea, but also in the Celtic or Irish Sea. Only during summer in the Central North Sea, does the model estimate meet the observation, as during the calm periods the suspended particles sink down, resulting in high Secchi Depth.

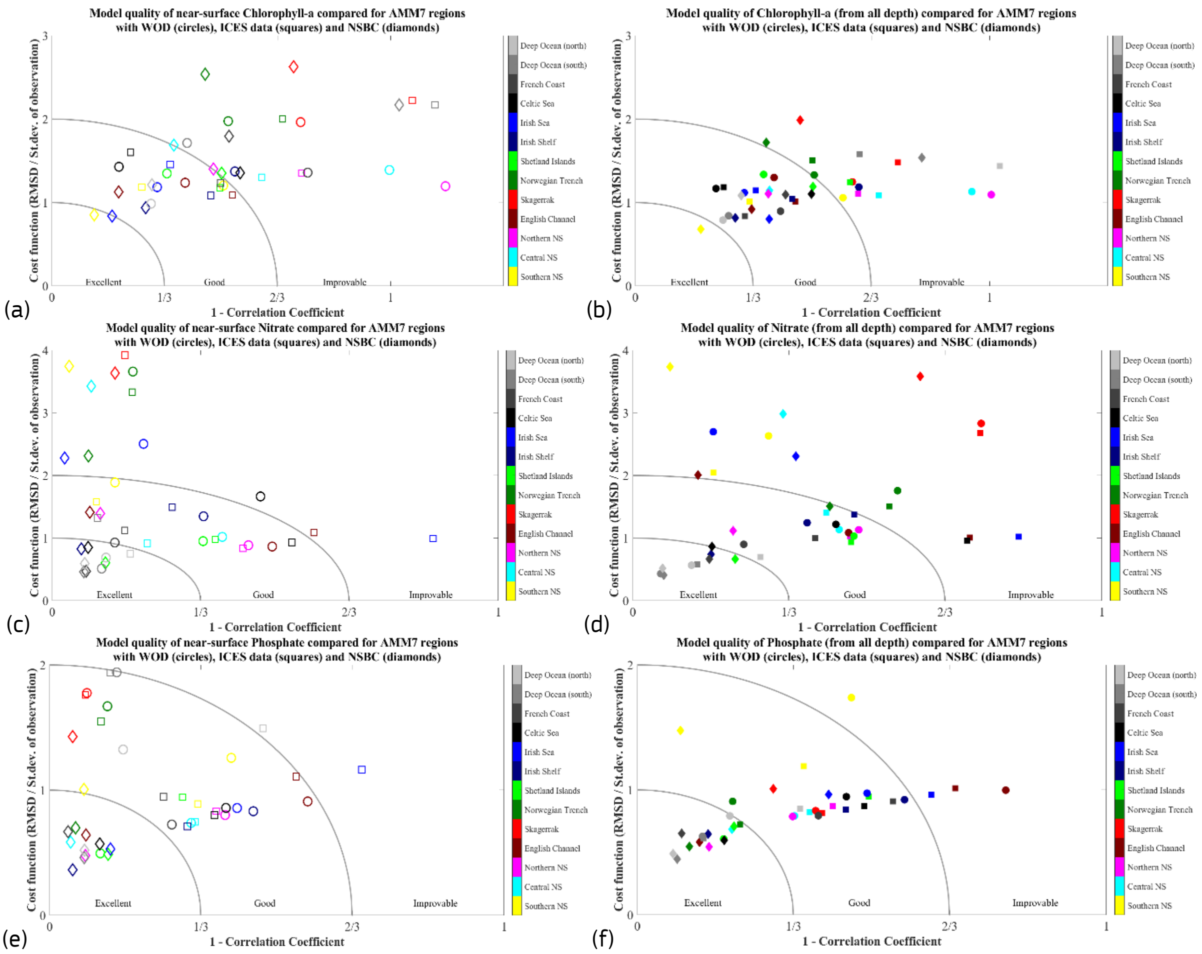

Figure 51: Classification of the model quality for Chlorophyll-a (a, b), Nitrate (c, d) and Phosphate (e, f) for the AMM7 regions (see Figure 19), evaluated only for near-surface values (a, c, e) and all depths (b, d, f)

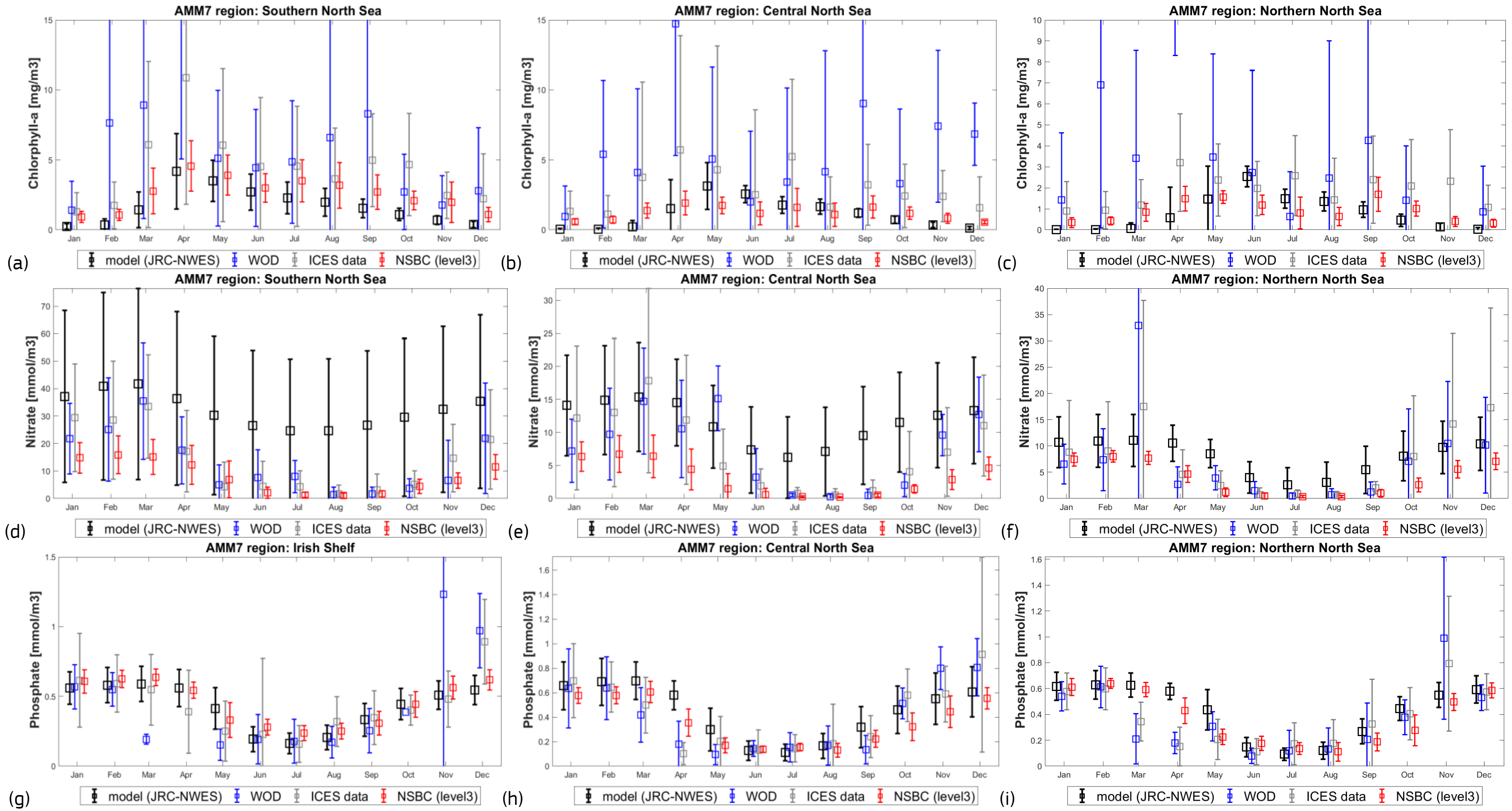

Figure 52: Monthly climatologies of model values (black) and different observations (blue: WOD; grey: ICES data; red: NSBC) computed Chlorophyll-a (a-c), Nitrate (d-f) and Phosphate (g-i) for three AMM7 regions (see Figure 19) covering the North Sea

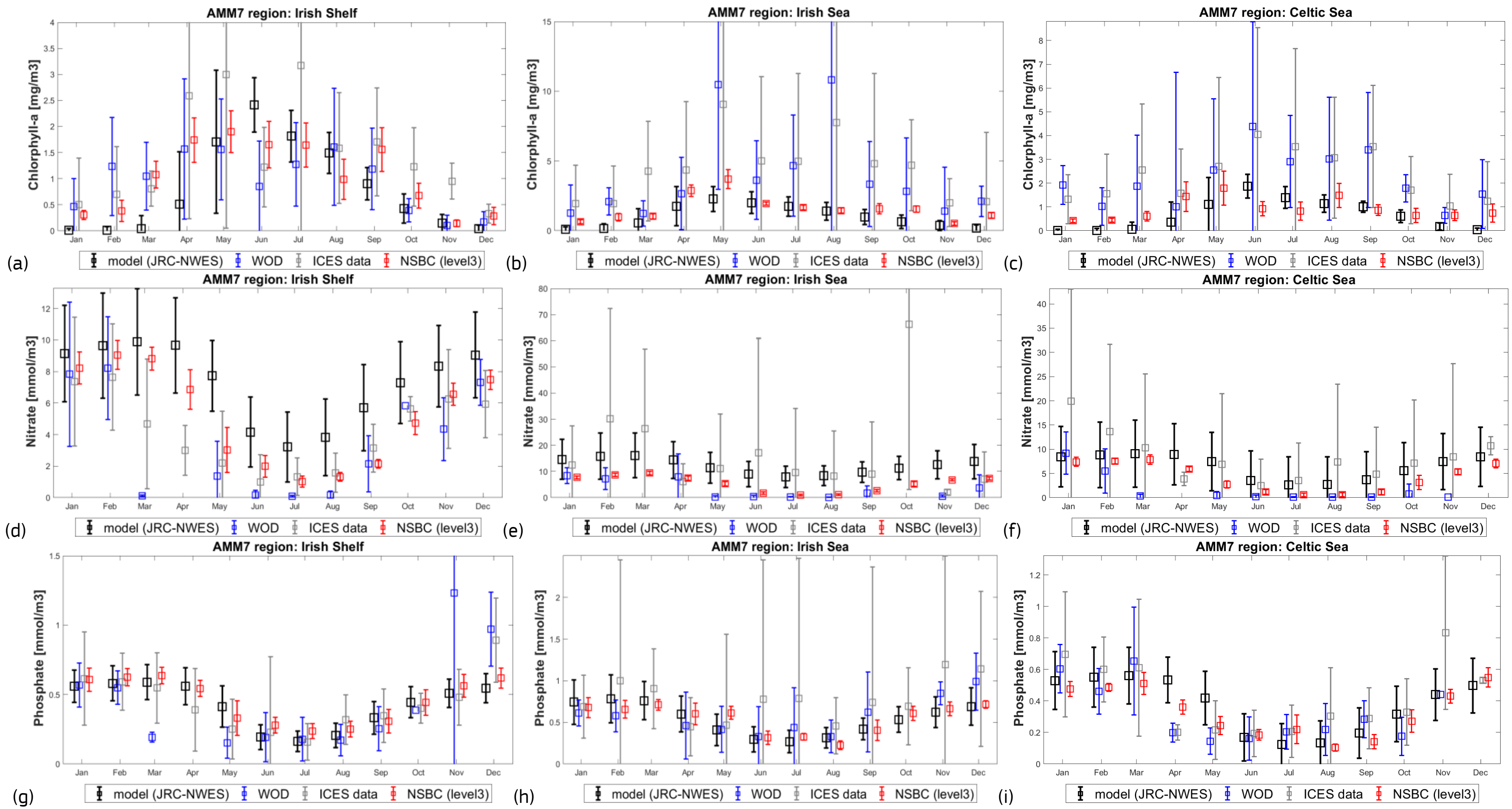

Figure 53: Monthly climatologies of model values (black) and different observations (blue: WOD; grey: ICES data; red: NSBC) computed Chlorophyll-a (a-c), Nitrate (d-f) and Phosphate (g-i) for three AMM7 regions (see Figure 19) covering the North Sea

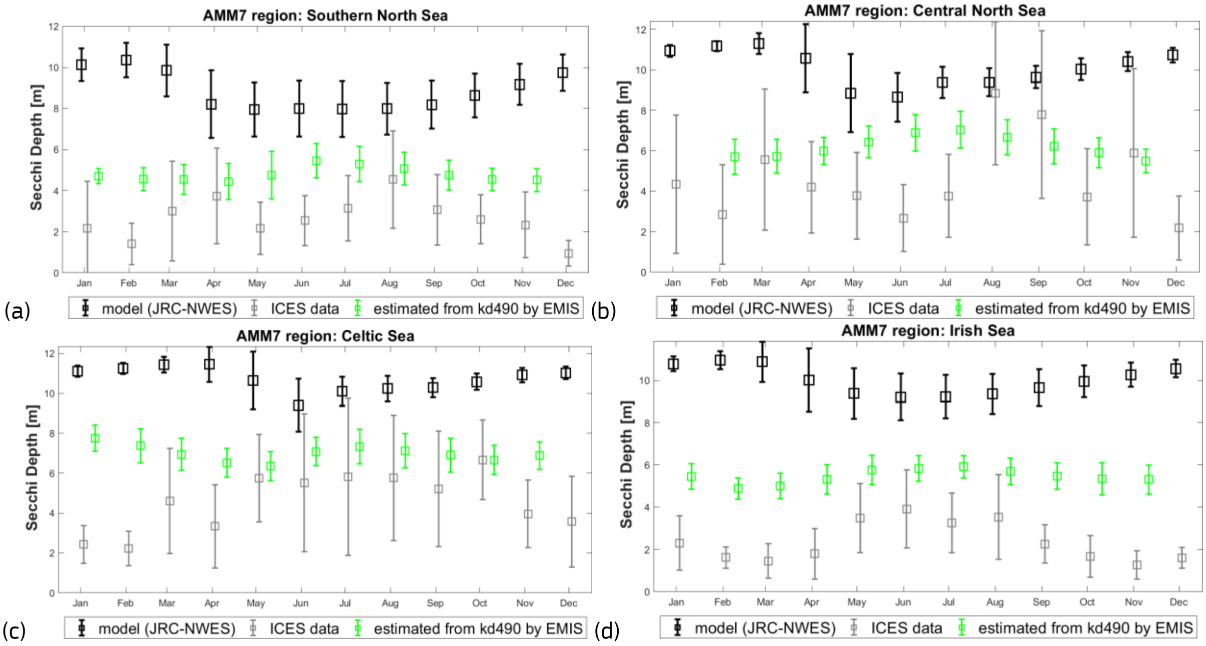

Figure 54: Monthly climatologies of Secchi Depth [m] computed from the model values (black), observations provided by ICES (grey) and estimated from the attenuation (kd490) taken from EMIS (green; see Figure 45)

3.11 Station data

Two stations (WCO long-term monitoring station L4 and Helgoland Reede) were selected for the validation (see Figure 55), representing the English Channel (L4) and the German Bight next to Helgoland, respectively. Both stations have distinctive annual cycles with high levels of Nitrate and Phosphate during winter and low levels during summer. This is reproduced well, although the strong overestimation of Nitrate in the south-eastern North Sea appears again, as well as the too low salinities. An opposite annual cycle occurs for Chlorophyll-a with lowest in values (possibly below observed values) and high values during spring and summer. While the annual maxima at L4 are well reproduced by the NWES model, at Helgoland they are too high, which might be caused by the too strong riverine influence, seen in the low salinity values.

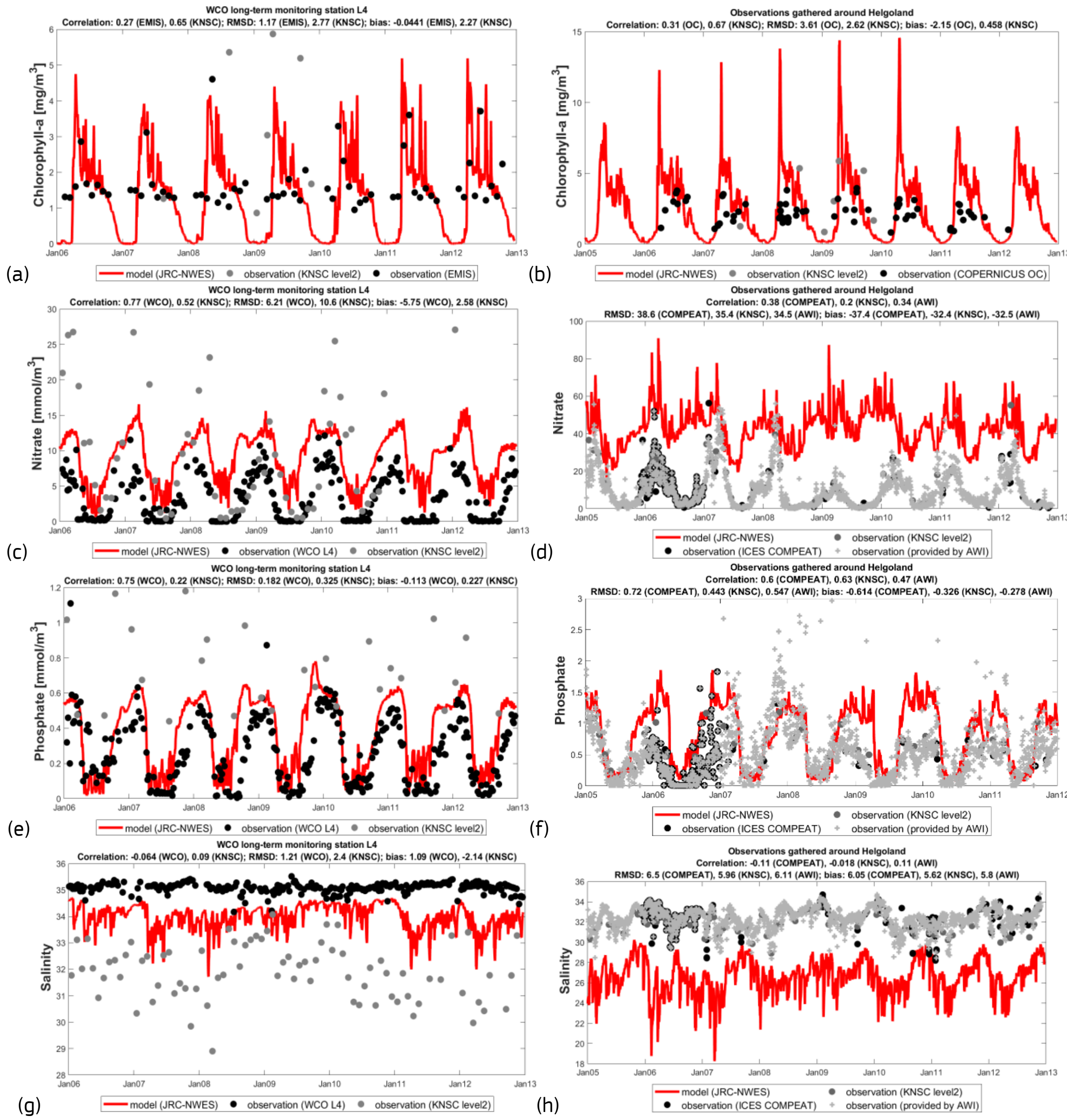

Figure 55: Comparison of model values and observation taken from several data sets regarding Chlorophyll-a (a, b), Nitrate (c, d), Phosphate (e, f) and salinity (g, h) evaluated for WCO long-term monitoring station L4 (a, c, e, g) and around Helgoland (b, d, f, h)

4 Summary

A coupled three-dimensional simulation model of the North-Western European Shelf including the hydrodynamics and a lower trophic level (biogeochemical) model was newly developed. Its results are mostly reliable and allow to apply the model for scenario simulations. All major hydrodynamic features, especially the tides, are well reproduced, as well as the dominating current fields (see Figure 33) or areas where mixing or stratification is mostly occurring (see Figure 32). The salinity gradients from central estuaries (like Rhine, Elbe or Humber) towards the marine waters are overestimated in the model (see Figure 31), as low salinity region extends too far into the sea. This could be improved by using a finer horizontal grid, which could be able to follow the complex topography of the estuaries in a more sophisticated way, so that a stronger mixing of sea water and riverine freshwater could take place already in the estuary.

Main biogeochemical variables used as eutrophication indicators (Chlorophyll-a, Phosphate, Nitrate and Ammonium) are included in the NWES model and mostly follow the annual cycles, which are also visible in the observations. On the other hand, the comparison of the model results with the large variety of available observations revealed strong differences between the individual data sets. This results in mixed signals, for example the simulated Chlorophyll-a concentration in the south-eastern North Sea is above the observations reported by Emodnet Chemistry (Figure 39), satellite data (Figure 43) or EMIS (Figure 44), but below the NSBC data (Figure 40), as well as below the data from WOD and ICES (Figure 52a). Overestimating the Chlorophyll-a concentration may be induced by too low light attenuation coefficients (Figure 45), as suspended inorganic particles (SPM) are missing, which lead especially in the southern and eastern North Sea to high attenuation coefficients.

Another improvable feature is that Nitrate and Ammonium (combined as Dissolved Inorganic Nitrogen, DIN) are in the NWES model mostly above the observed concentrations (e.g. visible in Figure 55d). This is most likely caused by the lacking denitrification in the sediments, which is the central process to convert DIN to atmospheric Nitrogen. Solving this issue requires the implementation of a more sophisticated benthic model, coupled to ERSEM. Another uncertainty is introduced by the riverine nutrient loads. The monthly DIN loads were computed from the annual loads (assuming climatological means) and constant conversion factors from the total Nitrogen load. This method is quite simplified and might be extended by incorporating conversion factors and seasonality from the riverine loads, where observations are available. The very same proceeding worked quite well for the Phosphate loads, seen in a quite good agreement to the observed Phosphate concentrations of the NWES region.

Other key elements of the biogeochemical model (like Dissolved Oxygen or Inorganic Carbon) were also assessed and validated, resulting in a good model quality (not shown). Silicate is included in some of the validation plots (e.g. Figure 39), revealing that model values especially in the southern and eastern North Sea are much too low. Due to its limitation, Diatoms are underestimated in the model simulation, what has only a limited influence on the overall Chlorophyll-a concentration, as the other Phytoplankton groups are not limited by Silicate and therefore their growth is enhanced. Nevertheless, improving the riverine Silicate loads seems important to achieve better model results, as rivers along the southern shore of the North Sea are the main source of Silicate to the NWES.

References

2008/56/EC M. Commission of the European Communities Directive 2008/56/EC of the European Parliament and of the Council of 17 June 2008. Establishing a Framework for Community Action in the Field of Marine Environmental Policy (Marine Strategy Framework Directive). In: Official Journal of the European Union L 164.

BERSCH M, GOURETSKI V, SADIKNI R, HINRICHS I. KLIWAS North Sea Climatology of Hydrographic Data (Version 1.0). In: World Data Center for Climate (WDCC) at DKRZ, 2013.

BOUTIN J, VERGELY J-L, KOEHLER J, ROUFFI F, REUL N. ESA Sea Surface Salinity Climate Change Initiative (Sea_Surface_Salinity_cci): Monthly Sea Surface Salinity product v1.8. In: Centre for Environmental Data Analysis, 2019.

BRUGGEMAN J, BOLDING K. A general framework for aquatic biogeochemical models. Environmental Modelling & Software. 2014;61:249-265.

BUTENSCHÖN M, CLARK J, ALDRIDGE JN, ALLEN JI, ARTIOLI Y, BLACKFORD J*, et al.* ERSEM 15.06: a generic model for marine biogeochemistry and the ecosystem dynamics of the lower trophic levels. Geosci. Model Dev. 2016;9(4):1293-1339.

CAPUZZO E, PAINTING SJ, FORSTER RM, GREENWOOD N, STEPHENS DT, MIKKELSEN OA. Variability in the sub-surface light climate at ecohydrodynamically distinct sites in the North Sea. Biogeochemistry. 2013;113(1):85-103.

CUMMINGS JA, SMEDSTAD OM. Variational Data Assimilation for the Global Ocean. In: Park SK, Xu L, editors. Data Assimilation for Atmospheric, Oceanic and Hydrologic Applications (Vol. II). Berlin, Heidelberg: Springer Berlin Heidelberg, 2013. p. 303-343.

DAEWEL U, SCHRUM C. Simulating long-term dynamics of the coupled North Sea and Baltic Sea ecosystem with ECOSMO II: Model description and validation. Journal of Marine Systems. 2013;119-120:30-49.

DE ROO APJ, WESSELING CG, VAN DEURSEN WPA. Physically based river basin modelling within a GIS: the LISFLOOD model. Hydrological Processes. 2000;14(11-12):1981-1992.

EDMAN M, OMSTEDT A. Modeling the dissolved CO2 system in the redox environment of the Baltic Sea. Limnology and Oceanography. 2013;58(1):74-92.

EDWARDS KP, BARCIELA R, BUTENSCHÖN M. Validation of the NEMO-ERSEM operational ecosystem model for the North West European Continental Shelf. Ocean Sci. 2012;8(6):983-1000.

FORD DA, VAN DER MOLEN J, HYDER K, BACON J, BARCIELA R, CREACH V*, et al.* Observing and modelling phytoplankton community structure in the North Sea. Biogeosciences. 2017;14(6):1419-1444.

GARCIA-GORRIZ E, MACIAS MOY D, STIPS A, MILADINOVA-MARINOVA S. JRC Marine Modelling Framework in support of the Marine Strategy Framework Directive: Inventory of models, basin configurations and datasets. In: JRC Technical Report, editor. EUR 27885. 2016.

GRÄWE U, HOLTERMANN P, KLINGBEIL K, BURCHARD H. Advantages of vertically adaptive coordinates in numerical models of stratified shelf seas. Ocean Modelling. 2015;92:56-68.

GRIZZETTI B, BOURAOUI F, ALOE A. Changes of nitrogen and phosphorus loads to European seas. Global Change Biology. 2012;18(2):769-782.

GRIZZETTI B, LIQUETE C, PISTOCCHI A, VIGIAK O, ZULIAN G, BOURAOUI F, *et al.* Relationship between ecological condition and ecosystem services in European rivers, lakes and coastal waters. Science of The Total Environment. 2019;671:452-465.

GROßE F, GREENWOOD N, KREUS M, LENHART HJ, MACHOCZEK D, PÄTSCH J*, et al.* Looking beyond stratification: a model-based analysis of the biological drivers of oxygen deficiency in the North Sea. Biogeosciences. 2016;13(8):2511-2535.

HARTMANN J, LEVY J, KEMPE S. Increasing dissolved silica trends in the Rhine River: an effect of recovery from high P loads? Limnology. 2011;12(1):63-73.

HESSE C, KRYSANOVA V. Modeling Climate and Management Change Impacts on Water Quality and In-Stream Processes in the Elbe River Basin. Water. 2016;8(2).

HINRICHS I, GOURETSKI V, PÄTSCH J, EMEIS K-C, STAMMER D. North Sea Biogeochemical Climatology (Version 1.1). In: World Data Center for Climate (WDCC) at DKRZ, 2017.

HOWDEN NJK, BURT TP, WORRALL F, WHELAN MJ, BIEROZA M. Nitrate concentrations and fluxes in the River Thames over 140 years (1868–2008): are increases irreversible? Hydrological Processes. 2010;24(18):2657-2662.

LENHART H-J, MILLS DK, BARETTA-BEKKER H, VAN LEEUWEN SM, DER MOLEN JV, BARETTA JW*, et al.* Predicting the consequences of nutrient reduction on the eutrophication status of the North Sea. Journal of Marine Systems. 2010;81(1):148-170.

MAAR M, MØLLER EF, LARSEN J, MADSEN KS, WAN Z, SHE J, *et al.* Ecosystem modelling across a salinity gradient from the North Sea to the Baltic Sea. Ecological Modelling. 2011;222(10):1696-1711.

MAYORGA E, SEITZINGER SP, HARRISON JA, DUMONT E, BEUSEN AHW, BOUWMAN AF, *et al.* Global Nutrient Export from WaterSheds 2 (NEWS 2): Model development and implementation. Environmental Modelling & Software. 2010;25(7):837-853.

MÉNESGUEN A, DUSSAUZE M, DUMAS F, THOUVENIN B, GARNIER V, LECORNU F, *et al.* Ecological model of the Bay of Biscay and English Channel shelf for environmental status assessment part 1: Nutrients, phytoplankton and oxygen. Ocean Modelling. 2019;133:56-78.

MINAUDO C, MEYBECK M, MOATAR F, GASSAMA N, CURIE F. Eutrophication mitigation in rivers: 30 years of trends in spatial and seasonal patterns of biogeochemistry of the Loire River (1980–2012). Biogeosciences. 2015;12(8):2549-2563.

MOCKLER EM, DEAKIN J, ARCHBOLD M, GILL L, DALY D, BRUEN M. Sources of nitrogen and phosphorus emissions to Irish rivers and coastal waters: Estimates from a nutrient load apportionment framework. Science of The Total Environment. 2017;601-602:326-339.

MOLL A, RADACH G. Review of three-dimensional ecological modelling related to the North Sea shelf system: Part 1: models and their results. Progress in Oceanography. 2003;57(2):175-217.

NIXON SW. Coastal marine eutrophication: a definition, social causes, and future concerns. Ophelia. 1995;41(1):199-219.

OSPAR. Commission for the Protection of the Marine Environment of the North-East AtlanticQuality Status Report. In: 2000.

OSPAR. Third OSPAR integrated report on the eutrophication status of the OSPAR Maritime Area. 2017.

PARCOM. PARCOM Recommendation 88/2: On the Reduction in Nutrients to the Paris Convention Area, Publication number 88/2, Paris Commission. In: 1988.

PASSY P, GYPENS N, BILLEN G, GARNIER J, THIEU V, ROUSSEAU V, *et al.* A model reconstruction of riverine nutrient fluxes and eutrophication in the Belgian Coastal Zone since 1984. Journal of Marine Systems. 2013;128:106-122.

PASSY P, LE GENDRE R, GARNIER J, CUGIER P, CALLENS J, PARIS F, *et al.* Eutrophication modelling chain for improved management strategies to prevent algal blooms in the Bay of Seine. Marine Ecology Progress Series. 2016;543:107-125.

PÄTSCH J, BURCHARD H, DIETERICH C, GRÄWE U, GRÖGER M, MATHIS M, *et al.* An evaluation of the North Sea circulation in global and regional models relevant for ecosystem simulations. Ocean Modelling. 2017;116:70-95.

RADACH G, PÄTSCH J. Variability of continental riverine freshwater and nutrient inputs into the North Sea for the years 1977–2000 and its consequences for the assessment of eutrophication. Estuaries and Coasts. 2007;30(1):66-81.

ROMERO E, GARNIER J, LASSALETTA L, BILLEN G, LE GENDRE R, RIOU P, *et al.* Large-scale patterns of river inputs in southwestern Europe: seasonal and interannual variations and potential eutrophication effects at the coastal zone. Biogeochemistry. 2013;113(1):481-505.

SKOGEN MD, MOLL A. Interannual variability of the North Sea primary production: comparison from two model studies. Continental Shelf Research. 2000;20(2):129-151.

STIPS A, BOLDING K, MACIAS D, BRUGGEMAN J, COUGHLAN C. Scoping report on the potential impact of on-board desulphurisation on the water quality in SOxEmission Control Areas. In: JRC Technical Report. 2016.

THIEU V, GARNIER J, BILLEN G. Assessing the effect of nutrient mitigation measures in the watersheds of the Southern Bight of the North Sea. Science of the Total Environment $V 408. 2010(6):1245-1255.

TOCKNER K, UEHLINGER U, ROBINSON CT. Rivers of Europe. Academic Press; 2009.

VAN DER KNIJFF JM, YOUNIS J, DE ROO APJ. LISFLOOD: a GIS-based distributed model for river basin scale water balance and flood simulation. International Journal of Geographical Information Science. 2010;24(2):189-212.

VAN DER MOLEN J, RUARDIJ P, GREENWOOD N. A 3D SPM model for biogeochemical modelling, with application to the northwest European continental shelf. Journal of Sea Research. 2017;127:63-81.

VAN LEEUWEN S, TETT P, MILLS D, VAN DER MOLEN J. Stratified and nonstratified areas in the North Sea: Long-term variability and biological and policy implications. Journal of Geophysical Research: Oceans. 2015;120(7):4670-4686.

WAKELIN SL, HOLT JT, BLACKFORD JC, ALLEN JI, BUTENSCHÖN M, ARTIOLI Y. Modeling the carbon fluxes of the northwest European continental shelf: Validation and budgets. Journal of Geophysical Research: Oceans. 2012;117(C5).

WESTBERRY T, BEHRENFELD MJ, SIEGEL DA, BOSS E. Carbon-based primary productivity modeling with vertically resolved photoacclimation. Global Biogeochemical Cycles. 2008;22(2).

WESTON K, FERNAND L, MILLS DK, DELAHUNTY R, BROWN J. Primary production in the deep chlorophyll maximum of the central North Sea. Journal of Plankton Research. 2005;27(9):909-922.

WILTSHIRE KH, MALZAHN AM, WIRTZ K, GREVE W, JANISCH S, MANGELSDORF P*, et al.* Resilience of North Sea phytoplankton spring bloom dynamics: An analysis of long-term data at Helgoland Roads. Limnology and Oceanography. 2008;53(4):1294-1302.

KJ-NA-30168-EN-N

The European Commission's science and knowledge service

Joint Research Centre

JRC Mission

As the science and knowledge service of the European Commission, the Joint Research Centre's mission is to support EU policies with independent evidence throughout the whole policy cycle.

EU Science Hub
ec.europa.eu/jrc

@EU_ScienceHub

EU Science Hub - Joint Research Centre

EU Science, Research and Innovation

EU Science Hub

Publications Office of the European Union

doi:10.2760/78173

ISBN: 978-92-76-17866-8